THE EFFECT OF HSA-MIR-105 ON PROSTATE CANCER GROWTH

by

David Rice Honeywell
Bachelor of Science, Queen's University, 2010

THESIS SUBMITTED IN PARTIAL FULFILLMENT OF
THE REQUIREMENTS FOR THE DEGREE OF

MASTER OF SCIENCE

In the
Department of Biochemistry, Microbiology and Immunology

ABSTRACT

Micro (mi)RNAs have recently been found to play an important role in cancer biology. In order to further understand how miRNAs affect prostate tumour progression, we evaluated miRNA expression in two invasive prostate tumour lines, PC3 and DU145. We then focused our evaluation on a novel miRNA, miR-105, whose levels were significantly decreased in both tumour cell lines as compared to normal prostate epithelial cells. As miR-105 levels were reduced in prostate tumour cell lines, we restored its expression following transfection of cells with mimic constructs to over-express miR-105 in both cell lines, in order to determine its effect on various tumourigenic properties. Over-expression caused decreased tumour cell proliferation, anchorage-independent growth and invasion *in vitro* and inhibited tumour growth *in vivo*. We further identified CDK6 as a putative target of miR-105, which likely contributed to its inhibition of tumour cell growth. Our results suggest that miR-105 inhibits tumour cell proliferation and may be an interesting target to regulate tumour growth or potentially used as a biomarker to differentiate between less and more aggressive tumours in patients.

ACKNOWLEDGEMENTS

First and foremost I would like to thank my supervisor, Dr. Christina Addison, for her constant support and advice throughout my studies. I would like to thank Grant Howe, Huijun (Jane) Zhao and Miguel Cabrita for the countless times they helped me in the lab with my experiments. I would like to thank my TAC members Dr. Jim Dimitroulakos and Dr. Bruce McKay for their valuable advice and criticism. I would like to thank everyone in the Cancer Centre who helped me, whether it was through advice, hands-on help or encouragement. Finally, I would like to thank my friends, family and significant other for their constant encouragement and support.

TABLE OF CONTENTS

ABBREVIATIONS

3’ untranslated region	3’UTR
5,10-methylenetetrahydrofolate reductase	MTHFR
5’ untranslated region	5’UTR
androgen receptor	AR
Argonaute-2	Ago2
basic fibroblast growth factor	bFGF
chronic lymphocytic leukemias	CLL
cold-shock domain-containing protein 2	CSDC2
coronary heart disease	CHD
cyclin-dependent kinase 6	Cdk6
cyclin-dependent kinase-8	Cdk8
Dead end 1	Dnd1
DNA-binding protein DiGeorge critical region 8	DGCR8
double-stranded RNA	dsRNA
Dulbecco’s Modified Eagle Medium	DMEM
E3 ubiquitin ligase identified by differential display	EDD
epidermal growth factor	EGF
epidermal growth factor receptor	EGFR

epithelial to mesenchymal transition	EMT
eukaryotic initiation factor 4E	eIF4E
extracellular matrix	ECM
fetal bovine serum	FBS
formalin-fixed, paraffin-embedded	FFPE
GABA A receptor alpha 3 subunit	GABRA3
Gamma-aminobutyric acid	GABA
glutathione S-transferase 1	GSTP1
hematoxylin and eosin	H&E
heterogeneous nuclear ribonucleoprotein A1	hnRNP A1
inositol polyphosphate multikinase	IPMK
microRNA	miRNA
miRNA-induced silencing complex	miRISC
Neural precursor cell expressed, developmentally down-regulated 4	NEDD4
open-reading frame	ORF
phosphatase and tensin homologue	PTEN
poly ADP ribose polymerase	PARP
poly(A)-binding protein	PABP
precursor miRNA	pre-miRNA
primary miRNA	pri-miRNA
processing bodies	P-bodies

propidium iodide	PI
prostate epithelial cell	PrEC
prostate-specific antigen	PSA
protein activator of PKR	PACT
Ran guanosine diphosphate	Ran-GDP
Ran guanosine triphosphate	Ran-GTP
Retinoblastoma	RB
Ribonuclease	RNase
ribonuclease (RNase) III enzyme Drosha	RNASEN
ribonucleoprotein complexes	RNP
RISC loading complex	RLC
RNA helicase A	RHA
RNA-induced silecing complex	RISC
single nucleotide polymorphism	SNP
Soft-agarose	SA
Tar RNA binding protein	TRBP
Toll-like Receptor 2	TLR2
tumour necrosis factor-alpha	TNF-alpha
Tumour-growth factor-B II receptor	TGFBRII

LIST OF FIGURES AND ILLUSTRATIONS

LIST OF TABLES

1: INTRODUCTION

1.1 Preamble

Prostate cancer is the most common cancer affecting Canadian men and its prevalence is increasing as our population grows older (48). Within Canada there will be an expected 26,500 new cases along with approximately 4000 deaths in 2012, which ranks prostate cancer third in terms of cancer mortality among males (183). Autopsies of men aged 30 to 40 revealed that up to 29 percent harboured prostatic carcinomas, and the percentage increased to 64 percent in the 60 to 70 age group (170). Many important genes are involved in the development of prostate cancer, including key targets such as androgen receptor (AR) (191), phosphatase and tensin homologue (PTEN) (118) and $p27^{Kip1}$ (32). Recently there is a new class of genes, called microRNAs (miRNAs), which have been shown to greatly influence prostate cancer progression.

miRNAs are small, 18-25 nucleotide RNA molecules that target specific mRNA sequences and usually repress or destroy their targets (76). Since their discovery in 1993 (113) (200) and subsequent understanding of their function, miRNAs have risen in prominence as an additional layer of complexity in gene expression. It is estimated that over 60% of genes, which include many key signaling pathways within the cell, are regulated by miRNAs (55). They are very important in the proper development of organs, such as the heart (50), brain (49) and reproductive organs (75), but also play a role in many diseases such as cancer (19), heart disease (190), and diabetes (101). miRNAs are also highly involved in the development and progression of prostate cancer (74). One area of interest is

miRNA involvement in prostate cancer metastasis. Most deaths in prostate cancer patients occur because the primary prostate tumour has metastasized and spread throughout the body, particularly to the bone (16). Understanding how miRNAs affect prostate cancer metastasis would aid in the understanding, detection and future treatment of the disease. To this end the miRNA expression of two metastatic prostate cancer cell lines, PC3 and DU145, was compared against that of normal prostate epithelial cells (PrECs). A novel target, hsa-miR-105, was identified as being significantly repressed in both metastatic cells lines and its effects on cell proliferation, anchorage-independent growth and invasion were thus evaluated.

1.2 Introduction to Prostate Cancer

1.2.1 Prostate cancer background

Prostate cancer was first described in 1853 when Dr. John Adams performed a histological examination of a patient's prostate and lymph nodes and found cancerous masses (39). The progression of prostate cancer from normal prostatic epithelium to advanced metastatic cancer lies with the alteration of key genes such as glutathione S-transferase 1 (GSTP1), PTEN, $p27^{Kip1}$, and AR. GSTP1 is a caretaker gene that protects the genome from oxidative stress-induced damage, and hyper-methylation of its promoter is the most common epigenetic change in early prostate cancers (92). PTEN is a canonical tumour-suppressor gene that normally suppresses the Akt/PKB growth pathway, and its loss leads to metastatic prostate cancer (194). $p27^{Kip1}$ normally regulates the cell cycle, and its loss in prostate cancer leads to increased proliferation and tumour growth in conjunction with loss of PTEN (40). Finally, AR mutations are crucial to late-stage prostate cancer because they

allow the cell to become androgen-independent (191). In addition to these examples there are thousands of other possible prostate cancer mutations that allow tumours to grow, survive and metastasize.

Today there are multiple therapeutic treatments available for prostate cancer, such as surgery, radiation therapy, hormonal therapy and chemotherapy. Radical prostatectomies were one of the first therapies used to treat prostate cancer. This method was pioneered in 1904 by Dr. Hugh Young when he performed the first radical perineal prostatectomy (85). Surgery, in combination with other advances such as improved biopsy techniques in 1988 (155) and prostate-specific antigen (PSA) tests in 1986 (103), led to increased survival rates for men with primary prostate cancers. Radiation therapy is another method that was initially used in the beginning of the 20th century by inserting radium, a radioactive element, into a patient's prostate (37). However, this was very inaccurate and radiation therapy fell out of use until new technology allowed the accurate placement of radioactive materials (156), along with the invention of accurate external beam radiotherapy that did not damage surrounding tissues (6). The first drug-based therapy arrived in the early 1940s when Charles Huggins developed androgen-ablation therapy. It was based on the discovery that prostate cell growth is driven by androgen hormones such as testosterone, and reducing their levels by chemical inhibition or physical castration leads to significantly reduced prostate size and growth (79). When applied to human prostate cancer patients it significantly reduced prostate cancer growth, and became one of the first successful prostate cancer treatments (78). This therapy is often used in conjunction with surgery or radiation treatment. Finally, chemotherapy is used less in prostate cancer compared with other cancers (60). Current research is focusing on creating chemotherapeutics that have a significant effect on

metastatic cancers, with limited but improving success (151). Today, primary prostate cancer is often caught early because of physical examinations and PSA testing, and this early cancer responds well to treatments such as surgery, radiation and androgen-ablation therapy. However, if prostate cancer develops and metastasizes, then there are no effective treatment options except for palliative care (52).

1.2.2 General models of prostate cancer

Cancer research requires immortalized cancer cell lines to study the disease *in vitro*. The standard prostate cancer cell lines PC3 and DU145 were used in our study as models of metastatic prostate cancer. They were compared to the normal prostate epithelial cell line (PrEC). PrEC cells are the standard representative cell line of pubertal prostate epithelial cells (182). PrECs express both basal and luminal prostate cell markers, which indicates that they are derived from basal epithelial stem cells and show signs of transition into the luminal cell type. Unlike cancer cell lines PrEC cells are not immortalized and cells can only be used for between 10-15 cell doublings. The PC3 cell line was derived from metastatic prostate tumours located in a lumbar vertebrae (89), and the DU145 cell line was derived from metastatic prostate tumour located in the central nervous system (139). PC3 cells are non-responsive to androgen, do not respond to external growth factors such as epidermal growth factor (EGF) and basic fibroblast growth factor (bFGF) and are able to grow in both anchorage-independent and nude mouse environments (198) (1). DU145 cells are similar except for the fact that they still respond to external growth factors such as EGF and bFGF. Both contain mutations in important cancer genes. For example, PC3 cells are p53 null, while DU145 cells are p53 heterozygous (24). Recent research has shown that both also

harbour changes in miRNAs that affect cancer phenotypes, such as miR-29b affecting epithelial to mesenchymal transition (EMT) in PC3 cells (169) and miR-375 affecting proliferation levels in DU145 cells (187).

1.3 Introduction to miRNAs

1.3.1 miRNA background

miRNAs are small RNA inhibitors which have been shown to play an important role in regulating gene expression in a number of organisms. miRNAs were first discovered in 1993 in *C. elegans* by two separate groups (113) (200). Both found that a small RNA product of the *lin*-4 gene was able to regulate levels of LIN14 protein. They determined that the small RNA contained complementary sequences to the 3' untranslated region (3'UTR) of the lin-14 mRNA, but they did not know if the relationship was based around a stable or transient binding. In 1998 it was discovered that small RNAs could cause post-transcriptional silencing of mRNA levels (53). A second miRNA, let-7, was discovered by two groups in 2000 (148) (159). Then in 2001 three studies (112) (105) (107) simultaneously found that there were an abundance of these small RNA molecules not just in C. *elegans* but also in many animal species, including *Drosophila melanogaster* and *Homo sapiens*. The three groups agreed to name this new, abundant class of small RNAs microRNAs, based on their small mature size of 18-25 nucleotides. They also suggested the nomenclature miR-# and *mir-#* for individual miRNAs and their genes, respectively. After this discovery came a flood of new miRNA discoveries in many species of animals (142) and plants (124). The function of miRNAs on their mRNA targets was discovered in 2002 when multiple groups demonstrated that miRNAs can act in a similar fashion to siRNAs by causing the destruction

of their mRNA partners by directing sequence-specific degradation (84) (125) (160). A breakthrough in miRNA identification appeared in 2004 when researchers used directional cloning to develop small cDNA libraries of endogenous small RNA molecules (27) (2). This was far more efficient at discovering large amounts of new miRNAs than previous techniques utilizing forward genetics. In recent years new techniques have been created to discover miRNAs such as the immunoprecipitation of Ago2 proteins, which are often bound to miRNAs (189).

Not all miRNAs are involved in the destruction of their mRNA targets. The first miRNA, lin-4, is in fact a transcriptional repressor that down-regulates protein levels but does not decrease levels of its corresponding mRNA (145). miRNAs often bind to the 3'UTR of mRNAs but have also been found to bind to the 5' untranslated region (5'UTR) (110), and even directly to genes by attaching to different promoter regions (152). Because of their importance in fine-tuning post-transcriptional gene expression, major dysregulation of important miRNAs leads to negative effects on cells that manifest in diseases such as cancer (19), heart disease (190), and diabetes (101). Today, after over 10,000 papers have been written on the subject, researchers have discovered over 1000 human-specific miRNAs and many more in other species (66), each regulating hundreds of potential gene targets (55).

1.3.2 miRNA biogenesis

The transcription and processing of miRNA into its mature form has been thoroughly investigated, but there are still new regulatory pathways and exceptions being discovered every year. miRNA genes are located on each chromosome except for the Y chromosome in *Homo sapiens*, and often come in clusters of independent miRNA genes (98). A large

percentage of miRNA genes are found within already defined transcriptional units (167), located within gene introns or exons (116). For example, miRNA genes can be located within the intronic regions of protein-coding genes (165) or non-coding genes (117). They can also be located in the intergenic regions between canonical protein-coding genes (215).

The biogenesis of miRNAs was originally viewed as a linear pathway that was universal for all microRNAs (see Figure 1). With new research it is now understood that there are many different regulatory elements that control different parts of the process, and that miRNAs can be processed in unique ways (202). miRNA biogenesis always begins in the nucleus with the creation of long primary miRNA (pri-miRNA) transcript, often thousands of base pairs in length. Within this large transcript are multiple smaller hairpin loops containing a hairpin stem of about 33 base pairs that ends in a terminal loop (180). The strand is transcribed either by RNA Polymerase II (18) (116) or RNA Polymerase III (12). RNA polymerase II transcripts are usually capped at their 5' end with 7-methyl guanosine, and joined with a poly-adenosine tail at their 3' end (116). Polymerases choose their miRNAs according to sequence, promoter or the genome context surrounding them, such as when RNA polymerase III transcribes miRNAs surrounded by many Alu repeats (12).

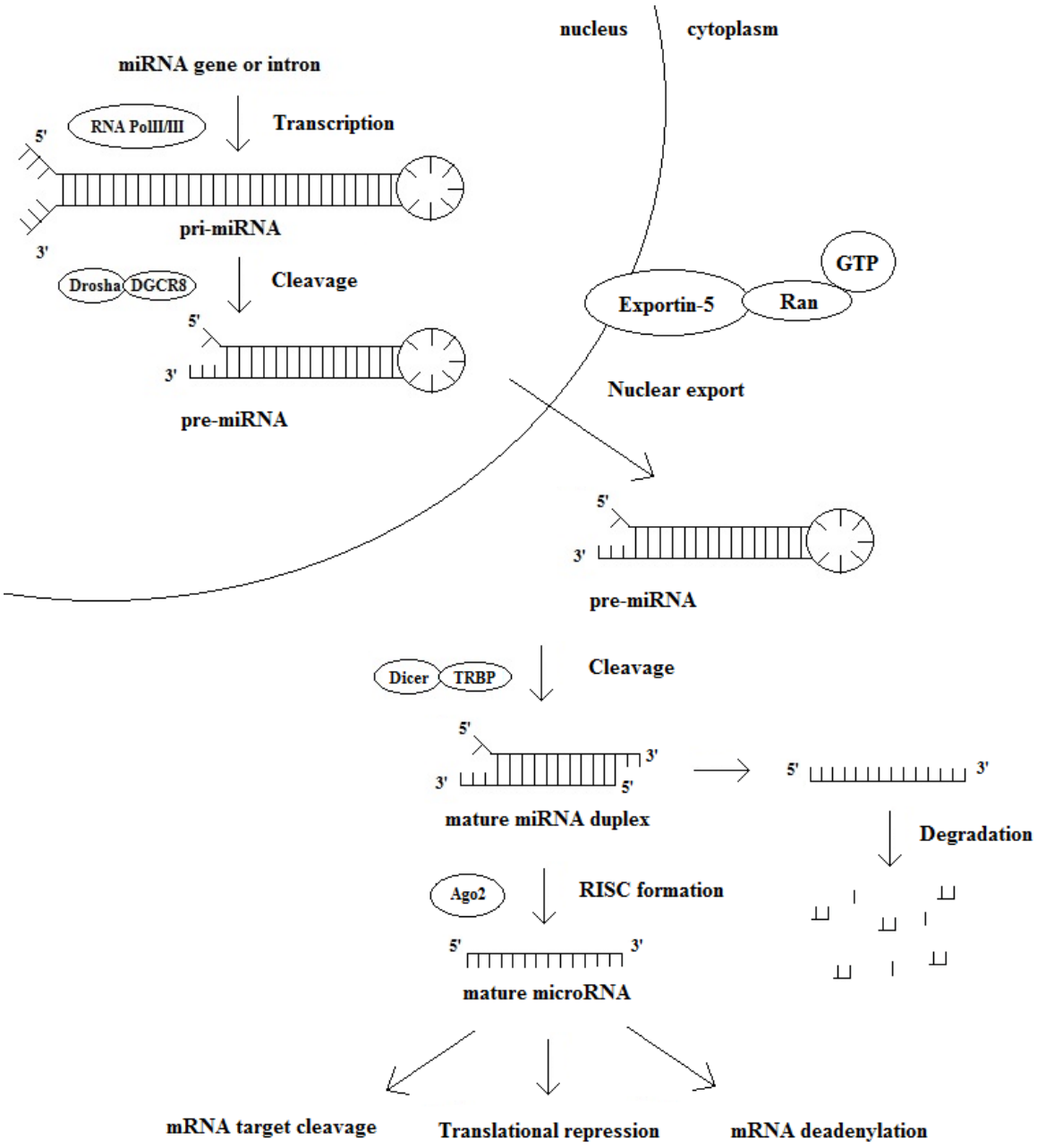
nucleus
cytoplasm
miRNA gene or intron
RNA PolII/III
Transcription
5'
3'
pri-miRNA
Drosha
DGCR8
Cleavage
5'
3'
pre-miRNA
GTP
Exportin-5
Ran
Nuclear export
5'
3'
pre-miRNA
Dicer
TRBP
Cleavage
5'
3'
3'
5'
mature miRNA duplex
5'
3'
Degradation
Ago2
RISC formation
5'
3'
mature microRNA
mRNA target cleavage
Translational repression
mRNA deadenylation

Figure 1: Standard view of the linear progression in miRNA biogenesis.

Figure adapted from Winter *et al.* 2009 (202). The miRNA gene is transcribed by RNA Polymerase II or III (RNA Pol II/III) into its primary-miRNA (pri-miRNA) form. This is then cleaved by the microprocessor complex, composed of the enzyme Drosha and its partner DNA-binding protein DiGeorge critical region 8 (DGCR8), into its precursor miRNA (pre-miRNA) form. This molecule is then exported from the nucleus by Exportin-5, where it is then cleaved into its mature miRNA duplex form by the enzyme Dicer and its partner Tar RNA binding protein (TRBP). The mature miRNA guide strand is attached to the Argonaute 2 (Ago2) protein, which joins with other associated proteins to form the RNA-induced silencing complex (RISC). The RISC uses the mature miRNA to guide its effects by specific 3'UTR binding, and this binding is followed by mRNA translational repression and degradation.

After edits, pri-miRNAs are then transformed into precursor miRNA (pre-miRNA) transcripts by the ribonuclease (RNase) III enzyme Drosha (RNASEN) and the DNA-binding protein DiGeorge critical region 8 (DGCR8) (114). These two proteins form what is called the Drosha/DGCR8 microprocessor complex, which is necessary for miRNA processing in all species (65). In this complex, DGCR8 binds to the pri-miRNA transcript like a molecular anchor and makes sure the microprocessor is in the exact location necessary for correct cleavage by Drosha (72). Once the complex is bound, Drosha proceeds to cleave both the 5' and 3' sides of the hairpin stem exactly 11 base pairs above the junction where the stem and single stranded RNA meet. Because of the helical structure of dsRNA, this results in a 2 nucleotide 3' overhang (71). The end result of this cleavage is a 60-70 nucleotide pre-miRNA transcript.

The next step after pre-miRNA creation is their export from the nucleus by the protein exportin-5, which is a member of the karyopherin β family of nuclear export proteins (214). This protein family helps shuttle almost all RNA molecules (with the exception of mRNAs) out of the nucleus through nuclear pores. To successfully export pre-miRNAs, exportin-5 must form a complex with Ran guanosine triphosphate (Ran-GTP), bind to the pre-miRNA transcript and then undergo cytoplasmic hydrolysis of Ran-GTP to Ran guanosine diphosphate (Ran-GDP) to induce cargo (eg. miRNA) release (131). This binding is highly specific to pre-miRNAs as exportin-5 recognizes the entire hairpin stem and 3' overhang, with any errors such as loss of 3' overhang or existence of a 5' overhang being significantly inhibitory to binding (217). Loss of exportin-5 by siRNA transfection causes a drop of 40-60% of mature miRNAs in the cytoplasm, indicating the possibility of alternate

routes for pre-miRNA export (131), or alternatively that that low levels of exportin-5 may be sufficient to maintain some level of pre-miRNA export.

Once the pre-miRNAs have been shuttled into the cytoplasm they are then processed into their final mature form by the RISC loading complex (RLC), which consists of four central proteins. There are two double-stranded transactivation-responsive RNA-binding proteins known as PACT (protein activator of PKR) (115) and TRBP (Tar RNA binding protein) (69), along with the core Argonaute-2 (Ago2) protein and the RNase III endonuclease Dicer protein (63), which transforms the pre-miRNA into its final form. The initial loading of pre-miRNA into the RLC is accomplished in two steps, physical association and activation. The second step is rate-limiting and governed by the thermodynamic stability of the pre-miRNA (67). Once loaded the pre-miRNA is ready for processing by Dicer. Dicer cuts off the hairpin loop at the end of the molecule and creates an approximately 22 nucleotide duplex with 2 nucleotide 3' overhangs on either end (108). This is the new mature miRNA duplex. Dicer is crucial to the miRNA biogenesis pathway, as without it mature miRNA levels are significantly down-regulated (83) and lack of Dicer leads to early embryonic lethality in mice (11). However, Dicer-independent pathways have been found that use the Ago proteins catalytic core to cleave the pre-miRNA, such as in the case of miR-451 (26).

Once cleaved, all the proteins disassociate from the RLC except for Ago2, which stays bound to the miRNA duplex (120). Recent crystal structures of Ago2 bound to miR-21 have shown that the binding of the mature miRNA to the Ago2 enzyme is remarkably stable and helps the complex exist for long periods of time (47). The miRNA duplex, bound to Ago2, is unwound by a variety of helicases so that the functional miRNA guide strand,

which will attach to the mRNA, is separated from the non-functional passenger strand, which will be degraded. The guide strand is determined by whatever strand has the lower thermodynamic stability at the 5' terminus (97). The initiator of duplex unwinding is the N-domain of the Ago2 protein (104). Helicases involved with this process include RNA helicase A (RHA) (166) and p68 (171). It is possible that the various helicases involved in miRNA unwinding represents another level of differential regulation specific to the certain miRNA families. Once the mature, cleaved guide strand is attached to the Ago2 protein it is now ready to bind to its targets (64).

1.3.3 Mechanisms of gene regulation by miRNA

miRNAs are non-coding RNA transcripts whose purpose is to bind to specific sequences in mRNA and DNA promoters. They are part of the miRNA-induced silencing complex (miRISC) and are only involved in the targeting aspect of miRNA down-regulation. The canonical function of the mature miRISC complex is to bind the 3'UTR region of a target mRNA using a 5-7-nt seed sequence within the mature miRNA strand (110). Once bound it can inhibit translation or degrade the mRNA molecule. The end results of miRISC binding to its target mRNA are accomplished by its main protein components, the Argonaute proteins (AGO1 through 4) (43) and Argonaute-bound GW182 (158), along with other proteins. Once the RLC disassembles the miRNA duplex, the new miRNA guide strand is attached to an Ago protein, which is then joined by the GW182 protein (51). In humans Ago2 is essential for the silencing effect of the miRISC complex (175). Ago2 was the first of the family known to associate with siRNAs such as miRNAs (70) and it controls the catalytic cleavage activity of the complex in mammalian cells (120). GW182 proteins are the

other main class of miRISC proteins. They are associated with processing bodies (P-bodies) inside the cytoplasm and were first shown in 2005 to be involved in miRNA silencing (121). Since then they have proven crucial for miRISC silencing effects, as inhibition of the Ago-GW182 interaction caused significant repression of miRISC silencing (212). GW182 is also known to associate with other proteins that can act as modules that alter miRISC effects, such as the E3 ubiquitin ligase identified by differential display (EDD) protein (184) and poly(A)-binding protein (PABP) (56).

The two main mechanisms of miRISC silencing are translational repression and mRNA degradation (see Figure 2). Recent studies *in vivo* using fruitfly and zebrafish models indicate that this is usually a two step process, with repression of the mRNA occurring first followed by degradation (41) (7).

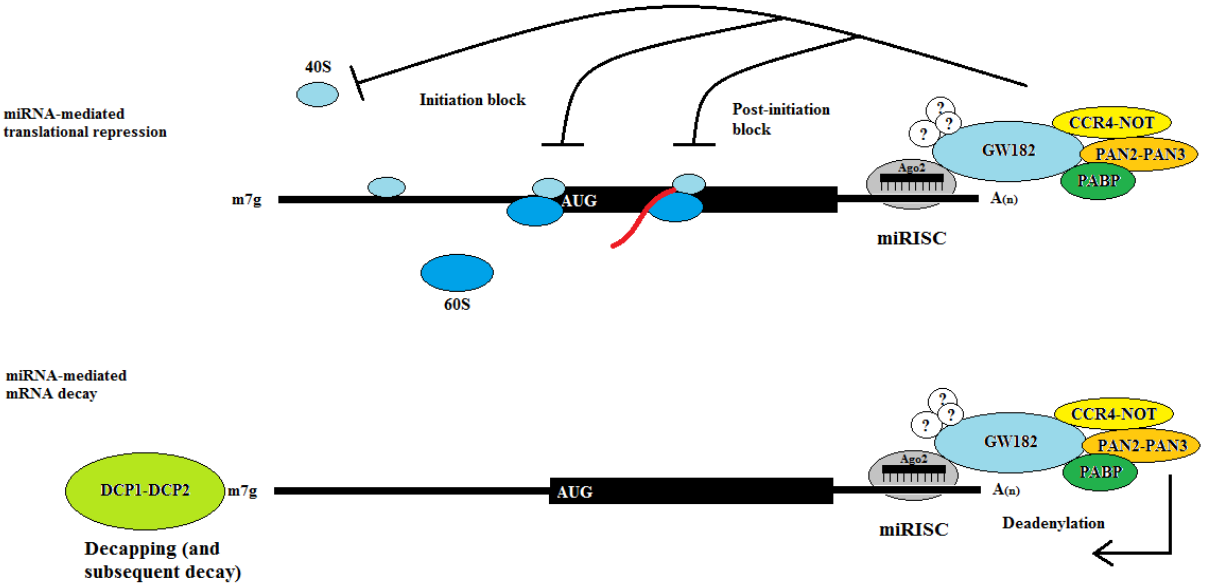
miRNA-mediated
translational repression
40S
Initiation block
Post-initiation
block
m7g
AUG
60S
Ago2
GW182
CCR4-NOT
PAN2-PAN3
PABP
A(n)
miRISC
miRNA-mediated
mRNA decay
DCP1-DCP2
m7g
AUG
Ago2
GW182
CCR4-NOT
PAN2-PAN3
PABP
A(n)
miRISC
Deadenylation
Decapping (and
subsequent decay)

Figure 2: Standard view of miRISC-related translational repression and mRNA degradation by deadenylation and decapping.

Figure adapted from Fabian *et al.* 2012 (51). The miRNA-associated RNA-induced silencing complex (miRISC) down-regulates mRNA activity by both translational repression and mRNA decay mechanisms. The miRISC is composed of the Argonaute 2 (Ago2) protein and GW182 protein, as well as additional proteins such as CCR4-NOT, PAN2-PAN3 and Poly(A) binding protein (PABP). In miRNA-mediated translational repression, the miRISC induces both an initiation block by interfering with 40S and 60S ribosomal subunits, along with a post initiation block on the translational machinery. In miRNA-mediated mRNA decay, the DCP1-DCP2 complex is directed to the decapping of the mRNA. The CCR4-NOT and PAN2-PAN3 complexes are directed to deadenylation of the poly(A) tail. After the mRNA has been stripped it is then degraded by RNA nucleases.

To ensure translational repression the miRISC often interferes with cap-dependent translation in the early initiation steps, such as eukaryotic initiation factor 4E (eIF4E)-cap recognition (80), along with blocking the recruitment and binding of ribosomal subunits such as 60S (193). In mRNA degradation, the CCR4-CAF1-NOT and PAN2-PAN3 deadenylase complexes attach to the miRISC through GW182 and deadenylate the poly(A) tail of the mRNA (15). In addition to loss of its poly(A)-tail, the mRNA also loses its 5'-cap because of DCP1-DCP2 action (158) (8) and is then degraded completely by the Xrn1 5'-3' exonuclease (86). miRNA-mRNA complexes have been proven to specifically localize to nearby P-bodies (122) and most of the actions taken by the miRISC complex happen in the P-bodies as it contains many RISC-related factors such as deadenylase proteins, cap degradation proteins and the Xrn1 5'-3' exonuclease (86). Overall in mammalian cell cultures it appears that miRNA-induced mRNA degradation plays a much larger role than inhibition of translation, but in real organisms the situation could be quite different (68) (81). Once their role is complete the miRNAs themselves are degraded by Xrn1, Xrn2, the exosome or other nucleases, although no studies have proven conclusively that there is one central pathway (86). The entire miRISC silencing process may be modified by a number of additional proteins that may bind to either Ago or GW182, or bind directly on or beside the mRNA binding region. For example, Dead end 1 (Dnd1) protein binds to miRNA binding regions in the mRNA, blocking the miRISC complex from attaching to its target (94).

New findings suggest that there are other modes of miRNA action besides the canonical 3'UTR targeting and subsequent inhibition and degradation of mRNA. miRNAs have been shown to target the 5'UTR and open-reading frame (ORF) regions in mRNA, in addition to the 3'UTR. This regulation acts in a similar mechanistic fashion to 3'UTR

binding, for example when miR-2 binding to either the 5'UTR or ORF causes mRNA deadenylation and cap degradation (141). However, compared with 3'UTR binding the overall effect on mRNA and protein levels is significantly weaker, which helps explain why the normal 3'UTR sites are favoured by miRNAs in nature. Another non-canonical miRNA activity is their binding to genes directly, often on their promoters. The first study to discover this effect found a miR-373 target site directly inside the promoter regions of both E-cadherin and cold-shock domain-containing protein 2 (CSDC2) genes (152). Elevated miR-373 levels induced expression of both proteins, which was driven by mature miR-373 binding to the promoters of both genes. To bind to DNA, it is necessary for miRNAs to return to the nucleus where they were created. miRISC complexes are able to travel back into the nucleus using proteins such as Importin-8 (199).

Overall, miRNAs attached to the RISC complex can accomplish multiple effects inside the cell. Even when miRISCs are set on one course of action, such as translational repression, they can be modified by additional factors to regulate their function. In the future there will likely be new discoveries of more RISC-binding proteins and even entirely new modes of action for miRNAs and the miRISC complex.

1.4 Role of miRNAs in disease

1.4.1 miRNAs in disease

Since their discovery two decades ago it has been shown that miRNAs regulate many biological processes within cells as a result of their ability to target hundreds of different mRNAs. These include crucial processes such as development (100), the cell cycle (22), and apoptosis (87). Thus in many diseases the alteration of miRNA's normal expression patterns

or their ability to target certain mRNAs can contribute to disease development and progression.

Altered miRNA levels because of gene mutation or dysfunctional biogenesis are found in diseases such as heart disease (206), diabetes (127) and cancer (192). Expression levels can be altered by affecting the miRNA gene itself, such as modifying the methylation status of its promoter to knock-down gene expression (73). miRNA levels can also be altered by interference in their normal biogenesis pathway, such as when exportin-5, the crucial pre-miRNA transporter, is down-regulated in cancer cells. Loss of exportin-5 leads to the down-regulation of the many miRNAs that use this transporter (137). Cancer is an informative example of the effect of altered miRNA expression patterns because of the high levels of mutations and chromosomal damage that tumour cells undergo. Certain cancers benefit from shutting off expression of tumour suppressor miRNAs that help control cell proliferation, apoptosis and DNA repair (144). Alternatively, cancers can also benefit from over-expression of certain miRNAs because they are oncogenes that contribute to tumourigenic phenotypes such as uncontrolled cell growth and apoptosis evasion (173).

miRNAs may also affect disease when crucial mRNAs escape their normal regulation through mutation or modification of their structure that stops proper miRNA binding from occurring (61). One example is alteration of a target mRNA's 3'UTR, either by a change in miRNA seed site or certain physical changes. As previously discussed in section 1.22, the 3'UTR is the central site for effective miRISC silencing. If something impedes a miRNA's ability to bind to the 3'UTR, such as loss of a miRNA's normal seed site, then it can reduce regulation of the mRNA. Alternatively, a mutation in the 3'UTR can cause the creation of new miRNA seed sites that lead to aberrant miRISC silencing. One example of

3’UTR alteration is in coronary heart disease (CHD). The single nucleotide polymorphism (SNP) rs4846049 in the protein 5,10-methylenetetrahydrofolate reductase (MTHFR) caused hsa-miR-149 to bind to the mutated MTHFR 3’UTR when it normally does not (206). This caused a decrease in MTHFR protein levels and an increased risk of CHD in a Chinese Han population that contained this SNP. In addition to changing the seed site, other examples of 3’UTR change include the loss of 3’UTR length or structure, such as shortening of the region. The first study to discover this shortening effect found that loss of 3’UTR length corresponded with higher cell proliferation levels, and also that a smaller 3’UTR meant more protein synthesis, possibly because of decreased miRNA binding sites and thus less regulation (172). Overall these are just a few of the most prominent ways that dysregulation of miRNA expression and targets is involved in many disease states.

1.4.2 miRNAs in cancer

Every major type of cancer has been shown to have some degree of miRNA dysregulation, which can affect crucial cell processes such as growth receptor pathway signaling or apoptosis. In 2002 the first study demonstrating that miRNAs could be involved in cancer found that a small region of chromosome 13q14, which contained the miR15/16 genes, was deleted in over 65% of chronic lymphocytic leukemias (CLL) (20). Intriguingly this exact region was also lost in other cancers such as prostate (42), indicating that miR-15/16 deletion could play a role in multiple tumour types. In 2004 the same group then investigated all 186 human miRNAs known at the time and how their genetic locations matched with fragile sites related to human cancer. They found that many of the miRNAs corresponded with regularly deleted or mutated genomic areas in cancers such as lung, breast and colon (21). In 2003 one

of the first published studies to look for a direct link between miRNAs and cancer investigated the expression levels of miRNAs in colorectal cancer. It was discovered that miR-143 and miR-145 levels were down-regulated in neoplastic colorectal tissue as compared with normal tissue (138). One of the first papers on miRNA regulation of a specific target associated with tumourigenesis showed that miR-15/16 repressed the apoptosis-related oncogene BCL2 in CLL (28), which helped explain why miR-15/16 are consistently deleted in that disease. This was one of the first examples of miRNAs acting to suppress tumour characteristics.

In 2005 one of the first miRNA oncogenes was found in the study of miR-155 expression in human B cell lymphomas. Significantly high copy numbers of miR-155 were found in this cancer compared with normal circulating B cells (46), and later miR-155 was shown to increase lymphoma motility by down-regulation of certain targets (35). The first paper to examine global expression of every miRNA across all cancers was published by Lu *et al.* in 2005 (128). They found that almost every miRNA known at the time was differentially expressed in tumours versus normal tissue. They also determined that miRNA expression patterns could provide a useful tool for classifying tumours and that the global levels of miRNAs are down-regulated in cancer. In 2006 Volinia *et al.* undertook the first in depth analysis of miRNA expression in six solid tumour types: lung, breast, stomach, prostate, colon and pancreatic. They found 26 over-expressed and 17 under-expressed miRNAs in these tumour types and observed that the spectrum of expressed miRNAs was very different in solid tumours compared with normal tissue (192). They also examined the levels of predicted gene targets such as Retinoblastoma (RB) and Tumour-growth factor-B II receptor (TGFBRII) and found that they were affected by miRNA expression. After these

studies were published the cancer miRNA field grew larger as researchers investigated the function of miRNAs that had already been shown to play a part in cancer, discovered entirely new cancer-related miRNAs and examined cancer-specific miRNA expression levels more closely. miRNAs have since been found to play important roles in all cancer types and areas of tumourigenesis. For example, important growth factor pathway proteins such as EGFR and Ras are affected by miRs such as miR-542-5p (210) and let-7a (143), respectively. Cell cycle regulation is affected by dysregulation of miR-449 in gastric cancer (13). Apoptotic pathways can be subverted by the aforementioned miR-15/16 deletion and the subsequent rise in anti-apoptotic Bcl2 protein (28). Reduction of miR-1 and miR-200 leads to increased EMT in prostate cancer (123), and loss of miR-101 in glioblastoma leads to increased angiogenesis (181). One of the main challenges facing researchers today is how to integrate all the new cancer miRNA findings into a more complete picture of cancer-specific miRNA dysregulation.

There are many ways in which tumourigenesis can affect the expression levels and basic function of miRNAs. As previously described, deletion of a specific chromosomal area (13q14) corresponded to loss of tumour-suppressors miR-15 and miR-16 in CLL (20). Following the reduction of the levels of these miRNAs, the normally down-regulated expression levels of BCL2 were able to rise and protect tumour cells from apoptosis. In addition to deletion, many oncogenic miRNAs are amplified in the cancer genome. For example, gene amplification of miR-26a was discovered in glioblastomas, which led to over-expression of the miRNA and corresponding loss of its target, the tumour-suppressor PTEN (82). In some cases miRNA genes are switched on or off according to cancer-related processes such as aberrant promoter methylation. It was found in the colorectal cancer cell

line HCT-116 that over 10% of the miRNAs were down-regulated by DNA methylation activity against their promoters (73). Another example of mRNA alteration in cancer is the loss of 3'UTR length in specific, often oncogenic mRNAs. This leads to increased stability of mRNAs and up to 10-fold increase in protein levels because of decreased regulation by miRNAs (135).

miRNAs represent exciting new therapeutic options in the treatment of cancer. miRNA profiles in different tumours could lead to new prognostic indicators of a cancer's stage, response to treatment and likelihood of metastasis by examining samples taken from biopsies or surgery. The use of miRNAs as biomarkers in patient serum samples is also advancing as certain miRNA levels are found to be correlated with patient outcomes (33). miRNAs also represent potential therapeutic treatments, with positive attributes such as their ability to target many genes and pathways simultaneously and the fact that they are endogenous factors not recognized as foreign agents in human cells, unlike many artificial drugs (59). Limitations include effective targeted delivery of the synthetic miRNA reagents to tumours and potential off-target effects in non-cancer cells. Overall, increasing our understanding of how miRNAs are dysregulated in cancer will help determine how the disease progresses from initiation to metastasis. It will also lead to the identification of important novel therapeutic targets, predictive biomarkers and prognostic indicators that are able to identify important cancer characteristics and patient status.

1.4.3 miRNAs in prostate cancer

miRNAs are involved in the tumourogenesis of prostate cancer and numerous studies have shown that miRNA dysregulation occurs in the majority of prostate tumours

(176) (62) (74). In 2005 the first study to link miRNAs and prostate cancer showed that prostate tumour samples exhibited a different global miRNA expression pattern than normal prostate tissue (128). In 2006 the previously mentioned study by Volinia *et al.* examined the expression levels of miRNAs in 6 solid tumours, including prostate, and found greatly altered patterns in tumour samples versus normal prostate tissue (192). One of the first miRNAs to be specifically investigated in relation to prostate cancer was miR-125b, a functional homologue to lin-4. It was found that miR-125b was elevated in most prostate cancer samples, including both patient and cell line derived, and its down-regulation by specific hairpin inhibitors caused reduced growth (177). Subsequently, miR-125b was found to target Bak1, a Bcl2 family member and a pro-apoptotic regulator, which would explain why its reduced levels would facilitate prostate cancer growth by reducing apoptosis in tumour cells. In 2010 the first comprehensive, prostate cancer specific miRNA study examined the difference in miRNA expression levels between benign peripheral zone tissue and prostate cancer tissue from radical prostatectomies. They found widespread deregulation of most examined miRNAs and altered expression of many novel miRNAs (174). Today, many dysregulated miRNAs have been identified that contribute to the prostate cancer phenotype by affecting crucial growth regulatory targets such as K-Ras (205), AR (178) and cyclin D1 (5). For example, miR-21 is a well-known prostate miRNA that acts as an oncogene. It is over-expressed in numerous cancers such as prostate (161), breast (31), and lung (58), and it has been shown to target tumour suppressor genes such as PTEN in prostate cancer (218). Another example is the tumour-suppressing miR-143, which is down-regulated in many cancers including prostate and has been shown to regulate genes that promote proliferation and migration, such as K-Ras and cyclinD1 (205). Experiments where miR-143

is artificially increased in PC3 prostate cancer cells showed decreased invasion and migration *in vitro* and decreased proliferation and bone metastasis *in vivo* (29).

Overall, the study of prostate cancer miRNAs is an exciting area of research that is still in its infancy. There is still much to be learned in order to fully understand how miRNA dysregulation affects various prostate tumour phenotypes and how best to use this knowledge to detect and treat prostate cancer.

1.5 The role of miR-105 in prostate cancer

1.5.1 miR-105 location and structure

Hsa-miR-105 is one of many poorly understood and undescribed miRNAs that exist. miR-105 was first discovered in 2002 by Mourelatos *et al. (142),* when they examined molecules associated with different ribonucleoprotein complexes (RNPs). miR-105 is located on the X-chromosome (Xq28), inside the Intron 1 region of the gammaaminobutyric acid (GABA) A receptor alpha 3 subunit (GABRA3) gene (106). Hsa-miR-767 also exists in this location (10). This receptor is involved in normal GABA neurotransmitter functioning and is associated with neurological diseases such as bipolar affective disorder (134). The sequence of mature miR-105 is 5'-UCAAAUGCUCAGACUCCUGUGGU-3' and is 23 nucleotides long (see Figure 3). The mature miR-105 strand targets hundreds of possible mRNA 3'UTRs according to the miRwalk miRNA target prediction program (http://www.umm.uni-heidelberg.de/apps/zmf/mirwalk/) (45).

Stem loop of pre-miR-105

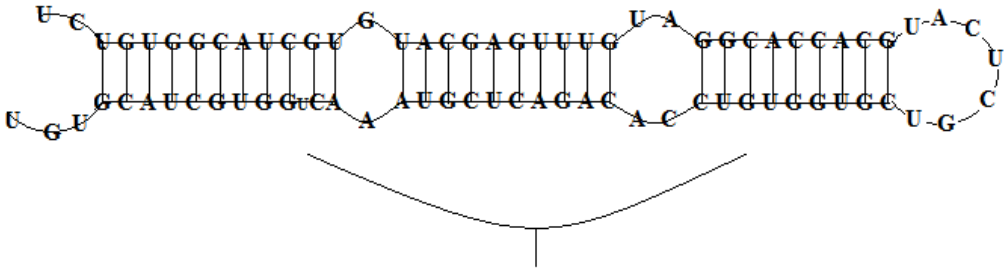

Mature miR-105 UCAAAUGCUCAGACUCCUGUGGU

Figure 3: Pre-miR and mature miR-105 sequences.

Figure adapted from Benakanakere *et al.* 2009 (10). The standard stem loop structure of the pre-miRNA can be seen above the mature miRNA strand, which shows the 23 nucleotide sequence of the mature single-stranded miR-105 guide strand.

1.5.2 Preliminary findings for miR-105

The only paper published to date which has directly studied miR-105 examined its role in Toll-like Receptor 2 (TLR2) regulation (9). The authors found that miR-105 directly targeted the TLR2 mRNA and caused a decrease in its protein levels in human gingival keratinocytes. Their conclusion was that miR-105 is involved in the innate immune response in certain cells. The current literature gives some clues as to miR-105's possible role in cancer. Research by Schmittgen *et al.* found that miR-105 belongs to a group of pre-miRNAs which are prevented from leaving the nucleus in pancreatic, colorectal, cervical and promyelocytic leukemia cancer cell lines after it is processed by Drosha/DGCR8 into its pre-miRNA form (109). More recently, a large meta-analysis of miRNA expression datasets indicated that down-regulation of miR-105 was common in hepatocellular carcinomas (195). A paper by Mlyncek *et al*. found that miR-105 may influence proliferation of primary ovarian granulosa cells as its over-expression was found to alter proliferative marker expression levels, including PCNA and Cyclin B1 (179). PCNA is involved with the S phase of the cell cycle, and cyclin B1 is involved in forcing the cell into mitosis during the G2 phase. Since miR-105 activity caused both an increase in PCNA levels and a decrease in Cyclin B1 levels, its function may be dependent on cell cycle timing. miR-105 was also of interest to us based on previous experiments in our lab looking into the effect of the extracellular matrix on miRNA levels. Given that previous research suggested miR-105 possibly alters cell proliferation and is down-regulated in multiple cancer cell lines, along with preliminary data from our laboratory suggesting it was down-regulated in metastatic prostate tumour cell lines as compared to normal prostate epithelial cells, we embarked on an investigation to determine the role of miR-105 in metastatic prostate cancer cell lines.

1.6 Summary, rationale and hypothesis

Recent research has highlighted the important role of miRNAs in modulating the tumourigenic phenotype, especially that of prostate cancer. Normal miRNA expression is crucial for healthy cell function while aberrant miRNA expression leads to cancer related effects such as uninhibited proliferation, increased invasion and inhibition of apoptosis. Many miRNAs have been shown to play a role in the development and progression of prostate cancer, but miRNAs that play a significant role in mediating the growth and invasion of aggressive prostate tumour cells have not been thoroughly examined. Previously, our lab performed a miRNA microarray to compare miRNA expression levels in normal prostate epithelial cells (PrEC) versus those of two well characterized metastatic prostate tumour lines (PC3 and DU145). Although a number of novel miRNAs showed altered expression levels, we decided to characterize the role of certain differentially expressed miRNAs which had not previously been indicated in prostate tumour progression. Therefore we began to examine the role of hsa-miR-105, one of these miRNAs. RT-qPCR validation showed that miR-105 had decreased expression in prostate tumour cell lines as compared to PrEC. It has also been shown that miR-105 plays a role in cellular proliferation (179) and levels of mature miR-105 are inhibited in other cancer types (109). The fact that it is involved in crucial pathways such as cell proliferation indicated that its loss may lead to dysregulation of these pathways and a subsequent increase in tumourigenic phenotypes such as uninhibited cell proliferation and increased invasion. Thus it is possible that this miRNA may act like other tumour-suppressing miRNAs. The experiments presented herein are designed to test the hypothesis: **MicroRNA-105 inhibits prostate tumour growth.**

1.7 Approach

1.7.1 Objective 1: To validate microarray findings indicating that certain miRNAs are dysregulated in metastatic prostate tumour cells compared with normal prostate epithelial cells.

RNA was collected from PC3 and DU145 cell lines and compared with RNA from PrEC cells by miRNA microarray to yield an original list of putative differentially regulated miRNAs. The miRNAs that showed altered expression patterns were validated by RT-qPCR to confirm their differential expression levels in these cell lines.

1.7.2 Objective 2: To evaluate the effect of differentially regulated miRNAs, specifically miR-105, on prostate cancer growth and invasion in vitro and in vivo.

The efficacy of miR-105 mimic and hairpin constructs to modulate cellular miR-105 levels were tested in PC3 and DU145 cells. The *in vitro* effects of miR-105 over-expression on PC3 and DU145 cell viability, apoptosis, anchorage-independent growth and cell migration and invasion were assessed. The effects of miR-105 over-expression on subcutaneous prostate tumour growth were assessed using xenograft models in mice.

1.7.3 Objective 3: To identify cellular targets of miR-105 that contribute to its effects on tumourigenesis.

miR-105 was over-expressed in PC3 cells using specific mimic constructs and cellular mRNA expression was compared to cells treated with control mimic using a Human Gene microarray. Changes in expression of the putative novel targets identified in the array were validated at the mRNA level by RT-qPCR, and protein level by the western immunoblot assay.

2: MATERIALS AND METHODS

2.1 Cells and Media

PC3 and DU145 human prostate carcinoma and A549 human lung carcinoma cells were obtained from ATCC (Manassas, VA). These cells were grown in Dulbecco's Modified Eagle Medium (DMEM, Mediatech Inc, Manassas, VA) supplemented with 10% HyClone fetal bovine serum (FBS, Fisher Scientific Co., Toronto, ON). PrEC (Normal Prostate Epithelial Cells) were obtained from Lonza (Walkersville, MD), and were grown in PrEGM (Lonza, Walkersville, MD) for expansion. PrEC were only used between passages 4-10. All cells were grown at 37^{o}C in 5% CO_2 in a HERAcell® (Kendro Laboratory Products, Newtown, CT) incubator.

The standard protocol for collecting cells was to wash twice with warm sterile PBS (Dulbecco's Phosphate Buffered Saline, Mediatech Inc., Manassas, VA) and trypsinise the cells for approximately 6 minutes. The cells were collected into 15 mL conical tubes then centrifuged at 1200 RPM for 5 minutes. The cell pellet was re-suspended in the appropriate amount of media then placed in 10 cm (BD Falcon, Franklin Lakes, NJ), 6 cm or 6 well / 24 well tissue culture plates (Corning Incorporated, Corning NY). Cell counting was performed in triplicate using a Bright-Line hemacytometer (Hausser Scientific, Horsham, PA). Cells were seeded in numbers corresponding to basic passaging needs or specific experimental designs. µL

2.2 Transfections

Cells were seeded at ~40-50% density, or approximately $5x10^4$ cells/mL, to achieve optimal distribution on 6 or 10 cm plates. Following adherence overnight, cells were transfected with 2, 10, 50 or 100 nM solutions of miR-105 specific mimics (based on the mature miR-105 sequence: 5'-UCAAAUGCUCAGACUCCUGUGGU-3'), or their respective cel-miR-67 (based on the mature cel-miR-67 sequence: 5'-UCACAACCUCCUAGAAAGAGUAGA-3') mimic controls (all from Dharmacon, Lafayette, CO) using Oligofectamine™ (Invitrogen, Carlsbad, CA) in Opti-MEM® (Invitrogen, Carlsbad, CA). Initially, a solution of 19% Oligofectamine™ and 81% Opti-MEM® was mixed and left at room temperature for 5 minutes. This solution was added to Opti-MEM® containing the appropriate concentration of mimic or hairpin reagents and left to incubate for 15-20 minutes at room temperature. The seeded plates were washed with Opti-MEM®, and a small volume of Opti-MEM® was placed on top of the cells. The reagent mixture was added to the plate, which was then left in the incubator. Four hours later a solution of DMEM + 30% FBS was added to the dish. Transfection efficiencies were monitored by examination of the fluorescence of the tagged control miRNAs and by quantitative reverse transcription polymerase chain reaction (RT-qPCR) for specific miRNAs as described below.

2.3 Microarrays

Genechip® Human Gene 1.0 ST and Genechip® microRNA microarrays (Affymetrix, Santa Clara, CA) were used for microarray analysis of samples. RNA samples in both cases were prepared according to the manufacturer's protocol using the miRNeasy kit (Qiagen, Velencia, CA). Samples for the Genechip® Human Gene 1.0 ST were prepared using the Whole-transcript Sense Target Labeling Assay (Affymetrix, Santa Clara, CA). Samples for the Genechip® microRNA microarrays were prepared with the Flashtag™ Biotin HSR kit (Genisphere, Hatfield, PA). Prepared labelled samples were sent to Stemcore Laboratories (Ottawa, ON) for microarray processing. Data was analyzed using the program FlexArray (McGill University, Montreal, QC). The Affymetrix website (www.affymetrix.com) was used to create target lists for Human Gene microarray data.

2.4 Quantitative Reverse Transcription-Polymerase Chain Reaction (RT-qPCR)

For microRNA RT-qPCR: Samples of total RNA were prepared from either human cancer cells or mouse tumour tissue using the miRNeasy kit (Qiagen, Valencia, CA). Total RNA concentration was assessed using a Nanodrop Spectrophotometer (Thermo Scientific, Wilmington, DE), RNA samples were diluted to 5 ng / µL in RNAse/DNAse free water and RT was performed using the Taqman® microRNA Reverse Transcription Kit (Applied Biosystems, Carlsbad, CA) as per manufacturer's instructions, primed from specific or endogenous control miRNA primers (TaqMan primer sets of 5x and 20x used: hsa-miR-103: Cat. #4427975, RNU24: Cat. # 4427975, hsa-miR-105: Cat. #4427975). For each RT

sample: 13 µL of master mix (MM) was created from 0.300 µL 100mM dNTP, 1.5 µL Reverse Transcriptase, 1.5 µL 10x RT Buffer, 0.19 µL RNAse inhibitor, 2.0 µL of each 5x TaqMan® microRNA Assay (Applied Biosystems, Carlsbad, CA) and the remaining volume with RNAse-free H_2O. The MM was gently mixed, centrifuged and placed on ice. Subsequently, 13 µL of MM was combined with 2 µL of the diluted RNA to make a total of 15 µL reaction volume. These samples were mixed, centrifuged and placed in the PCR machine for amplification.

The miRNA RT program was then used for template amplification (Hold: 16^{o}C for 30 minutes, Hold: 42^{o}C for 30 minutes, Hold: 85^{o}C for 5 minutes, Hold: 4^{o}C indefinitely) on a GeneAmp® PCR System 9700 (Applied Biosystems, Carlsbad, CA). For the qPCR analysis a new master mix (qMM) was created. For this, 9 µL of qMM was created from 5 µL TaqMan® 2x PCR Master Mix (Roche, Branchburg, NJ), 3.5 µL ddH_2O, and 0.5 µL 20x TaqMan® microRNA Assay (Applied Biosystems, Carlsbad, CA). This 9 µL of qMM was then mixed with 1 µL of the RT solution to form 10 µL in each well of a MicroAmp® Fast Optical 96-well Reaction Plate with Barcode (Applied Biosystems, Carlsbad, CA). After the plate was loaded with solution, it was centrifuged at 500 RPM for 5 minutes at 4^{o}C, RT miRNA templates, were then specifically amplified by qPCR using TaqMan primers (see above) in a 7500 Fast Real-Time PCR system (Applied Biosystems, Carlsbad, CA), using the following standard machine amplification conditions: Holding stages: 50^{o}C for 20 seconds, 95^{o}C for 10 minutes, Cycling stage (40 cycles): 95^{o}C for 15 seconds, 60^{o}C for 1 minute. Results were normalized to the levels of miR-103 or RNU24 and fold differences calculated using the integrated Applied Biosciences program.

For mRNA qPCR: For each reaction with RNA, 1 ug total isolated RNA, 1 µL of a 50uM dilution of dN6 random primers and 1 µL of 10mM dNTP mix (both from Invitrogen, Carlsbad, CA) were added to a nuclease-free microcentrifuge tube. Sterile distilled water was added to make the final volume in each tube 12 µL. The mixture was heated to 65^{o}C for 5 minutes then quickly chilled on ice. The contents were collected by brief centrifugation and further reagents were added: 4 µL of 5x First Strand buffer, 2 µL 0.1 M DTT and 1 µL RNaseOUT Recombinant Ribonuclease Inhibitor (all from Invitrogen, Carlsbad, CA). The tubes were gently mixed and incubated at 37^{o}C for 2 minutes. Following this, 1 µL of M-MLV Reverse Transcriptase (Invitrogen, Carlsbad, CA) was added, and the solution was gently mixed and incubated at room temperature for 10 minutes. The tubes were then incubated for 50 minutes at 37^{o}C and the reaction was then inactivated by heating the tubes at 70^{o}C for 15 minutes. For the quantitative PCR mix, each reaction in 10 µL total consisted of: 5.0 µL RT^{2} Fast SYBR® Green/Rox™ qPCR Master Mix (SABiosciences, Frederick, MD), 3.6 µL ddH2O, 1.0 µL from the previously made template cDNA and 0.4 µL of custom gene-specific 10uM PCR primer pair stock (all ordered from Invitrogen, Carlsbad, CA). For quantitative PCR, specific templates were amplified using the following primer pairs:

β-actin, Forward: 5'-GGGCATGGGTCAGAAGGAT-3',

Reverse: 5'-GTGGCCATCTCTTGCTCGA-3'

Cdk6, Forward: 5'-TGATCAACTAGGAAAAATCTTGGAC-3'

Reverse: 5'-GGCAACATCTCTAGGCCAGT-3'

The RT^2 Fast SYBR® Green/Rox™ qPCR Master Mix (SABiosciences, Frederick, MD) was used for amplification in an ABI 7500 FAST Real Time PCR System under the following standard machine conditions: Holding stages: 50°C for 20 seconds, 95°C for 10 minutes, Cycling stage (40 cycles): 95°C for 15 seconds, 60°C for 1 minute, Melt curve stage in continuous mode: 95°C for 15 seconds, 60°C for 1 minute, 95°C for 30 seconds, 60°C for 15 seconds. The results were analyzed using the integrated Applied Biosciences program, and levels of specific targets were normalized to levels of β-actin for all cases.

2.5 MTT Assays

Cells were transfected with miRNA mimics or hairpin inhibitors as described in Section 1.2, and seeded 24 hours post-transfection into 96-well plates at 2500 cells per well. Each condition contained 8 wells for a total of 8 replicates. At 24 hour intervals, 42 µL of 5 mg/mL MTT (3-(4,5-dimethylthiazol-2-yl)-2,5-diphenyltetrazolium bromide) solution (Sigma, St.Louis, MO) was added to wells and incubated for a further 3-4 hours at 37°C, followed by addition of 82 µL of lysis solution composed of 0.01 N HCl in 10% SDS (Fisher Scientific Co., Toronto, ON). The plate was then incubated overnight and read the following morning at 570nm in a Multiskan Ascent plate reader (MTX Lab Systems Inc., Vienna, VA). Absorbance readings were taken of plates which had been incubated for either 24, 48, 72 or 96 hours prior to addition of MTT reagent.

2.6 Apoptosis Assays

Cells were transfected according to section 2.2. Twenty-four hours post-transfection, normal cell media was replaced by serum-free media. After 96 hours, cells were collected for either analysis by flow cytometry (FACS) or western blot. During cell collection the media in each well was collected along with two washes of warm sterile PBS and the trypsinized cell solution to ensure collection of any floating apoptotic cells. The collected cells were pelleted by 5 minutes of centrifugation at 1200 RPM. The pellet was washed twice with cold PBS and pelleted a final time. For FACS, cell pellets of non-adherent cells pooled with trypsinized adherent cells were washed with cold PBS and then permeabolized in 100% ethanol by incubation at -20^{o}C for a minimum of 24h. After incubation cells were again washed in PBS, followed by staining with propidium iodide (PI, Sigma, St.Louis, MO) solution (48 µg/ml propidium iodide, 40 µg/ml RNase A in PBS) followed by a 30 minute incubation at 4^{o}C. Samples were then analysed using a Coulter EPICS XL flow cytometer (Beckman-Coulter, Mississauga, ON) on the FL2 channel. The percentage of apoptotic cells was calculated by examining cells with less then 2N DNA content using FCS Express flow cytometry analysis software (De Novo Software, Los Angeles, CA). The proportion of cells in G1 and G2/M was determined using ModFit LT (Verity Software House, Topsham, ME).

For western blot analysis, total protein lysates from harvested cells (adherent and non-adherent) were generated following lysis in Frack's lysis buffer as described in section 2.11. Western blots were performed as described in Section 2.11, to visualize the cleavage of PARP as an indication of the degree of apoptosis occurring in treated cells.

2.7 Anchorage-independent 3D Growth Assays

Cells were transfected as described in Section 1.2. Sterile ultraPure™ low-melting point agarose (Gibco-BRL, Rockville, MD) solutions (1% and 1.5%) were melted by heating in the microwave and placed overnight in a 37^{o}C water bath. The next day solutions of agar and media were created by combining the two at a 1:1 ratio in a pre-warmed TC bottle. For the base underlay, 1.5% LMP agarose was mixed with 2x αMEM + 20% FBS to create a 0.75% agarose media solution. For the overlay 1.0% agarose was mixed with 2x αMEM + 20% FBS to create a 0.5% agarose media solution. The solutions were stored in a water bath when not in use to prevent solidification. Initially, 400 µL of agarose base underlay was placed in each well of a 24 well tissue culture plate, and the base was allowed to solidify and was then stored in a 37^{o}C incubator until it was needed. Transfected cells were then trypsinized and counted according to Section 2.1. A total of 2.84 x 10^4 cells were placed in the first 15 mL conical tube, in a row of six, and then 5 mL of the 0.5% overlay agarose solution was mixed with the cells in the first tube. Subsequently 2.5ml of the cell-agarose solution was transferred to the next tube containing 2.5 mL of 0.5% agarose solution and mixed to create the next cell dilution. The solutions were then serially diluted down the row of tubes to create the required cell dilutions to plate 2000, 1000, 500, 250, 125 or 62.5 cells per well in 700µL total. This 700 µL was added to the solidified base underlays in triplicate for each dilution. The solutions were then cooled at room temperature for approximately 5-10 minutes until the overlay agarose mixture developed the desired viscous consistency. Plates were then incubated in a 37^{o}C incubator for 2 weeks. At the end of two weeks each well was assessed for number of colonies and their relative size. Plate identity was blinded by a labmate to eliminate bias. Representative photos were taken using an inverted light

microscope (Axiovert S100, Zeiss, Germany) with attached camera (Axiocam, Zeiss, Germany).

2.8 Scratch Wound Assays

Cells were transfected as described in section 2.2. Subsequently, 24 hours post-transfection they were seeded into 6-well tissue culture plates at a density that would ensure cell confluency the next day. The following day the cell monolayers were scratched in a straight line using a sterile wounding tool, and four images per well were acquired with a digital camera (Nikon, Mississauga, ON) for time 0 hours. Additional photos were taken at 24 hours and 48 hours time-points using a 4x objective attached to an Eclipse TE2000-U microscope (Nikon). Wound diameters in images were measured and percentage wound closure was calculated as follows: [(wound diameter at 24 hours - wound diameter at 0 hours) / wound diameter at 0 hours] x 100.

2.9 Invasion Assays

Cells were transfected as described in Section 1.2. The next day, cells were trypsinized and collected according to Section 2.1. Matrigel-coated transwell invasion plates (BD Biocoat Growth-factor reduced Matrigel Invasion Chamber, PET membranes, Mississauga, ON) were thawed and prepared according to the manufacturer's instructions. In a 24 well tissue culture plate the invasion chambers were lowered into a solution of DMEM + 5% FBS, which acted as a chemoattractant. 5.0×10^4 transfected cells were suspended in serum-free DMEM and 500 µL, containing 2.5×10^4 cells, were placed on top of the Matrigel invasion chambers. The cells were left for 24 hours in a 37^oC incubator, which

allowed them to migrate through the Matrigel and 8 um pores towards the chemoattractant solution in the bottom well. After 24 hours the matrigel and all uninvaded cells were removed physically by dry and then moist sterile swabs. Invaded cells on the underside of the invasion filter were visualized following staining with Crystal Violet (0.5% crystal violet solution in 25% methanol). The invasion membranes were placed in the ice-cold Crystal Violet solution, gently washed in sterile water and then left to dry at room temperature in the tissue culture hood for at least 30 minutes. Invaded cells on the dried, stained membranes were then quantified using microscopic quantification at 10x magnification, across the entire membrane. Results are expressed as the mean of 2 wells, counting all the invaded cells per well, across three independent experiments.

2.10 In Vivo Tumour Xenograft Models

Five-week old CD1 nude mice were purchased from Charles River Laboratories (Wilmington, MA) and housed in the Animal Care and Veterinary Services facility at the University of Ottawa. All protocols performed using mouse models were approved by the University of Ottawa Animal Care Committee and conformed to the guidelines set by the *Animals for Research Act* and the Canadian Council on Animal Care's *Guide to the Care and Use of Experimental Animals*, Vol. 1, 2nd edn., 1993) and meet standards of practice in the disciplines of laboratory animal science, laboratory animal veterinary medicine.

For xenograft models, PC3 or DU145 cells were transfected as described in Section 2.2. Twenty-four hours post-transfection, $1x10^6$ cells in 150 µL of sterile PBS were injected subcutaneously into both hind flanks of the mice. Tumour measurements were taken weekly following caliper measurements of visible subcutaneous tumours. Volume was calculated

using the formula [Volume = (width)^2 x (length/2)]. At necropsy, dissected tumours were measured in three dimensions to calculate tumour volume, wet tumour weight was obtained, and tumour, lung, liver and bone tissue samples were obtained and immediately fixed in 10% formalin solution (Sigma, St.Louis, MO) for histological analysis. After two weeks the lung, liver and tumour samples were sent to the Roger-Guindon Hall Pathology department (Ottawa, ON) to undergo hematoxylin and eosin (H&E) staining, along with creation of unstained slides of the tumour samples. After two weeks of formalin fixation the bone samples were treated with 10% EDTA in pH 8.0 PBS. This solution was changed every 4 days over the course of 3 weeks until the bones were sufficiently decalcified. The samples were then sent to the Pathology department for H&E staining. Tumour samples were taken and processed for RNA according to Section 2.4

2.11 Antibodies and Western Immunoblotting

Monoclonal mouse anti-β-actin from Sigma-Aldrich (St. Louis, MO) was used at a 1:10,000 dilution. Monoclonal rabbit anti-Cdk6 (Novus Biologicals, Littleton, CO) was used at a 1:500 dilution. Polyclonal rabbit anti-PARP (Cell Signaling, Danvers, MA) was used at a 1:000 dilution. Horse-radish peroxidase (HRP) conjugated secondary antibodies to mouse or rabbit IgG were obtained from Sigma and used at a 1:7000 dilution.

Total protein from cells was generated following lysis in Frack's lysis buffer (10mM Tris-HCL, pH 7.4, 150mM NaCl, 5mM EDTA, 1% Triton X-100, ddH_2O) on an ice-cold surface. Plates were scraped using rubber policemen and the lysis solution was transferred to a 1.5 mL tube and sonicated at 1.0 power in 4-5 10 second bursts using a Sonicator 3000

(Misonix, Newtown, CT). The homogenized samples were centrifuged for 30 minutes at 4^{o}C. Supernatants were stored at -20^{o}C.

Total protein concentration was assessed using the BioRad Bradford (Hercules, CA) detection system according to the manufacturer's protocol and protein absorbance was measured at 595 nm. For western blot analysis, equal amounts of total protein per sample, normally 50 ug, were separated on a 10% SDS-PAGE gel (per 10 mL resolving gel: 4.0 mL ddH_2O, 3.3 30% Acrylamide/Bis solution, 2.5 mL 1.5M Tris (pH 8.8), 0.1 mL 10% SDS, 0.1 mL 10% ammonium persulfate, 0.004 mL TEMED. Per 5 mL stacking gel: 3.4 mL ddH_2O, 0.83 mL Acrylamide/Bis solution, 0.63 mL 1.5M Tris (pH 8.8), 0.05 mL 10% SDS, 0.05 mL 10% ammonium persulfate, 0.005 mL TEMED). The gels were placed in freshly made 1x Running Buffer (from 10x solution: 29g Tris base, 144 g Glycine, 10 g SDS, fill to 1L ddH_2O) and run at 100V. Proteins were then transferred to Hybond™ -C Extra nitrocellulose membranes (GE Healthcare, Piscataway, NJ) in 1x Transfer buffer (from 1x solution: 3g Tris base (12mM), 58g Glycine (96mM), 200mL methanol, fill to 1L ddH_2O) with 20% methanol. The membranes were examined for successful transfers by staining for transferred protein using a Ponceau S stain (0.1% PonceauS (w/v) in 5% (v/v) acetic acid). For western blot detection, membranes were first washed with Tris-buffered saline with Tween (TBST containing 10nM Tris-HCL pH 8.0, 150mM NaCl, 0.05% Tween-20), and blocked using 5% skim milk powder in TBST (5% milk) or 5% bovine serum albumin (BSA) in TBST (5% BSA) for an hour. The membrane was then placed in a solution of diluted primary antibody in 5% milk or 5% BSA and was left to incubate in antibody with rocking overnight at 4^{o}C. The next day membranes were washed with TBST 3 times for 5 minutes each, and rabbit or mouse horse-radish peroxidase (HRP) conjugated secondary

antibodies were added, followed by incubation at room temperature for 1 hour. Membranes were again washed 5 times for 5 minutes each with TBST, and blots visualized using the Immobilon Western chemiluminescent HRP substrate (Millipore, Billerica, MA) and exposure of HyBlot CL autoradiography sheets (Denville Scientific, Metuchen, NJ). For re-probing of blots, membranes were stripped using Restore PLUS Western Blot stripping buffer (Thermo Scientific, Rockford, IL) and re-probed with additional antibodies.

2.12 Graphical and Statistical Analysis

All data was plotted using GraphPad Prism software (version 3.02, GraphPad Software, San Diego, CA). Statistical differences for single comparison tests were determined using two-tailed unpaired t-test with a 95% confidence interval. For multiple comparisons parametric one-way ANOVA tests with a 95% confidence interval were used along with Tukey's post-test. Tests were performed using the statistical programs within the GraphPad Prism software (version 3.02, GraphPad Software, San Diego, CA). Results with a p-value of less than 0.05 were deemed significant.

3: RESULTS

The status of miRNAs in metastatic prostate cancer has not yet been fully determined. To this end, we performed a microRNA microarray comparing the metastatic prostate cancer cell lines PC3 and DU145 with the normal prostate epithelial cell line PrEC. We discovered many miRNAs that were differentially expressed in metastatic prostate cells. We then proceeded to validate targets of interest using RT-qPCR. One of those validated targets, hsa-miR-105, was investigated further for its effect on processes important for cancer progression. Cell growth was measured with cell viability assays and data was supplemented with the use of apoptosis assays to more closely define the reasons for differences in viability. Soft agarose assays were used to measure differences in anchorage-independent growth, and scratch wound assay and Matrigel invasion assay were used to measure cell migration and invasion, respectively. An *in vivo* xenograft experiment was performed in nude mice to measure the effect of miR-105 over-expression on subcutaneous tumour growth. Finally, potential miR-105 targets were determined by a human gene microarray, and novel targets were validated for differences in mRNA and protein levels by RT-qPCR and western blot, respectively.

3.1 Differences in microRNA expression between normal prostate epithelial cells and prostate cancer cell lines

We were interested in determining whether various miRNAs were differentially expressed in prostate tumour cells as compared to normal prostate epithelial cells. To this end, we isolated miRNA from normal prostate epithelial cells (PrECs) and compared its profile to that isolated from PC3 and DU145 prostate cancer cell lines using Affymetrix chip profiling as described in section 2.3. A number of miRNAs were found to be differentially expressed between the two tumour cell lines as compared to PrEC, including many miRNAs already shown to be associated with prostate cancer (Tables 1 and 2 for PC3 and DU145 cells, respectively). The changes seen in many of these microarray miRNAs corresponded to the changes in expression seen in other cancer studies, such as the down-regulation of miR-205 (57) and miR-200c (102) and the up-regulation of miR-210 (77). As the roles for many of these miRNAs have been previously well described, we were interested in looking at the miRNAs on our list whose roles in cancer have not yet been defined. It should be noted that although this microarray revealed many interesting targets, it was only performed once, and thus could only be regarded as a guide to possible targets of interest. Validation of targets of interest was performed by RT-qPCR on PrEC, PC3 and DU145 RNA samples. Examples of validated targets such as miR-105 and miR-720 are shown in Figure 4 (4A and 4B respectively) and showed changes in expression that mirrored those observed in the microarray. We chose to look at a novel target, miR-105, which was found to be down-regulated in both PC3 and DU145 cells as compared to PrEC cells.

Down-regulated miRs	Fold decrease	Up-regulated miRs	Fold increase
hsa-miR-205	0.000474	hsa-miR-720	118.0248
hsa-miR-200c	0.001128	hsa-miR-1280	84.70152
hsa-miR-27a	0.00301	hsa-miR-1274b	29.38159
hsa-miR-20a	0.003338	hsa-miR-132-star	26.7977
hsa-miR-125a-5p	0.005982	hsa-miR-122	26.42372
hsa-miR-18a	0.006036	hsa-miR-936	17.01789
hsa-miR-455-3p	0.007481	hsa-miR-877	16.47615
hsa-miR-15b	0.013204	hsa-miR-181c-star	14.00186
hsa-miR-155	0.013789	hsa-miR-584	13.25543
hsa-miR-105	0.5890568	hsa-miR-210	12.13903

Down-regulated miRs	Fold decrease	Up-regulated miRs	Fold increase
hsa-miR-205	0.000461612	hsa-miR-886-3p	33.37576
hsa-miR-708	0.01245537	hsa-miR-720	31.3976
hsa-miR-20b	0.01703499	hsa-miR-1274b	28.55562
hsa-miR-455-3p	0.02073617	hsa-miR-25-star	19.78027
hsa-miR-155	0.03973436	hsa-miR-1280	18.35272
hsa-miR-127-3p	0.03973436	hsa-miR-768-3p	13.42583
hsa-miR-203	0.04756468	hsa-miR-513a-5p	12.42781
hsa-miR-1271	0.05093031	hsa-491-5p	12.00252
hsa-miR-27a	0.05169601	hsa-miR-210	10.86714
hsa-miR-105	0.78701	hsa-miR-27b-star	9.595465

Table 1: Differentially expressed miRNAs in PC3 cells versus PrEC cells.

Human miRNAs that showed the greatest increase or decrease in expression in the microRNA microarray comparing PC3 and PrEC cells are shown here. miR-105 is shown at the bottom of the down-regulated miRs table.

Table 2: Differentially expressed miRNAs in DU145 cells versus PrEC cells.

Human miRNAs that showed the greatest increase or decrease in expression in the microRNA microarray comparing DU145 and PrEC cells are shown here. miR-105 is shown at the bottom of the down-regulated miRs table.

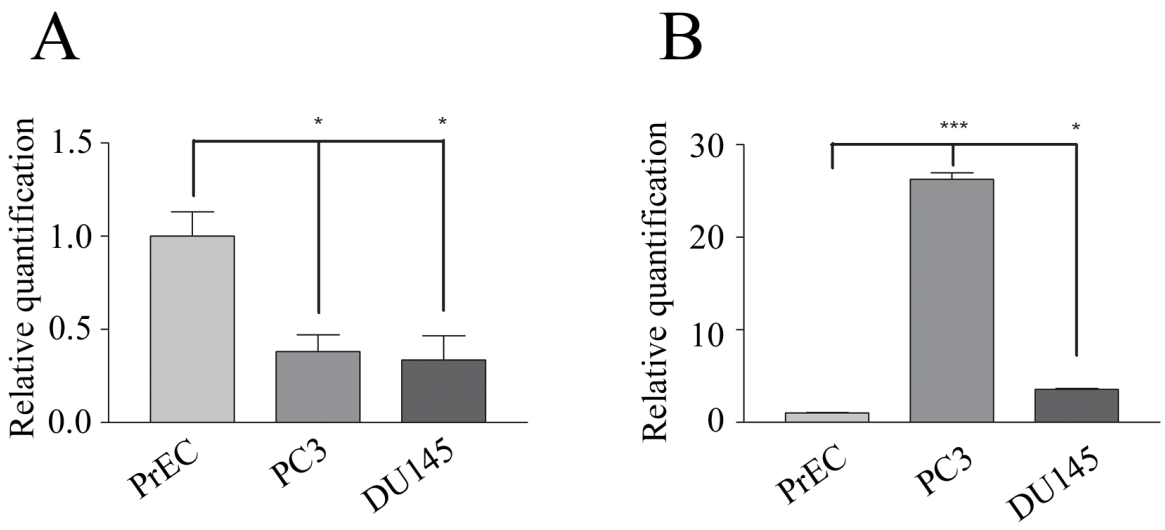
A
B
Relative quantification
1.5
1.0
0.5
0.0
*
*
PrEC
PC3
DU145
Relative quantification
30
20
10
0
***
*
PrEC
PC3
DU145

Figure 4: miR-105 levels are reduced and miR-720 levels are increased in prostate tumour cells compared to normal prostate epithelial cells.

Levels of miR-105 (A) and miR-720 (B) were quantified in PrEC, PC3 and DU145 cells using TaqMan RT-qPCR. Relative levels of miR-105 and miR-720 were normalized to endogenous levels of RNU24 and miR-103 as a control then expressed as relative levels compared to PrEC. Levels were quantified in 8 replicates for each cell line and the graph represents the pooled mean and standard error of 8 replicates from two independent experiments. The relative levels of miR-105 were significantly decreased ($p<0.05$) in PC3 and DU145 cells compared to PrEC. The relative levels of miR-720 were significantly increased in PC3 ($p<0.001$) and DU145 ($p<0.05$) cells compared to PrEC.

As miR-105 was also found to be a miRNA that was regulated in cells following integrin signalling which was another avenue of investigation of great interest to us, we chose to focus on its role in prostate cancer as opposed to some of the identified miRNAs that may have been more highly downregulated in tumour cells for this reason. Endogenous levels of RNU24 and miR-103 were used as normalization controls as both have been shown to be very stably expressed in tumour and normal cells (23) (149). Specifically, the expression level of miR-105 was found to be reduced by 62% and 67% in PC3 and DU145 cells, respectively, as compared to PrEC cells (Fig.4A). Given that miR-105 is reduced in both metastatic prostate tumour cell lines compared to normal prostate epithelium, we hypothesized that miR-105 expression may inhibit prostate tumour cell growth or invasion.

3.2 Characterization of efficacy of miRIDIAN miRNA mimics

As we wished to study the effects of modulation of miR-105 expression on various aspects of tumourigenesis, we evaluated the utility of using miRIDIAN miRNA mimics (Dharmacon) for this purpose. Hsa-miR-105 and cel-miR-67 were used as the specific and control mimic miRNAs, respectively. miRNAs were transfected into PC3 or DU145 cells using Oligofectamine as described in section 2.2. To determine the most effective mimic concentration for use in miR-105 over-expression, we initially transfected different concentrations (2nM, 10nM, 50nM, and 100nM) of mimics and compared the level of miR-105 expression in the transfected cells using RT-qPCR (Fig.5A). We found that 50nM of mimic was sufficient to significantly over-express miR-105. miR-105 over-expression at this concentration in transfected PC3 cells was significantly higher than normal miR-105 levels seen in non-transfected PrEC cells.

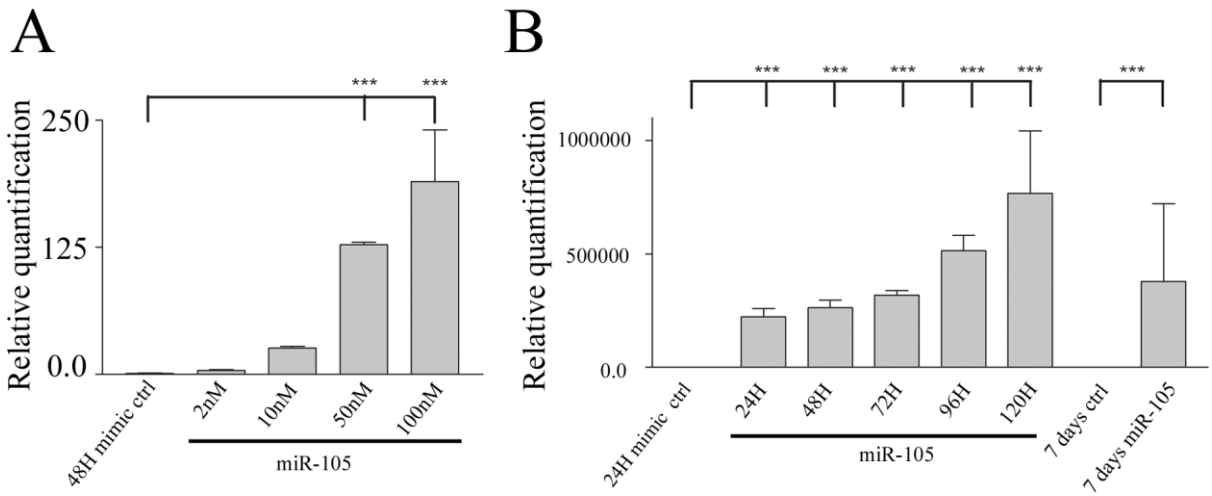
A
Relative quantification
250
125
0.0
***
***
48H mimic ctrl
2nM
10nM
50nM
100nM
miR-105
B
Relative quantification
1000000
500000
0.0
***
***
***
***
***
***
24H mimic ctrl
24H
48H
72H
96H
120H
miR-105
7 days ctrl
7 days miR-105

Figure 5: Evaluation of efficacy of miRIDIAN mimics for modulation of miR-105 levels.

(A) PC3 cells were treated with increasing concentrations (2, 10, 50, 100 nM) of miR-105 specific or 100nM control (cel-miR-67) mimics (Dharmacon). After 48 hours samples were evaluated for relative levels of miR-105 using TaqMan RT-qPCR. miR-105 levels specifically increased in a dose-dependent fashion in miR-105 compared to control mimic transfected cells. The graph represents the mean and standard error of 8 replicates from one experiment. Statistical analysis showed that the 50 nM and 100 nM transfections showed significantly greater miR-105 levels than the mimic control ($p<0.001$). (B) PC3 cells were treated with 50nM of miR-105 or control cel-miR-67 mimics, and relative levels of expression of miR-105 were assessed over time using TaqMan RT-qPCR. miR-105 expression increased over time, and peaked at 120 hours post-transfection before declining, while miR-105 levels in control transfected cells showed no change between 24 h and 7 days post transfection. In all cases levels were normalized to endogenous levels of RNU24 as an internal control. The graph represents the mean and standard error of 3 replicates from one experiment. Statistical analysis showed that all time points showed significantly greater miR-105 levels compared to mimic control ($p<0.001$).

We next tested the duration of over-expression of miR-105 following transfection of specific mimic at the 50nM concentration, and quantified miR-105 levels over 7 days post-transfection (Fig.5B). We found that the levels of miR-105 expression peaked at 120 hours (5 days) post-transfection of mimic, and began to decline at 7 days. Control miRNA-treated cells showed no change in expression of miR-105 levels over the course of the week. In all cases, miR-105 levels were normalized to the levels of RNU24 as the endogenous control.

3.3 Over-expression of miR-105 suppresses tumour cell growth in vitro.

In order to evaluate the effects of miR-105 over-expression on tumourigenic properties, we transfected prostate cancer cell lines with hsa-miR-105 specific or cel-miR-67 control mimics at 50nM as described in section 2.2. Cells were used in the various assays described below at 24 hours post-transfection when sufficient levels of miR-105 over-expression were detectable (Fig. 5B). We initially examined the effect of miR-105 over-expression on tumour cell growth and viability in PC3 (Fig. 6A) and DU145 (Fig. 6B) cells using the MTT assay system in 96-well plates as described in section 2.5. Cell viability was assessed over time, and at 96 hours post-seeding (120 hours post-transfection) we found that elevated miR-105 levels significantly reduced the relative viable cell number by 55% and 18% for PC3 and DU145 respectively, as compared to cel-miR-67 control over-expressing cells. We also found that cell viability in A549 lung carcinoma cells was decreased by miR-105 over-expression (Fig. 7A). Thus miR-105 over-expression inhibited prostate cancer cell viability *in vitro*, but as MTT is a measure of viable cell number, the results could be attributed to miR-105 affecting either cell proliferation or apoptosis.

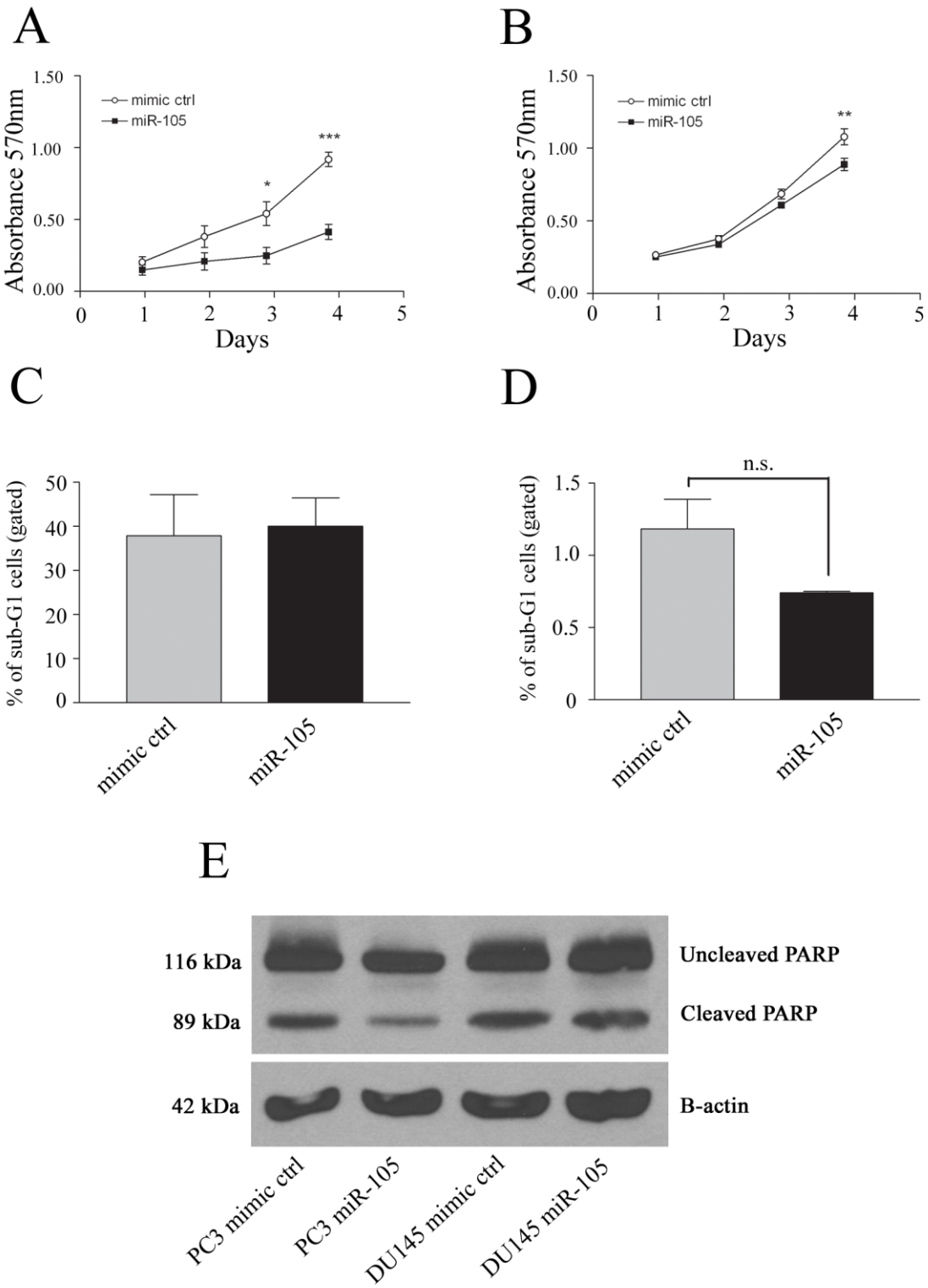
A
Absorbance 570nm
mimic ctrl
miR-105
*
***
Days
B
Absorbance 570nm
mimic ctrl
miR-105
**
Days
C
% of sub-G1 cells (gated)
mimic ctrl
miR-105
D
% of sub-G1 cells (gated)
n.s.
mimic ctrl
miR-105
E
116 kDa
89 kDa
42 kDa
Uncleaved PARP
Cleaved PARP
B-actin
PC3 mimic ctrl
PC3 miR-105
DU145 mimic ctrl
DU145 miR-105

Figure 6: Over-expression of miR-105 inhibits tumour cell growth but does not induce apoptosis.

(A-B) Tumour cells were transfected with either 50 nM miR-105 or control mimic and subsequently seeded into 96-well plates in replicates of 8. Cell viability was assessed over time using the MTT assay as described in section 2.5. Graphs represent the pooled mean and standard error of 8 replicates from three independent experiments. Both miR-105 over-expressing PC3 (A) and DU145 (B) cells showed a significant decrease in cell number/viability at 96 hours ($p<0.001$ and $p<0.01$ respectively) as compared to control mimic transfected cells. (C-E) To analyze apoptosis, cells were transfected with 50 nM of miR-105 or control mimic as described in section 2.2 and then serum-starved over 96 hours. The percentage of all sub-G1 cells representing the apoptotic portion was assessed by FACS as described in section 2.6. Bars represent the pooled mean and standard error of duplicate dishes from two independent experiments. There was no significant difference in the number of apoptotic cells between the miR-105 and control mimic-treated populations for either the PC3 (C) or DU145 (D) cells. (E) Serum starved cells as described above, were also analyzed for PARP cleavage by specific western blot analysis. A small decrease in both uncleaved and cleaved PARP was observed in PC3 cells, but this change was likely due to loading issues. No differences in the levels of PARP were observed in DU145 cells. β-actin was used as a loading control for equivalent amounts of total protein.

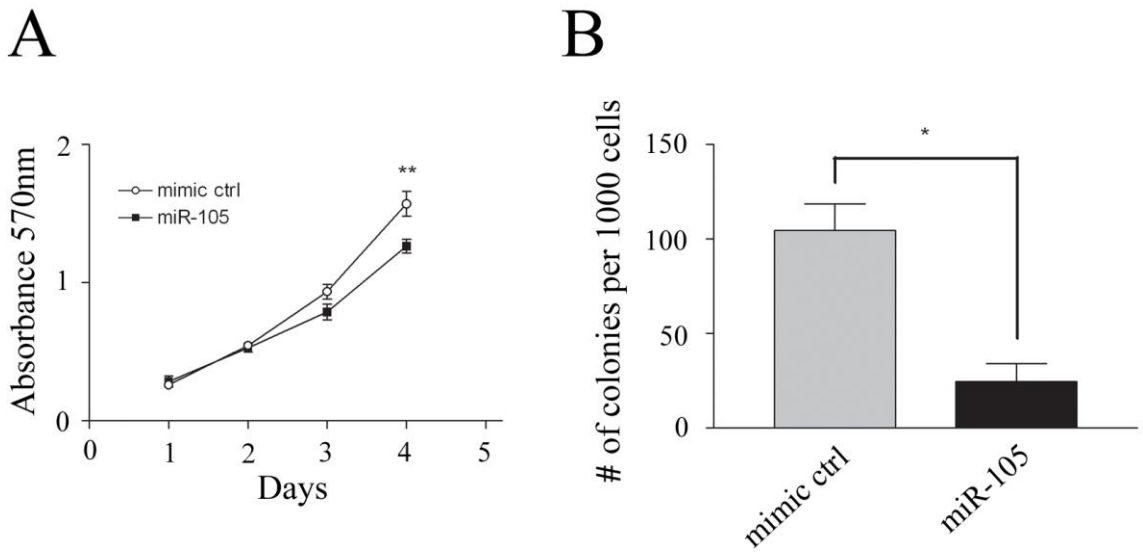
A
B
Absorbance 570nm
Days
mimic ctrl
miR-105
**
*
# of colonies per 1000 cells
mimic ctrl
miR-105

Figure 7: Effects of elevated miR-105 levels on A549 cell viability and anchorage-independent growth.

(A) A549 lung carcinoma cells were transfected with either 50 nM miR-105 or control mimic and subsequently seeded into 96-well plates in replicates of 8. Cell viability was assessed over time using the MTT assay as described in section 2.5. Graph represents the pooled mean and standard error of 8 replicates from three independent experiments. miR-105 over-expressing A549 cells showed a significant decrease in cell number/viability over time ($p<0.01$) as compared to control mimic transfected cells. (B) A549 cells were transfected with either 50 nM miR-105 or control mimic and 24 hours post-transfection were seeded in a soft-agarose. The number of colonies were then counted in the wells generated from the 1000 cell dilution in triplicate wells. Bars represent the pooled mean and standard error for triplicate wells from two independent experiments. miR-105 over-expressing A549 cells showed a significant decrease in colony number ($p<0.05$) as compared to control mimic transfected cells.

To test whether miR-105 has an effect on either of these processes, we further examined the effect of miR-105 on apoptosis in the prostate cancer cell lines.

3.4 miR-105 over-expression does not cause increased apoptosis in vitro.

As cell number/viability was assessed by MTT assay, the reduction observed following miR-105 over-expression could be due to either increased levels of apoptosis or decreased cell proliferation. To determine whether miR-105 over-expression induced tumour cell apoptosis, we evaluated apoptosis of PC3 and DU145 cells using two standard methods: propidium iodide (PI) flow cytometry and detection of PARP protein cleavage by western blot analysis. The PI flow cytometry method allowed quantification of the percentage of cells in the subG1 population in treated cell samples, which represented the total proportion of apoptotic cells (Fig.6C and 6D for PC3 and DU145 cells respectively). Apoptosis was also assessed by evaluating the level of PARP cleavage in treated cells by western blot (Fig. 6E). In this assay, increased levels of cleaved PARP (lower band) compared to uncleaved PARP (upper band) represents an increase in apoptosis. In PC3 cells we observed no increase in the apoptosis of miR-105 over-expressing cells when measured by PI flow cytometry (Fig. 6C). Similarly, there was no increase in the relative proportion of cleaved to un-cleaved PARP in miR-105 compared to control mimic transfected cells, although there was a drop in overall protein levels which could be attributed to loading issues. With DU145 cells, although we observed reduced numbers of apoptotic cells by PI flow cytometry, this decrease was not statistically significant (Fig. 6D). These findings were supported by the analysis of PARP cleavage, where the levels of cleaved PARP were similar between miR-105 over-expressing cells and control cells (Fig. 6E). Under non serum-starvation

conditions, with cells collected at 48 hours past transfection, we observed a 5-10% increase in the percentage of miR-105 over-expressing PC3 cells in the G1 phase versus the control transfected PC3 cells. This indicated that miR-105 was affecting cell cycle mechanisms, such as G1 checkpoint activity. Overall, as we did not observe significant increases in apoptosis in either PC3 or DU145 miR-105 over-expressing cells, this suggests that the reduced viable cell numbers observed in the MTT assays were likely a result of inhibition of tumour cell proliferation, not induction of apoptosis.

3.5 miR-105 over-expression suppresses anchorage-independent growth in vitro.

We tested the effect of miR-105 over-expression on the ability of prostate tumour cell lines to grow under anchorage-independent 3D conditions using soft-agarose assays as described in section 2.7. Anchorage-independent growth is an important measure of cell tumourigenicity (93). Normal non-cancerous cells are unable to grow in the isolated agarose environment, while cancer cells are able to proliferate and form colonies. Cell types with higher tumourigenicity are able to form colonies more readily and at increased frequency. After a two week incubation period, the number of colonies was counted in each well at appropriate dilutions. The ability of miR-105 over-expressing PC3 (Fig. 8A) or DU145 (Fig. 8B) cells to form colonies in 3D was reduced by 36% and 43% respectively, as compared to the control-treated cells. A549 lung carcinoma cells also showed a reduction in colony-forming ability (Fig. 7B). Representative photos were taken of the PC3 and DU145 colonies (Fig. 8C and D) There was no qualitative change in colony size or shape between miR-105 and control-treated cells at the end of the 2 weeks in any cell line.

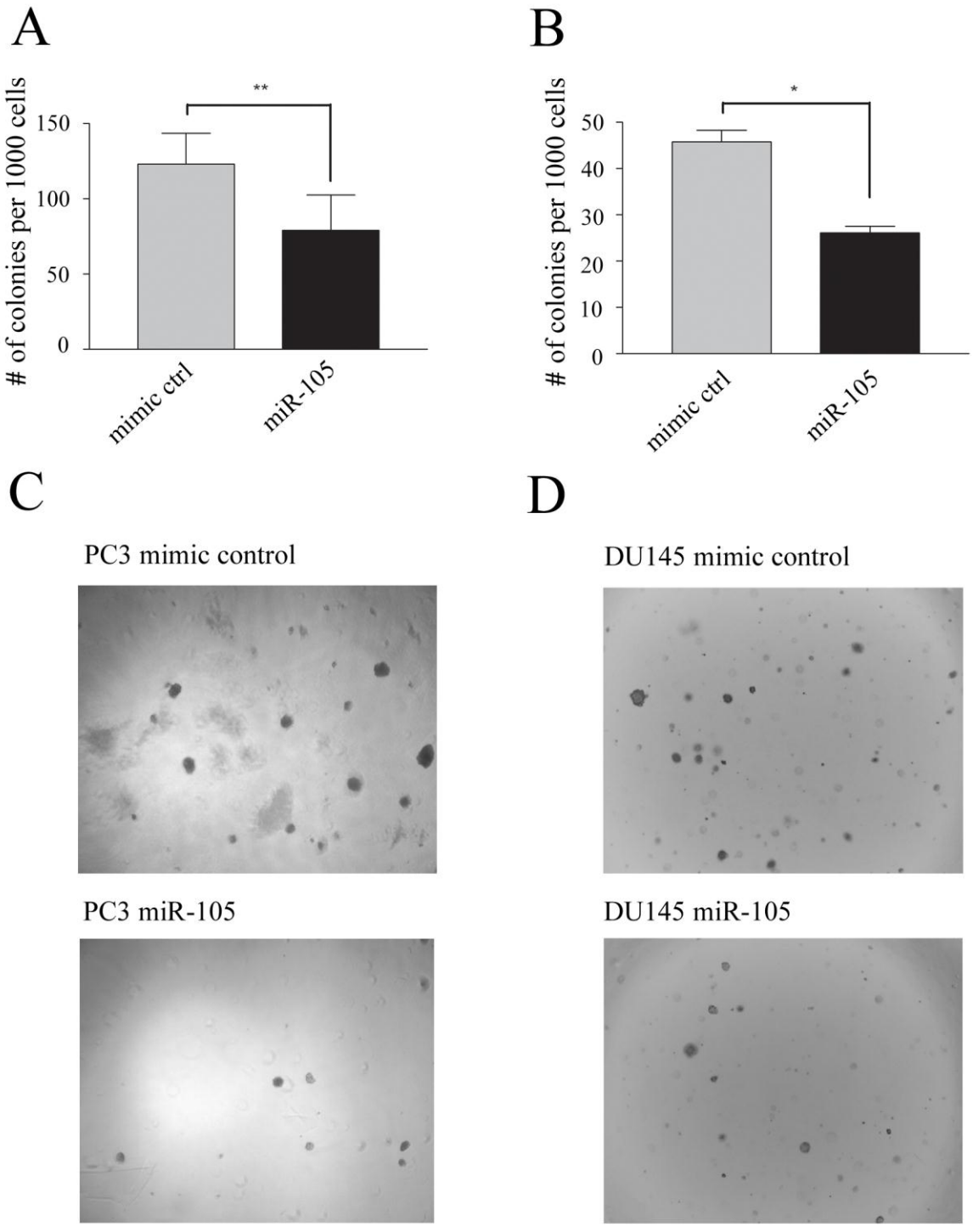
A
# of colonies per 1000 cells
150
100
50
0
**
mimic ctrl
miR-105
B
# of colonies per 1000 cells
50
40
30
20
10
0
*
mimic ctrl
miR-105
C
PC3 mimic control
PC3 miR-105
D
DU145 mimic control
DU145 miR-105

Figure 8: Over-expression of miR-105 inhibits anchorage-independent growth of prostate tumour cells.

(A-D) PC3 (A) and DU145 (B) cells were transfected with either 50 nM miR-105 or control mimic and 24 hours post-transfection were seeded into soft-agarose. The number of colonies were then counted 14 days later in the wells generated from the 1000 cell dilution in triplicate wells. Bars represent the pooled mean and standard error for triplicate wells from three independent experiments. There was a significant decrease in colony formation in cells treated with miR-105 as compared to control mimic-transfected cells for both PC3 ($p<0.01$) and DU145 ($p<0.05$) cells. (C-D) Representative photos showing reduced colony formation in soft-agarose for miR-105 versus control mimic transfected PC3 (C) and DU145 (D).

Taken together, our results suggest that increased levels of miR-105 suppress 2D and 3D growth in PC3, DU145 and A549 cells.

3.6 Over-expression of miR-105 inhibits PC3 tumour cell migration and invasion.

We next evaluated whether miR-105 over-expression affected tumour cell migration or invasion as described in sections 2.8 and 2.9, respectively. To test the effects of miR-105 over-expression on cell migration, transfected PC3 cells were used in a scratch wound assay. Confluent cell monolayers were scratched to create a wound opening, and then the percentage wound closure at various times was calculated following comparison to the wound diameter at time 0. We found that the migration of miR-105 mimic treated PC3 cells over a 48 hour time period was significantly inhibited as compared to control mimic transfected cells (Fig. 9A and B). However, as wound closure rates can be influenced by cell proliferation, and we had previously noted the ability of miR-105 to inhibit PC3 cell growth, we investigated the ability of miR-105 to inhibit tumour cell invasion using Matrigel-coated transwell invasion chambers. As this assay is of shorter duration, the influence of differences in cell proliferation play a less significant role and effects are mostly attributable to direct effects in cell migration and invasive capabilities. In this assay system we found that the number of invaded cells transfected with miR-105 mimics was significantly reduced as compared to control mimic transfected cells (Fig.9C). Thus, over-expression of miR-105 also appears to inhibit PC3 cell invasion *in vitro*.

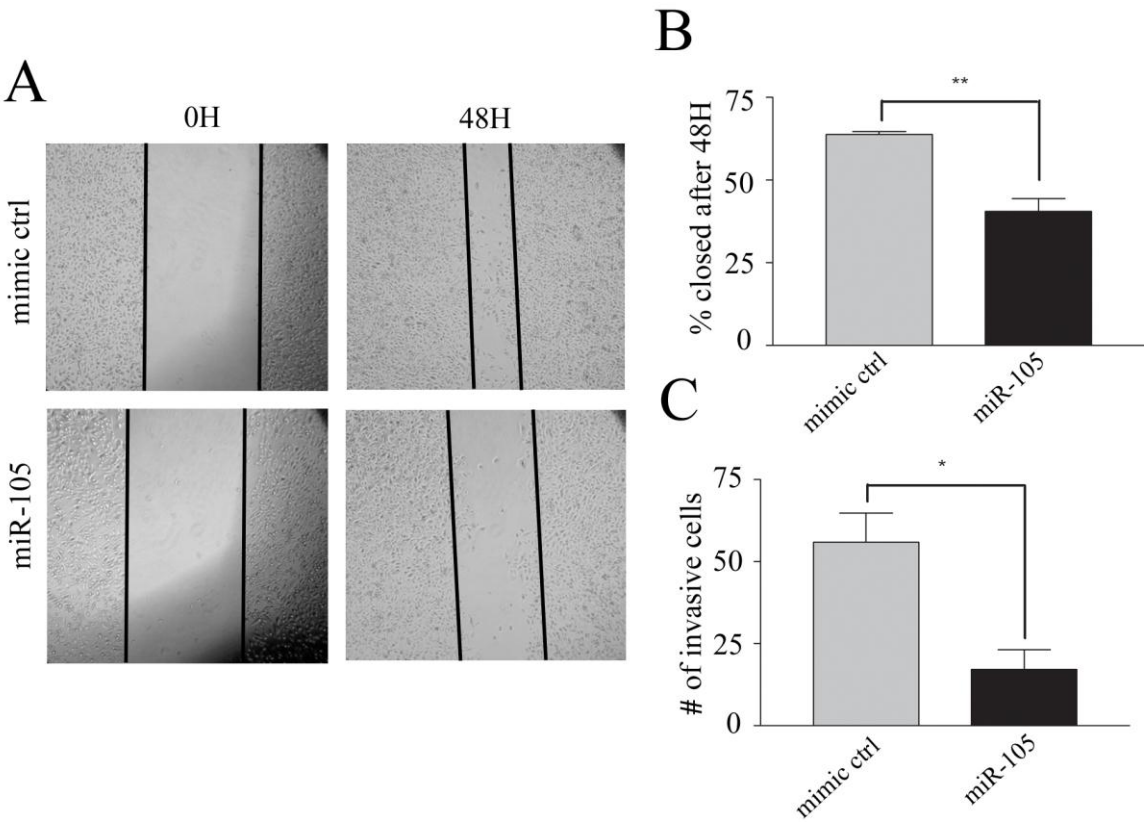
A
0H
48H
mimic ctrl
miR-105
B
% closed after 48H
75
50
25
0
**
mimic ctrl
miR-105
C
# of invasive cells
75
50
25
0
*
mimic ctrl
miR-105

Figure 9 Over-expression of miR-105 inhibits tumour cell migration and invasion.

(A) Representative photos of scratch wound assays at 0 and 48 hours post wounding for miR-105 compared to control mimic transfected PC3 cells showing impaired wound closure in miR-105 mimic over-expressing cells. Photos were taken at 10x magnification. (B) PC3 migration was measured as percentage wound closure in assays in (A) as described in section 2.8. Average wound closure measurements at three different points along wound edge was quantified in each of two independent wells. Bars represent pooled mean and standard error of duplicates in each of two independent experiments. Wound closure after 48 hours was significantly less ($p<0.01$) in the miR-105 mimic expressing compared to control mimic transfected cells. (C) PC3 invasion was measured over 24 hours using Matrigel coated transwells as described in section 2.9. The total number of invaded cells on the underside of each filter were counted and expressed in the graph as the pooled mean and standard error from duplicate wells in three independent experiments. There were significantly less ($p<0.05$) miR-105 mimic over-expressing invaded cells compared to control cells.

3.7 Over-expression of miR-105 inhibits growth of prostate tumour cells in vivo in xenograft models.

We decided to examine the effects of miR-105 over-expression on *in vivo* tumour growth using xenografts in immunocompromised mouse models as described in section 2.10. PC3 or DU145 cells were transfected with either miR-105 specific mimic or control mimics, and 24 hours later were harvested and $1x10^6$ cells were injected subcutaneously into both flanks of each nude mouse. A total of 8 mice were used in each experiment, with 4 receiving bilateral injections of miR-105 treated cells and 4 receiving control cells, for a total of 16 PC3 and 16 DU145 tumours. Tumour growth was measured weekly, and tumour volumes over time assessed for PC3 (Fig. 10A) and DU145 (Fig. 10B) tumours. We found that the growth of PC3 tumours was significantly inhibited following over-expression of miR-105 mimics as compared to control mimic transfected PC3 cells (Fig. 10A). At the termination of the experiment, wet tumour weight was also determined, and it was confirmed that miR-105 over-expressing tumours weighed on average 73% less than the control tumours (Fig.10C). Although not statistically significant, we also observed reduced DU145 tumour growth in miR-105 transfected as compared to control mimic transfected cells over time (Fig.10B). At endpoint, the weight of tumours derived from miR-105 transfected DU145 cells were approximately 82% less than those derived from control mimic transfected cells (Fig.10D). In addition, sections of tumour sample were taken, H&E stained and photographed. Both PC3 (Fig.10E) and DU145 (Fig.10F) tumours showed no major histological differences between control-treated and miR-105-treated cells. At endpoint, total RNA was extracted from tumour samples and the levels of miR-105 expression were assessed using RT-qPCR (Fig.10G). Slightly higher levels of miR-105 expression were observed in PC3 tumours

derived from miR-105 mimic transfected cells as compared to control mimic transfected cells following analysis by RT-qPCR. These results support our contention that miR-105 inhibits prostate tumour cell growth, which results in delayed tumour progression.

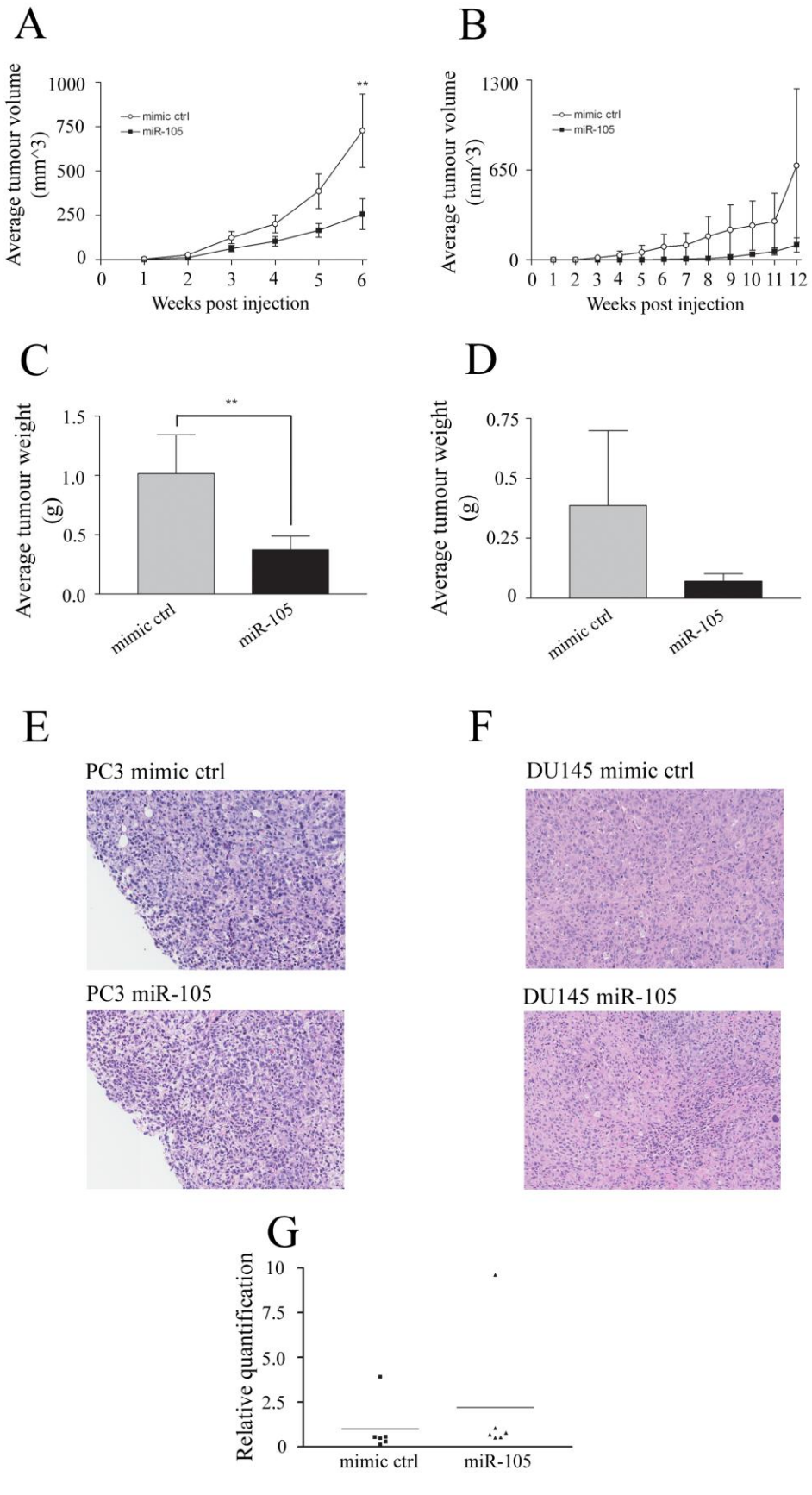
A
Average tumour volume (mm^3)
1000
750
500
250
0
mimic ctrl
miR-105
**
0 1 2 3 4 5 6
Weeks post injection
B
Average tumour volume (mm^3)
1300
650
0
mimic ctrl
miR-105
0 1 2 3 4 5 6 7 8 9 10 11 12
Weeks post injection
C
Average tumour weight (g)
1.5
1.0
0.5
0.0
**
mimic ctrl
miR-105
D
Average tumour weight (g)
0.75
0.5
0.25
0
mimic ctrl
miR-105
E
PC3 mimic ctrl
PC3 miR-105
F
DU145 mimic ctrl
DU145 miR-105
G
Relative quantification
10
7.5
5.0
2.5
0
mimic ctrl
miR-105

Figure 10: Over-expression of miR-105 inhibits in vivo subcutaneous tumour growth.

(A-G) PC3 and DU145 cells were were transfected with either 50 nM miR-105 or control mimics and injected subcutaneously in the hind flanks of 5-week old CD1 nude mice as described in section 2.10. For each condition, data is representative of 8 bilateral tumours from 4 mice. (A-B) Tumour size was measured by calipers over time for PC3 (A) and DU145 (B) derived tumours until humane endpoints were reached. Tumours derived from miR-105 over-expressing PC3 cells were significantly smaller ($p<0.01$) than tumours derived from control mimic transfected PC3 cells, while tumours derived from miR-105 mimic transfected DU145 cells tended to be smaller than their respective controls. (C-D) Tumour wet weight at experimental endpoint was also measured for PC3 (C) and DU145 (D) derived tumours. The mean weight in grams and associated standard errors is plotted, and shows that at endpoint miR-105 mimic transfected PC3 were significantly lighter ($p<0.01$) compared with control mimic transfected cells. DU145 tumours showed similar trends but did not quite reach statistical significance. (E-F) At endpoint, tumour sections were analyzed by H&E staining. No significant differences in tumour morphology were observed between miR-105 and control mimic transfected cell derived tumours for either PC3 (E) or DU145 (F) tumours. (G) Small pieces of PC3 tumours were collected and processed for isolation of miRNA and anlaysis of miR-105 expression. No significant difference in average miR-105 was detected between the miR-105 and control-treated tumour samples, although the level of miR-105 seemed to be slightly higher in miR-105 treated cells. There were two outliers, one in each population. RNU24 was used as internal control in all cases.

3.8 miR-105 targets multiple proteins, including Cdk6, in prostate tumour cells

In an attempt to determine by what mechanism miR-105 over-expression was modulating the tumour growth and invasive phenotypes we observed, we attempted to identify relevant mRNA targets of miR-105. To do this, the gene expression profile of miR-105 mimic compared to control mimic transfected PC3 cells was compared using Affymetrix GeneChip Human Gene 1.0 ST microarrays (see Appendix for target lists). As we presumed that the main mechanism of miR-105 modulation of the observed phenotypes was via down-regulation of specific gene messages, we focused on targets that were down-regulated in miR-105 transfected as compared to control transfected cells. The most down-regulated target was Cdk6, an important cell-cycle regulatory protein, and a likely candidate to explain the reduced 2D growth we previously observed. We thus validated the microarray findings using RT-qPCR for Cdk6 message (as compared to β-Actin as an endogenous control). We found that the level of expression of Cdk6 was significantly reduced in PC3 cells treated with 50nM of miR-105 mimic over 24 – 96 hours as compared to control mimic transfected cells (Fig.11A). We also found that Cdk6 mRNA expression was significantly reduced 48 hours after transfection with 100nM of miR-105 mimic (Fig.11C). To confirm these findings, we also examined the protein levels of Cdk6 by western blot as described in section 2.11. We found that the level of Cdk6 protein was also reduced in PC3 cells transfected with miR-105 over 96 hours (Fig.11B), as well as reduced in the 48 hour 100nM miR-105 transfections, compared to 100 nM control transfected cells (Fig.11D).

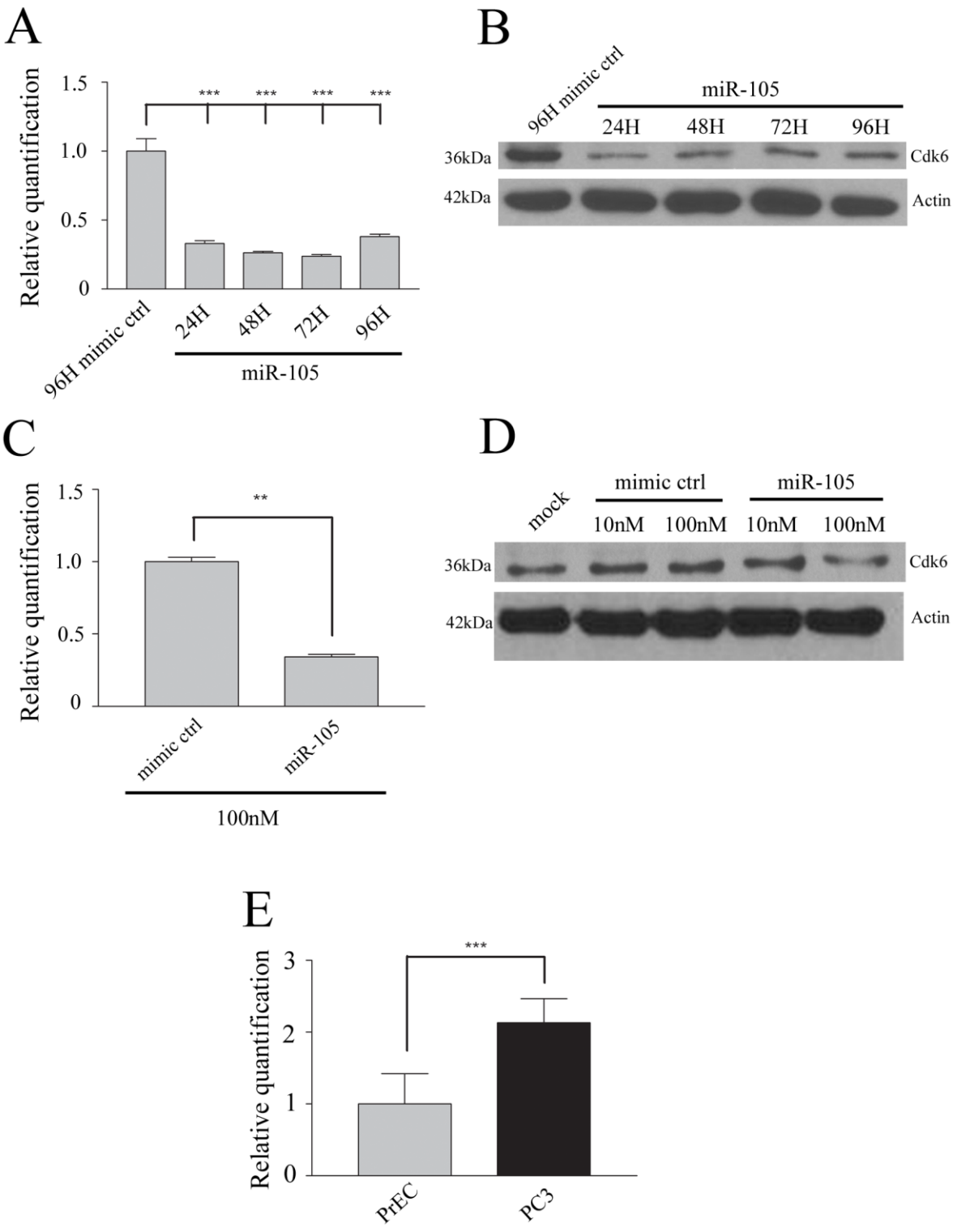
A
Relative quantification
1.5
1.0
0.5
0
***
***
***
***
96H mimic ctrl
24H
48H
72H
96H
miR-105
B
96H mimic ctrl
miR-105
24H
48H
72H
96H
36kDa
Cdk6
42kDa
Actin
C
Relative quantification
1.5
1.0
0.5
0
**
mimic ctrl
miR-105
100nM
D
mock
mimic ctrl
miR-105
10nM
100nM
10nM
100nM
36kDa
Cdk6
42kDa
Actin
E
Relative quantification
3
2
1
0
***
PrEC
PC3

Figure 11: miR-105 results in decreased Cdk6 expression at both the mRNA and protein levels.

(A-B) PC3 cells were transfected with 50nM of miR-105 mimic or control mimic as described in section 2.2 and relative Cdk6 expression levels were assessed over 24 - 96 hours. Both the mRNA and protein samples were isolated from paired PC3 dishes transfected with the same control or miR-105 reagents. (A) Relative levels of Cdk6 mRNA were determined following RT-qPCR analysis and normalization to endogenous levels of β-actin as a control. The graph represents the mean and standard error of 4 replicates from one experiment. We observed a significant decrease ($p<0.001$) in Cdk6 mRNA at the 24, 48, 72 and 96 hour timepoints in 50nM miR-105 over-expressing cells as compared to control mimic transfected PC3 cells. (B) We also observed a decrease in Cdk6 protein expression in miR-105 over-expressing cells as compared to control mimic transfected PC3 cells over the full 96 hour time period. (C-D) PC3 cells were transfected with 10 or 100 nM of miR-105 mimic or control mimics as described in section 2.2 and relative Cdk6 expression levels were assessed over 48 hours. Both the mRNA and protein samples were isolated from paired PC3 dishes transfected with the same control or miR-105 reagents. (C) Relative levels of Cdk6 mRNA were determined following RT-qPCR analysis and normalization to endogenous levels of β-actin as a control. The graphs represent the mean and standard error of 4 replicates from one experiment. We observed a significant decrease ($p<0.01$) in Cdk6 mRNA between 100nM miR-105 over-expressing cells as compared to 100nM control mimic transfected PC3 cells. (B) We observed a decrease in Cdk6 protein expression between the 100nM miR-105 over-expressing cells as compared to 100nM control mimic transfected PC3 cells. (E) Cdk6 mRNA levels were also compared between normal PrEC cells and cancerous PC3 cells using RT-qPCR and normalization to endogenous β-actin levels as a control. Consistent with reduced endogenous miR-105 levels (Fig. 4A), PC3 cells had a significantly higher ($p<0.001$) Cdk6 expression when compared to PrEC. The graph represents the mean and standard error of 4 replicates from one experiment.

This confirmed our results and suggested that Cdk6 is a putative target for miR-105. In our original studies we determined that miR-105 was higher in normal prostate epithelial cells as compared to tumour cells, so we examined the expression of Cdk6 between normal PrEC cells and PC3 tumour cells. Consistent with our results, we found that that the message levels of Cdk6 were elevated in the PC3 cell line as compared to PrEC (Fig.10E), further demonstrating the inverse correlation between miR-105 and Cdk6 expression. In conclusion, our results suggest that miR-105 inhibits tumour cell growth in part via its ability to down-regulate the expression of the important cell cycle regulator Cdk6.

4: DISCUSSION

4.1 Modulation of tumorigenesis by over-expression of miR-105 in PC3 and DU145 cells

Tumour-suppressive miRNAs have been discovered in most forms of cancer as researchers study the relationship between miRNAs and cancer. From our overall data we observed that hsa-miR-105 acts as a tumour-suppressive miRNA in prostate cancer cells both *in vitro* and *in vivo*. It shares many of the same characteristics as other miRNAs that suppress cancer, such as miR-205 (36, 57, 203) and miR-143 (29, 205). Cdk6, one of miR-105's central targets, is also a known target of other tumour-suppressive miRNAs (111, 204, 211) and helps to explain the miRNA's effect on cell proliferation and growth. miR-105's new role in prostate cancer will aid our understanding of prostate cancer biology and provide a potential candidate for future biomarkers and therapeutic treatments.

4.1.1 Analysis of PrEC vs PC3 / DU145 cells using miRNA microarrays

Aberrant expression of miRNAs in cancer is associated with significant changes in tumour phenotypes, and the study of these miRNAs aids in the understanding of cancer biology. Understanding what miRNAs are altered in metastatic prostate cancer will help us to both detect and treat the disease better. However, to date we have found no studies examining the broad miRNA signatures of metastatic prostate cancer cell lines compared to non-cancerous prostate cells. Thus, we compared the relative miRNA expression levels

between normal prostate epithelial and metastatic prostate cancer cell lines using a miRNA microarray to determine which miRNAs contribute to the modulation of metastatic prostate cancer's tumourigenic phenotype. It is important to note that the microarray was only performed once for each cell line, therefore the data resulting from the microarray was regarded only as an indicator of possible differences in miRNA expression. Further validation by RT-qPCR was necessary to establish true differences in expression. From the microarray we found altered expression of many miRNAs that are reported to be involved in multiple cancer types, such as the down-regulated miR-205 and miR-200c, and up-regulated miR-210. miR-205 was the most down-regulated target in both PC3 and DU145 cell lines. It is a well-studied tumour suppressive miRNA in cancers such as prostate (57), breast (203) and melanoma (36), where it suppresses cancer phenotypes such as cell proliferation, anchorage-independent growth, invasion, and EMT. miR-200c was another down-regulated miRNA and is a tumour suppressive miRNA in breast (88) and melanoma (209) cancers where it is able to repress migration, invasion and anchorage-independent growth. miR-210 was one of our common up-regulated targets in both PC3 and DU145 cells and is found to be over-expressed in advanced lung cancer (153) where it contributes to cell survival in hypoxic environments through modulation of HIF-1 activity. A prostate cancer study found that decreased miR-210 levels significantly decreased the survival of PC3 cells in hypoxic environments (154). Further study into miR-210's status in metastatic prostate cancer could yield a potential biomarker.

Overall, as the direction of miRNA changes in our microarrays matched what has been previously reported in the literature, we were encouraged that our microarray results could be relatively accurate despite the small sample size. Hence we proceeded to validate

many of the originally identified targets. As much literature exists supporting some of the miRNAs we did identify, we chose not to pursue study of these in detail, and instead chose to investigate miRNAs that were novel and not previously reported to be associated with prostate cancer, such as miR-105 and miR-720. Initially, miR-105 caught our attention because it appeared in another study in our lab, where we were examining the influence of the extracellular matrix (ECM) on miRNA expression. Previous research showed that miR-105 plays a role in cell proliferation (179) and that it was down-regulated in pancreatic, colorectal, cervical and promyelocytic leukemia cancer cell lines (109). miR-105's location on the X chromosome is also an interesting factor, as men inherit only one copy from their mothers. This raises the risk of possible mutations fully disabling or altering genes contained within the X chromosome, because there is no additional copy on an identical chromosome in men to compensate. In addition, previous studies have found evidence for a prostate cancer susceptibility locus in the Xq27-28 region, which is where miR-105 is located (207). When validated by RT-qPCR miR-105 was shown to have lower expression levels in the metastatic cell lines. This data led us to hypothesize that miR-105 over-expression could inhibit tumour cell growth in a similar way to other tumour-suppressive miRNAs.

4.1.2 miR-105 over-expression leads to altered *in vitro* tumour phenotypes

One of the most common methods used to examine miRNA function is the transfection of synthetic mimic or hairpin molecules into cells, which cause over-expression or under-expression of their target miRNA. This approach has been used successfully in previous studies on cancer miRNAs (95, 157). We utilized a system whereby miR-105 levels were artificially over-expressed using synthetic mimic constructs in the PC3 and DU145 cell lines.

This over-expression countered the down-regulation of miR-105 we observed in the metastatic prostate cancer cell lines. In our studies, transfection of 50nM of mimic was sufficient to significantly cause miR-105 over-expression. This concentration of mimic corresponds well with other studies, where mimic concentrations ranged between 10-200 nM (26, 96, 216). It is important to note that the miR-105 levels at this concentration in PC3 cells are significantly higher than normal miR-105 levels seen in PrEC cells. These transfected cancer cells were tested using experiments already established in previous tumour-suppressive miRNA studies, such as testing for differences in cell proliferation, anchorage-independent growth, cell invasion and apoptosis. In all of our assays we compared control transfected cells with miR-105 transfected cells, but we did also test mock transfections. On average the mock and control transfections were relatively similar, with the control transfected cells usually showing a approximately 10-20% decrease in the phenotype being tested compared with the mock transfected cells.

Cell proliferation is often tested in studies looking at cancer miRNAs by using MTT assays. For example, Chang *et al.* examined the effect of miR-21 and miR-494 alteration on cellular proliferation using MTT assays (25). They found that transfection of miR-494 mimic caused a 61.7% decrease in cell growth compared to controls, which was similar to the 55% drop seen in our transfected PC3 cells. Both PC3 and DU145 metastatic cell lines showed significant decreases in viability levels following elevated miR-105 expression. However, the limitations of the assay must be mentioned. MTT assays are used to test cell viability directly, not cell proliferation. They are based on cell metabolism, as tetrazolium salts such as MTT are taken up by viable cells and metabolically reduced into highly coloured end products called formazans, which can be measured (185). The decrease in cell viability

following miRNA up-regulation we observed could be due to a decrease in cell proliferation or an increase in cell apoptosis, because in both cases fewer cells are present to metabolize the chemical. Therefore, we examined apoptosis using assays to test for both PARP and PI staining. PARP is a DNA repair protein that is located in the nucleus, and during cell apoptosis it is cleaved by caspases which results in a signature 89 kDa fragment (44). PI staining causes measurable PI binding to cellular DNA, and in apoptotic cells there is a large increase in fragmented DNA leading to hypodiploid (sub-G1) cells which retain less PI than diploid cells (G1). For both cell lines there was no measurable increase in apoptosis levels. Taken together with our data from the MTT assay we determined that over-expression of miR-105 caused a decrease in cellular proliferation. Although we did not test this directly, miR-105's effect on cell proliferation could be further confirmed using techniques designed to directly measure cell proliferation, such as BrdU incorporation assays.

Soft-agarose (SA) assays are considered to be one of the most accurate indicators of tumourigenicity *in vitro* (93). In SA assays, cells are suspended in a matrix of agar that prevents them from contact with other cells, and those that are able to divide and form colonies demonstrate anchorage-independent growth. Previous studies of tumour-repressive miRNAs have examined altered miRNAs in agarose to determine their effect on anchorage-independent growth. Cole *et al.* used this assay to show that over-expression of the tumour-suppressive miR-34a led to a decrease in colony formation in soft agar (30). This decrease in colony growth caused by increased tumour-suppressive miRNA was similar to what we observed when we examined the effect of miR-105 over-expression on anchorage-independent growth. Both cell lines showed significantly less colonies compared with control-treated cells after transfection. It is possible that miR-105's effect on cell

proliferation may play a role in this assay by reducing the number of colonies of a "countable" size by preventing proliferation of single cells that progress into observable colonies. Overall the results of the cell proliferation and soft agarose assays indicate that miR-105 acts like miR-494 and miR-34a as a negative regulator of tumour growth.

miRNAs have previously been shown to significantly affect cell migration and cell invasion. Cell migration is often measured using scratch wound assays, for example in the case of miR-320 inhibition which led to increased migration of myocardial microvascular endothelial cells (MMVEC) (197). Cell invasion is often measured using Matrigel invasion chambers. Ma *et al.* successfully used the Matrigel invasion chamber system to show that miR-10b, which is over-expressed in metastatic breast cancer, is involved in breast cancer invasion. When miR-10b was knocked down in the invasive breast cancer cell line MDA-MB-231 there was a significant reduction of invasion *in vitro* (132). In further experiments, over-expression of miR-10b in non-invasive breast cancer cells with low endogenous miR-10b levels caused a significant increase in *in vitro* invasion. When we examined the role of miR-105 in migration and invasion, we found that increased miR-105 caused a decrease in both these phenotypes. We first observed a decrease in cell migration using a simple 2D scratch wound assays. However, in our study this difference could have been affected by inhibition of cell proliferation by miR-105, which would result in fewer cells to fill the wound site as compared to control-mimic transfected cells, which had a higher proliferation rate. Therefore we then used the Matrigel invasion chamber system to remove the variability of altered cell proliferation from our observations. Using this method, we observed a decrease in invasion in PC3 cells that was not affected by differences in cell proliferation due to the shorter duration of the experiment. This decrease in invasion corresponded with

the behaviour of other tumour-suppressive miRNAs that cause decreased invasion in prostate cancer cells, such as miR-205 (57) and miR-143 (205) .

Overall our *in vitro* assays indicated that miR-105 acts as a tumour-suppressive miRNA in PC3 and DU145 cells by inhibiting cell proliferation and anchorage-independent growth, and cell invasion in PC3 cells specifically. In this respect miR-105 resembles other tumour-suppressive miRNAs that also inhibit these characteristics. One of the best comparisons to miR-105 in the literature is miR-205, which is a tumour-suppressive miRNA that acts in prostate cancer to inhibit cell proliferation, anchorage-independent growth and invasion (57). miR-205 is also involved in altering EMT in cancer cells, and based on their similarities it is possible that miR-105 could affect EMT as well. Gandellini *et al.* examined the effect of miR-205 on EMT markers such as E-cadherin and vimentin, which are indicators of cancer aggressiveness and metastatic potential (90). Versican, another EMT marker (91), is a putative target of miR-105 that will be discussed later. miR-105's possible effect on versican levels, along with its similarities to miR-205, strengthens the possibility that miR-105 may affect EMT in prostate cancer cells.

4.1.3 miR-105 over-expression leads to altered *in vivo* tumour growth

Although many *in vitro* tests can indicate the tumourigenic properties of a given tumour cell line, the true test is its ability to regenerate tumours *in vivo*. Multiple studies have used this method to show the impact of altered miRNAs on tumour growth. For example, Clapé *et al.* used over-expression of miR-143 to inhibit subcutaneous prostate tumours and showed that it acts as a tumour suppressive miRNA *in vivo* (29). Therefore based on our *in vitro* results we were interested to evaluate whether miR-105 over-

expression could inhibit tumour growth *in vivo*. As PC3 and DU145 cells are of human origin, we used CD1 nude mouse models which are immuno-compromised to allow for growth of human tumours in mice without risk of rejection as foreign agents. As our previous results suggested that we could achieve over-expression of miR-105 mimic in these cells lines for at least 7 days, we hypothesized that the initial one to two weeks of miR-105 over-expression would be sufficient to cause a significant defect in the early stages of tumour growth, which would then still be detectable at the end of the experiment as differences in tumour sizes. We found that PC3 tumours treated with miR-105 mimic showed a significant decrease in both tumour volume and weight by endpoint. In DU145 cells, although there was a trend for smaller miR-105 mimic treated DU145 tumours the differences were not statistically significant. This was not surprising as we found that growth of DU145 in our xenograft models was significantly slower than that of PC3 tumours, which had experimental endpoints of 12 weeks compared to 6 weeks, respectively. The fact that transient over-expression of miRNA mimics was used means it is likely that the duration of expression in DU145 tumours *in vivo* was not sufficient to demonstrate significant growth differences over the extended period of time. However, it was encouraging that transient over-expression of miR-105 in this manner was sufficient to inhibit tumour growth, which supports the important role it seems to play in prostate tumour growth. In addition to tumour samples, lungs, liver and bones were taken from the animals at endpoint and examined by H & E staining for evidence of metastasis. None were seen in any of the organs after examination by a pathologist, which can be explained by the fact that both experiments finished at a relatively early endpoint and thus there was not enough time for tumours to metastasize and form detectable colonies. In addition, there were no obvious differences in

tumour appearance when comparing sections taken from the tumour samples, which supports the notion that miR-105 over-expression impairs tumour proliferation and hence tumour size, but does not affect tumour phenotype or cell morphology. At endpoint the PC3 tumours were also tested for miR-105 expression, which was slightly increased in the miR-105 over-expressing tumours versus control-treated tumours. We expected to observe very similar levels because of our previous studies on the duration and stability of miR-105 mimic levels. These indicated that after 5 days past initial transfection the levels of miRNA mimic began to steadily decrease. However, relative to the level of miR-105 expression seen 24 – 120 hours after transfection this difference was very small and likely inconsequential.

4.1.4 miR-105 targets Cdk6 to cause changes in cell proliferation

Determining a tumour-suppressive miRNA's mRNA targets is important because it allows us to discover how it affects specific cancer phenotypes. We found a number of mRNA targets that were down-regulated in miR-105 transfected cells by using a Human Gene 1.0 ST microarray to compare PC3 cells transfected with either control or miR-105 mimic (see Appendix for list of targets). However, as this microarray was only performed once it served only as an indication of potential targets, and interesting targets from these microarrays were thus analyzed by specific RT-qPCR and western blot to determine their validity. Some of these encoded for proteins that are involved in cell proliferation, anchorage-independent growth and cell invasion, which would help explain the differences in these phenotypes that we observed after miR-105 over-expression. We discovered that the top down-regulated microarray target in miR-105 over-expressing cells was the Cdk6 protein, whose decreased expression was validated at both the mRNA and protein levels.

miR-105 joins many other cancer-associated miRNAs, such as miR-107 (111), miR-129 (204), and miR-449a/b (211), that target and down-regulate Cdk6 to reduce cell proliferation. Cdk6 is an important cell-cycle regulator protein that acts with Cdk4 to bind CyclinD1 and phosphorylate the Retinoblastoma (Rb) protein and allow cell cycle progression (147). It regulates the transition from G1 to S phase and its dysregulation is important in many cancer types, including prostate (119) and breast cancer (129). In prostate cancer Cdk6 is linked to both alteration of the cell cycle and modulation of the transcriptional activity of the androgen receptor. Stably over-expressed Cdk6 in LNCaP cells causes a significant increase in both 2D and 3D growth *in vitro (119).* An abundance of Cdk6 leads to loss of control in the G1 to S phase checkpoint, which is followed by uninhibited cell proliferation (34). It is possible that miR-105 targets Cdk6 directly, as the mRNA 3'UTR is a predicted target of miR-105 by the online miRNA target prediction programs miRDB(196) (St. Louis, MO, http://mirdb.org/miRDB/), miRWalk(45) (Heidelberg, Germany, http://www.umm.uni-heidelberg.de/apps/zmf/mirwalk/index.html) and Targetscan (Cambridge, MA, USA, http://www.targetscan.org/). Predicted miR-105 seed regions in the CDK6 mRNA 3'UTR include positions 287-293, 538-544, 2625-2632 and 7613-7619. Although our findings of reduced CDK6 message levels in miR-105 over-expressing cells suggests it may be a direct target, we would have to confirm this using reporter gene constructs. Whether by direct or indirect mechanisms, the down-regulation of Cdk6 protein by miR-105 helps explain the effects on cell proliferation observed in our results (see Figure 12 for mechanistic diagram). Differences in the mutational status of cell cycle proteins between PC3 and DU145 cells help explain the difference we see in our proliferation assays. Most importantly, PC3 cells are Rb normal while DU145 cells are Rb

null. This means that PC3 cells still have a partially intact G1 checkpoint, while DU145 cells lack this altogether. If miR-105 down-regulates Cdk6 in PC3 cells it would cause a decrease in Rb phosphorylation, which would lead to the decrease in cell proliferation that we observed in this cell line. However, if miR-105 down-regulates Cdk6 in DU145 cells this likely would not have a major impact, as there is no Rb for the increased Cdk6 to affect. Therefore the smaller difference in proliferation we see in our DU145 cell experiments is likely due to another target, such as NEDD4, which will be discussed shortly. We also observed increased expression of CDK6 mRNA in the prostate tumour cell lines versus PrEC cells. This lends further support to the argument that miR-105 may be down-regulated in PC3 and DU145 cells partly because of its suppressive effect on Cdk6 and ability to inhibit malignant cell growth. Finally, the increase in miR-105 over-expressing PC3 cells in the G1 phase compared to control can be explained by miR-105's effect on Cdk6, as decreased Cdk6 protein levels would make it more difficult for cells to proceed past the G1 checkpoint system.

There are other miR-105 targets revealed by the mRNA microarray but not yet validated by RT-qPCR that could play a role in miR-105's affect on prostate cancer. These targets could help explain the other effects of miR-105 that we see, such as anchorage independent growth and cell migration and invasion. One of them, versican, is a proteoglycan that is sent outside the cell to become a part of the extracellular matrix (ECM) (99), where it regulates cell adhesion and motility (163). It is also used as a marker of EMT, as previously discussed. In prostate cancer it is over-expressed (162) and acts as a tumour promoter by promoting cell migration, invasion and proliferation (164).

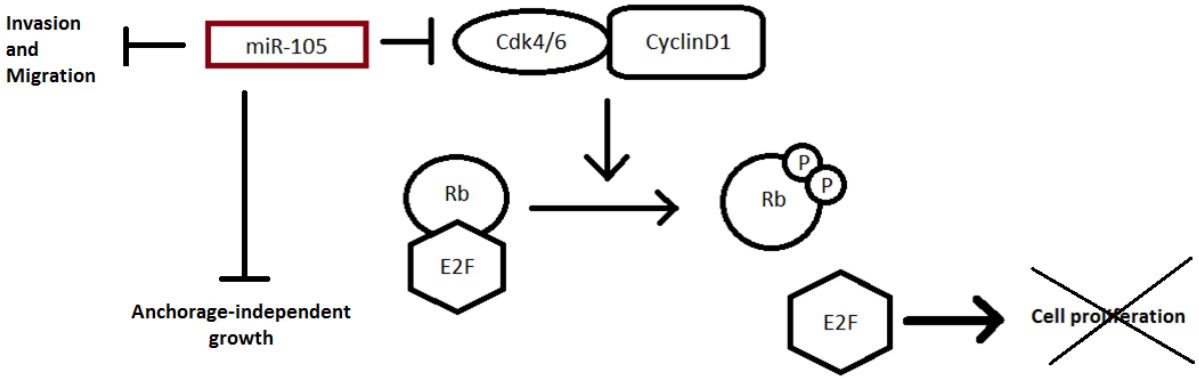
Invasion
and
Migration
miR-105
Cdk4/6
CyclinD1
Rb
E2F
P
P
Rb
E2F
Cell proliferation
Anchorage-independent
growth

Figure 12: Diagram of miR-105's putative effect on Cdk6 and cancer phenotypes

miR-105's inhibition of Cdk6 leads to a decrease in phosphorylation of Rb and ultimately a decrease in cell proliferation. Its other effects on cancer phenotypes such as anchorage-independent growth and cell migration and invasion will need to be explained by investigation of other putative miR-105 targets.

Versican down-regulation by miR-105 would help explain the defects we see in PC3 cell invasion in Matrigel invasion chambers. Down-regulated versican protein could also coincide with the effects of down-regulated Cdk6 protein levels to explain the inhibition of cell proliferation we observed in PC3 and DU145 cells.

Another potential miR-105 target is cyclin-dependent kinase-8 (Cdk8), a protein normally involved in the multi-subunit Mediator complex which regulates the actions of RNA Polymerase II (208). It has been shown to act as an oncoprotein in colorectal cancer by dysregulation of cell proliferation and is necessary for B-catenin-driven transformation (54). Recently, researchers have found that suppression of Cdk8 in malignant melanoma cells inhibits proliferation and is linked directly to histone variant macroH2A (mH2A) expression. Thus it is possible that Cdk8 may play a currently unknown oncogenic role in prostate cancer tumourigenesis and be a target of miR-105.

Neural precursor cell expressed, developmentally down-regulated 4 (NEDD4) is another possible miR-105 target. It is an E3 ubiquitin ligase that is known to target the tumour suppressor gene PTEN. It has been shown that NEDD4 plays a role in cancers such as non-small-cell lung carcinomas, where it acts in an oncogenic fashion to suppress PTEN levels and facilitate cell proliferation and anchorage-independent growth (3). In our study, PC3 cells contain a homozygous deletion of the PTEN allele (136), thus miR-105's effects on cell proliferation would not be related to NEDD4 targeting. However, it is possible that, as an E3 ubiquitin ligase, NEDD4 has other important targets in PC3 cells that affect cell proliferation and other cancer phenotypes. DU145 cells still retains one functional PTEN gene so it is possible that miR-105 affects cell proliferation through NEDD4 in this cell line,

which would help explain the decrease in cell proliferation we observed in this cell line after miR-105 over-expression.

A final novel target of miR-105 is inositol polyphosphate multikinase (IPMK), a physiologic PI3-kinase that creates PIP(3) (133). PIP(3) in turn causes the downstream activation of the oncogene Akt/PKB, which promotes cell proliferation and protects against apoptosis. miR-105 down-regulation of IPMK could reduce cell proliferation and help explain some of the effects we see on cell proliferation and anchorage-independent growth as a result of miR-105 over-expression.

In conclusion, besides Cdk6 there are multiple putative miR-105 targets that could aid in explaining how different cancer phenotypes are affected in PC3 and DU145 cells. The difference in mutations between these cell lines could also help explain the differences we observed between the two in our cell proliferation and tumour growth experiments. Further research in this area will help elucidate the validity of these targets in relation to miR-105 and prostate cancer.

4.2 Altered miRNA expression levels in cancer

Broad miRNA expression profiles of human tissues and cancers allow researchers to determine which miRNAs are relevant to specific cancers and cell processes. To date there have been many studies undertaken to examine the level of miRNAs in a wide variety of cancers. Examining this data can give us indications as to what role miR-105 may play in prostate cancer and even other cancer types.

4.2.1 Presence of miR-105 in expression studies

There have been multiple studies that examine the unique miRNA profiles associated with different cancer types, including prostate cancer. However, to date none of them have found significant differences in miR-105 expression levels between prostate tumour and normal tissue. For example, one of the largest miRNA expression studies in prostate cancer examined the miRNA profile of malignant primary prostate tissue compared to matched normal prostate tissue using microarray analysis and RT-qPCR (174). Schaefer *et al.* discovered ten miRs that were down-regulated and five miRs that were up-regulated. However, miR-105 was not one of their down-regulated targets. There are multiple possibilities as to why miR-105 did not appear on the top hits of the study's microarrays. In the study paired prostate samples were taken from patient's primary prostate tumours, while the cell lines we used were obtained from secondary metastatic tumours. Specifically, the PC3 cell line was initiated from metastatic tissue located in a lumbar vertebrae (89), and the DU145 cell line was initiated from metastatic tissue located in the central nervous system (139). Metastatic tumours can have very different profiles in terms of gene and mRNA expression than primary prostate tumours. For example, Dat *et al.* performed a genome wide gene expression profile of metastatic bones, lung and liver lesions obtained from a mouse model of human non-small cell lung cancer cells (38). They identified 77 bone-specific altered genes, with 8 genes being confirmed up-regulated exclusively in bone metastasis tumours by RT-qPCR. Thus it is possible that miR-105 is part of a host of genes that are altered more significantly or even exclusively in metastatic prostate cancer lesions as opposed to primary prostate tumours. In the future we hope to see more studies that examine

the expression levels of miRNAs in metastatic prostate cancer, and would expect to see miR-105 as a target in these studies.

In addition to the choice of cancer stage, the microarray results of Shaefer *et al* were confounded by the fact that the investigators did not use laser capture microdissection to isolate prostate tumour tissue away from intervening normal stromal cells (146). As prostate tumours are very heterogenous, the relative levels of expression of various miRNAs in cancer cells could be altered by the contribution of the stromal cell expression levels. This means that miR-105 expressed in stromal cells may remain elevated and interfere with detection of cancer cell-specific miR-105 expression levels. In the future, all studies performing miRNA microarray analysis needs to take care to eliminate the influence of confounding factors such as non-cancerous support cells, which contain completely different miRNA signatures compared with cancer cells. In support of our findings, a recent meta-analysis of miRNA expression datasets from hepatocellular carcinomas suggested that down-regulation of miR-105 was a common feature (195). miR-105's involvement in hepatocellular carcinoma lends support to our findings that it is down-regulated in metastatic prostate tumour cells, and suggests that additional studies be performed in other cancers, including prostate cancer, to ascertain its expression status.

4.2.2 Status of miR-105 in cancer cell lines and tissues

We observed that miR-105 was significantly repressed in PC3 and DU145 cells compared with normal prostate cells (PrEC). However, the mechanism by which prostate cancer cells cause this repression is unclear. It was previously shown that the mature form, but not pri- or pre-miRNA forms, of miR-105 is undetectable in certain pancreatic,

colorectal, cervical and blood cancer cell lines compared with abundant precursor miR-105 molecules present in the nucleus (109). An oncogenic defect that might explain the lower levels of miR-105 in these cancer types is lower levels of functional exportin-5, an important miR biogenesis protein (137). Exportin-5 mediates pre-miRNA nuclear transport into the cytoplasm, and some cancers hold loss-of-function mutations in this gene, which inhibits mature miRNA production. It has been shown that PC3 cells have lower levels of exportin-5 than normal prostate cells (RWPE) (213), so it is possible that the lower levels of exportin-5 in PC3 cells lead to the decrease in mature miR-105 levels we see in our experiments. Further research into the relative levels of pri-, pre- and mature miR-105 in prostate cancer will be necessary to determine if this particular defect is applicable. If it is not, there are other possible methods of miR down-regulation by cancer such as transcriptional silencing by aberrant promoter hypermethylation (126). Inappropriate promoter hypermethylation can cause the down-regulation of tumour-suppressor miRNAs such as miR-124a, which leads to an increase of its target Cdk6 and subsequent Rb phosphorylation in the colorectal cancer cell line HCT-116 (130). miR-124a is hypermethylated in multiple cancers such as cervical and gastric carcinomas (4, 201).

Our study of miR-105 focused on its expression levels and effects in prostate cancer. However, other cell lines have been shown to have decreased mature miR-105 expression, including HCT-116 (colorectal carcinoma), HeLa (cervical carcinoma), HL-60 (promyelocytic leukemia) and HS766T, MiaPaca2 and Panc1 (pancreatic carcinomas) (109). In addition to its effects in PC3 and DU145 cells, we found that miR-105 over-expression in A549 lung carcinoma cells caused a significant decrease in cell proliferation and anchorage-

independent growth. Thus, it is likely that miR-105 acts as a tumour-suppressive miRNA in cancer types beyond prostate cancer.

4.3 Applications for miR-105 in the future

Every year new miRNAs are discovered which play a role in cancer initiation, development and metastasis. The first reason to study these miRNAs is to resolve the complex web of interconnected signals and pathways that defines cancer biology. The second reason is to determine their relevance to the future detection and treatment of cancer. Two main therapeutic areas where miR-105 may play a part are in the expanding study of miRNAs as cancer biomarkers, and the new field of miRNA-specific targeted therapies.

4.3.1 miRNAs as biomarkers

One promising application of our results is the use of miRNAs as biomarkers to predict tumour progression and metastasis. Mitchell *et al.* first looked at the possible use of miRNAs as endogenous cancer biomarkers in human patients (140). They found that endogenous miRNAs are surprisingly stable in the blood and are also resistant to RNAses that exist in human plasma. They examined prostate cancer patient serum samples and looked for miRNAs that were both highly expressed in prostate cancer cells and patient serum but not expressed in non-cancerous patients. One of their identified miRNAs, miR-141 fit these criteria, and they found that serum miR-141 levels could detect prostate cancer patients with high sensitivity. Later studies have found additional miRNAs that can detect metastatic prostate cancer specifically, such as miR-375 (14). Serum levels of miR-105

could potentially give useful information about the status of metastatic prostate cancer in patients.

Beyond serum biomarkers, miR-105 could also play a role as a tissue biomarker, especially combined with formalin-fixed, paraffin-embedded (FFPE) tissue samples. FFPE miRNA expression patterns are closely correlated with fresh tissue samples and are stable for many years before being slowly degraded (186). Thus, FFPE samples provide a useful platform for research into miRNA tissue biomarkers. A recent study used the FFPE platform to identify miRNA signatures that could identify certain types of cancer from patient tissue samples (168). Determining the miRNA signature of metastatic cancer could help guide treatment options by identifying where the cancer originated, which can be difficult to do in many advanced cancer patients (150). In conclusion, miR-105 could become a useful biomarker in the detection of aggressive prostate cancer depending on its detectable expression levels in patient serum and tissue samples.

4.3.2 miRNAs in targeted therapies

Another application of our results is the use of cancer miRNAs in targeted therapies. Altering the level of miRNAs in cancer, through the use of synthetic replacements for down-regulated tumour suppressive miRNAs or inhibitors against up-regulated oncogenic miRNAs, shows promise both in the lab and in clinical trials. In one experiment, experimenters injected synthetic miR-16, a down-regulated tumour suppressor miRNA, into mice with prostate cancer bone metastases (188). This resulted in a significant decrease in metastases compared with mice injected with control miRNA. Although there have been no prostate-cancer specific miRNA clinical trials to date, there are significant advances being

made in other areas of miRNA therapy. For example, miravirsen, a miR-122 inhibitor that is used to treat Hepatitis C infections (17), has completed Phase I trials successfully and has moved into Phase II trials to further test safety and efficacy. As miRNA-targeting therapies become more widespread and technical and safety issues are solved, an understanding of which miRNAs are dysregulated in prostate cancer will help guide future therapeutic targets and treatments.

4.4 Conclusion

Overall our findings suggest that miR-105 is a novel miRNA that regulates tumour growth in prostate cancer cells and is likely to play a role in other cancer types. Further investigation is necessary to evaluate its relative expression in tissue from prostate cancer patients, which will help determine its clinical significance. Given miR-105's role in inhibiting tumour growth, testing its relative level of expression in patients may help to identify more aggressive tumours within each relative risk group. miR-105 joins a growing list of miRNAs that have a direct impact on cancer proliferation, anchorage-independent growth and invasion. In the future, this knowledge could have applications in both novel cancer biomarker studies and in direct targeted therapies to treat cancer.

APPENDIX

Human Gene 1.0 ST array – targets down-regulated by miR-105 - less than 0.5 fold

Transcript Cluster ID	Gene Title	Gene Symbol
7898574	chromosome 1 open reading frame 151	C1orf151
7900030	eukaryotic translation initiation factor 2C, 1	EIF2C1
7901418	basic transcription factor 3-like 4	BTF3L4
7908861	ovarian cancer-related protein 1	OCR1
7910379	dual specificity phosphatase 5 pseudogene	DUSP5P
7916167	origin recognition complex, subunit 1-like (yeast)	ORC1L
7918284	TAF13 RNA polymerase II, TATA box binding protein (TBP)-associated factor, 18kDa	TAF13
7923189	kinesin family member 14	KIF14
7923707	transmembrane protein 81	TMEM81
7924107	lysophosphatidylglycerol acyltransferase 1	LPGAT1
7929078	kinesin family member 20B	KIF20B
7929438	helicase, lymphoid-specific	HELLS
7933723	inositol polyphosphate multikinase	IPMK
7948424	mitochondrial ribosomal protein L16	MRPL16
7952673	FLJ45950 protein	FLJ45950
7954388	golgi transport 1 homolog B (S. cerevisiae)	GOLT1B
7968199	cyclin-dependent kinase 8	CDK8
7969060	fibronectin type III domain containing 3A	FNDC3A
7973743	BCL2/adenovirus E1B 19kDa interacting protein 3	BNIP3
7982294	hypothetical LOC440261 /// OTU domain containing 7A	MGC131512 /// OTUD7A
7989094	neural precursor cell expressed, developmentally down-regulated 4	NEDD4
7996393	core-binding factor, beta subunit	CBFB
8006187	ATPase family, AAA domain containing 5	ATAD5
8006325	suppressor of zeste 12 homolog (Drosophila)	SUZ12
8015642	MAX-like protein X /// PSMC3 interacting protein	MLX /// PSMC3IP
8020349	coiled-coil domain containing 29 /// hypothetical LOC644249	CCDC29 /// RP11-195B21.3
8020903	UDP-N-acetyl-alpha-D-galactosamine:polypeptide N-acetylgalactosaminyltransferase 1 (GalNAc-T1)	GALNT1
8021286	chromosome 18 open reading frame 54	C18orf54
8027348	zinc finger protein 730	ZNF730
8046408	pyruvate dehydrogenase kinase, isozyme 1	PDK1
8054769	HBV preS1-transactivated protein 4	PS1TP4

8056572	SPC25, NDC80 kinetochore complex component, homolog (S. cerevisiae)	SPC25
8059350	adaptor-related protein complex 1, sigma 3 subunit	AP1S3
8063755	chromosome 20 open reading frame 177	C20orf177
8069561	basic transcription factor 3-like 4	BTF3L4
8083594	pentraxin-related gene, rapidly induced by IL-1 beta /// pentraxin 3, long	PTX3 /// PTX3
8088680	chromosome 3 open reading frame 64	C3orf64
8091283	procollagen-lysine, 2-oxoglutarate 5-dioxygenase 2	PLOD2
8096098	COP9 constitutive photomorphogenic homolog subunit 4 (Arabidopsis)	COPS4
8100328	ubiquitin specific peptidase 46	USP46
8101143	nucleoporin 54kDa	NUP54
8105842	centromere protein H	CENPH
8106743	versican	VCAN
8108693	protocadherin beta 4	PCDHB4
8109712	hyaluronan-mediated motility receptor (RHAMM)	HMMR
8113800	fibrillin 2	FBN2
8115851	stanniocalcin 2	STC2
8117225	geminin, DNA replication inhibitor	GMNN
8119067	potassium channel tetramerisation domain containing 20	KCTD20
8124518	histone cluster 1, H2aj	HIST1H2AJ
8128329	chromosome 6 open reading frame 167	C6orf167
8128669	osteopetrosis associated transmembrane protein 1	OSTM1
8140955	cyclin-dependent kinase 6	CDK6
8144228	hypothetical LOC645524	FLJ36840
8150149	similar to Potassium channel tetramerisation domain containing 9	LOC642513
8151532	fatty acid binding protein 4, adipocyte	FABP4
8151559	solute carrier family 10 (sodium/bile acid cotransporter family), member 5	SLC10A5
8152582	defective in sister chromatid cohesion 1 homolog (S. cerevisiae)	DSCC1
8157233	hydroxysteroid dehydrogenase like 2	HSDL2
8170097	solute carrier family 9 (sodium/hydrogen exchanger), member 6	SLC9A6
8170119	four and a half LIM domains 1	FHL1
8173732	TAF9B RNA polymerase II, TATA box binding protein (TBP)-associated factor, 31kDa	TAF9B
8176263	TAF9B RNA polymerase II, TATA box binding protein (TBP)-associated factor, 31kDa	TAF9B

Human Gene 1.0 ST array – targets up-regulated by miR-105 - more than 2.0 fold

Transcript Cluster ID	Gene Title	Gene Symbol
7952036	myelin protein zero-like 3	MPZL3
7968029	C1q and tumor necrosis factor related protein 9B /// prostate collagen triple helix	C1QTNF9B /// PCOTH
7972239	SLIT and NTRK-like family, member 6	SLITRK6
7994058	sodium channel, nonvoltage-gated 1, gamma	SCNN1G
8001564	docking protein 4	DOK4
8008627	noggin	NOG
8017885	ATP-binding cassette, sub-family A (ABC1), member 8	ABCA8
8021635	serpin peptidase inhibitor, clade B (ovalbumin), member 10 /// serpin peptidase inhibitor, clade B (ovalbumin), member 2	SERPINB10 /// SERPINB2
8022747	UDP-Gal:betaGlcNAc beta 1,4-galactosyltransferase, polypeptide 6	B4GALT6
8037205	carcinoembryonic antigen-related cell adhesion molecule 1 (biliary glycoprotein)	CEACAM1
8072678	heme oxygenase (decycling) 1	HMOX1
8077160	arylsulfatase A	ARSA
8086530	transmembrane protein 158 (gene/pseudogene)	TMEM158
8087825	abhydrolase domain containing 14B	ABHD14B
8105077	caspase recruitment domain family, member 6	CARD6
8111915	selenoprotein P, plasma, 1	SEPP1
8131179	tweety homolog 3 (Drosophila)	TTYH3
8148917	major facilitator superfamily domain containing 3	MFSD3
8156770	UDP-N-acetyl-alpha-D-galactosamine:polypeptide N-acetylgalactosaminyltransferase 12 (GalNAc-T12)	GALNT12
8160452	cyclin-dependent kinase inhibitor 2B (p15, inhibits CDK4)	CDKN2B
8167560	G antigen 10 /// G antigen 12J /// G antigen 13 /// G antigen 8 /// G antigen 7 /// G antigen 12I /// G antigen 12G /// G antigen 12F /// G antigen 12B /// G antigen 2C /// G antigen 6 /// G antigen 2A /// G antigen 12D /// G antigen 12C /// G antigen 12E /// G antigen 12H /// G antigen 2E	GAGE10 /// GAGE12J /// GAGE13 /// GAGE8 /// GAGE7 /// GAGE12I /// GAGE12G /// GAGE12F /// GAGE12B /// GAGE2C /// GAGE6 /// GAGE2A /// GAGE12D /// GAGE12C /// GAGE12E /// GAGE12H /// GAGE2E
8174598	interleukin 13 receptor, alpha 2	IL13RA2

REFERENCE LIST

1. **Alimirah, F., J. Chen, Z. Basrawala, H. Xin, and D. Choubey.** 2006. DU-145 and PC-3 human prostate cancer cell lines express androgen receptor: implications for the androgen receptor functions and regulation. FEBS Lett **580:**2294-2300.

2. **Ambros, V., and R. C. Lee.** 2004. Identification of microRNAs and other tiny noncoding RNAs by cDNA cloning. Methods Mol Biol **265:**131-158.

3. **Amodio, N., M. Scrima, L. Palaia, A. N. Salman, A. Quintiero, R. Franco, G. Botti, P. Pirozzi, G. Rocco, N. De Rosa, and G. Viglietto.** 2010. Oncogenic role of the E3 ubiquitin ligase NEDD4-1, a PTEN negative regulator, in non-small-cell lung carcinomas. Am J Pathol **177:**2622-2634.

4. **Ando, T., T. Yoshida, S. Enomoto, K. Asada, M. Tatematsu, M. Ichinose, T. Sugiyama, and T. Ushijima.** 2009. DNA methylation of microRNA genes in gastric mucosae of gastric cancer patients: its possible involvement in the formation of epigenetic field defect. Int J Cancer **124:**2367-2374.

5. **Aqeilan, R. I., G. A. Calin, and C. M. Croce.** 2010. miR-15a and miR-16-1 in cancer: discovery, function and future perspectives. Cell Death Differ **17:**215-220.

6. **Bagshaw, M. A., G. R. Ray, D. A. Pistenma, R. A. Castellino, and E. M. Meares.** 1975. External beam radiation therapy of primary carcinoma of the prostate. Cancer **36:**723-728.

7. **Bazzini, A. A., M. T. Lee, and A. J. Giraldez.** 2012. Ribosome profiling shows that miR-430 reduces translation before causing mRNA decay in zebrafish. Science **336:**233-237.

8. **Behm-Ansmant, I., J. Rehwinkel, T. Doerks, A. Stark, P. Bork, and E. Izaurralde.** 2006. mRNA degradation by miRNAs and GW182 requires both CCR4:NOT deadenylase and DCP1:DCP2 decapping complexes. Genes Dev **20:**1885-1898.

9. **Benakanakere, M. R., Q. Li, M. A. Eskan, A. V. Singh, J. Zhao, J. C. Galicia, P. Stathopoulou, T. B. Knudsen, and D. F. Kinane.** 2009. Modulation of TLR2 protein expression by miR-105 in human oral keratinocytes. J Biol Chem **284:**23107-23115.

10. **Berezikov, E., G. van Tetering, M. Verheul, J. van de Belt, L. van Laake, J. Vos, R. Verloop, M. van de Wetering, V. Guryev, S. Takada, A. J. van Zonneveld, H. Mano, R. Plasterk, and E. Cuppen.** 2006. Many novel mammalian microRNA candidates identified by extensive cloning and RAKE analysis. Genome Res **16:**1289-1298.

11. **Bernstein, E., S. Y. Kim, M. A. Carmell, E. P. Murchison, H. Alcorn, M. Z. Li, A. A. Mills, S. J. Elledge, K. V. Anderson, and G. J. Hannon.** 2003. Dicer is essential for mouse development. Nat Genet **35:**215-217.

12. **Borchert, G. M., W. Lanier, and B. L. Davidson.** 2006. RNA polymerase III transcribes human microRNAs. Nat Struct Mol Biol **13:**1097-1101.

13. **Bou Kheir, T., E. Futoma-Kazmierczak, A. Jacobsen, A. Krogh, L. Bardram, C. Hother, K. Gronbaek, B. Federspiel, A. H. Lund, and L. Friis-Hansen.** 2011. miR-449 inhibits cell proliferation and is down-regulated in gastric cancer. Mol Cancer **10:**29.

14. **Brase, J. C., M. Johannes, T. Schlomm, M. Falth, A. Haese, T. Steuber, T. Beissbarth, R. Kuner, and H. Sultmann.** 2011. Circulating miRNAs are correlated with tumor progression in prostate cancer. Int J Cancer **128:**608-616.

15. **Braun, J. E., E. Huntzinger, M. Fauser, and E. Izaurralde.** 2011. GW182 proteins directly recruit cytoplasmic deadenylase complexes to miRNA targets. Mol Cell **44:**120-133.

16. **Bubendorf, L., A. Schopfer, U. Wagner, G. Sauter, H. Moch, N. Willi, T. C. Gasser, and M. J. Mihatsch.** 2000. Metastatic patterns of prostate cancer: an autopsy study of 1,589 patients. Hum Pathol **31:**578-583.

17. **Burnett, J. C., and J. J. Rossi.** 2012. RNA-based therapeutics: current progress and future prospects. Chem Biol **19:**60-71.

18. **Cai, X., C. H. Hagedorn, and B. R. Cullen.** 2004. Human microRNAs are processed from capped, polyadenylated transcripts that can also function as mRNAs. RNA **10:**1957-1966.

19. **Calin, G. A., and C. M. Croce.** 2006. MicroRNA-cancer connection: the beginning of a new tale. Cancer Res **66:**7390-7394.

20. **Calin, G. A., C. D. Dumitru, M. Shimizu, R. Bichi, S. Zupo, E. Noch, H. Aldler, S. Rattan, M. Keating, K. Rai, L. Rassenti, T. Kipps, M. Negrini, F. Bullrich, and C. M. Croce.** 2002. Frequent deletions and down-regulation of micro- RNA genes miR15 and miR16 at 13q14 in chronic lymphocytic leukemia. Proc Natl Acad Sci U S A **99:**15524-15529.

21. **Calin, G. A., C. Sevignani, C. D. Dumitru, T. Hyslop, E. Noch, S. Yendamuri, M. Shimizu, S. Rattan, F. Bullrich, M. Negrini, and C. M. Croce.** 2004. Human microRNA genes are frequently located at fragile sites and genomic regions involved in cancers. Proc Natl Acad Sci U S A **101:**2999-3004.

22. **Carleton, M., M. A. Cleary, and P. S. Linsley.** 2007. MicroRNAs and cell cycle regulation. Cell Cycle **6:**2127-2132.

23. **Carlsson, J., G. Helenius, M. Karlsson, Z. Lubovac, O. Andren, B. Olsson, and K. Klinga-Levan.** 2010. Validation of suitable endogenous control genes for expression studies of miRNA in prostate cancer tissues. Cancer Genet Cytogenet **202:**71-75.

24. **Carroll, A. G., H. J. Voeller, L. Sugars, and E. P. Gelmann.** 1993. p53 oncogene mutations in three human prostate cancer cell lines. Prostate **23:**123-134.

25. **Chang, S. S., W. W. Jiang, I. Smith, L. M. Poeta, S. Begum, C. Glazer, S. Shan, W. Westra, D. Sidransky, and J. A. Califano.** 2008. MicroRNA alterations in head and neck squamous cell carcinoma. Int J Cancer **123:**2791-2797.

26. **Cheloufi, S., C. O. Dos Santos, M. M. Chong, and G. J. Hannon.** 2010. A dicer-independent miRNA biogenesis pathway that requires Ago catalysis. Nature **465:**584-589.

27. **Chen, P. Y., H. Manninga, K. Slanchev, M. Chien, J. J. Russo, J. Ju, R. Sheridan, B. John, D. S. Marks, D. Gaidatzis, C. Sander, M. Zavolan, and T. Tuschl.** 2005. The developmental miRNA profiles of zebrafish as determined by small RNA cloning. Genes Dev **19:**1288-1293.

28. **Cimmino, A., G. A. Calin, M. Fabbri, M. V. Iorio, M. Ferracin, M. Shimizu, S. E. Wojcik, R. I. Aqeilan, S. Zupo, M. Dono, L. Rassenti, H. Alder, S. Volinia, C. G. Liu, T. J. Kipps, M. Negrini, and C. M. Croce.** 2005. miR-15 and miR-16 induce apoptosis by targeting BCL2. Proc Natl Acad Sci U S A **102:**13944-13949.

29. **Clape, C., V. Fritz, C. Henriquet, F. Apparailly, P. L. Fernandez, F. Iborra, C. Avances, M. Villalba, S. Culine, and L. Fajas.** 2009. miR-143 interferes with ERK5 signaling, and abrogates prostate cancer progression in mice. PLoS One **4:**e7542.

30. **Cole, K. A., E. F. Attiyeh, Y. P. Mosse, M. J. Laquaglia, S. J. Diskin, G. M. Brodeur, and J. M. Maris.** 2008. A functional screen identifies miR-34a as a candidate neuroblastoma tumor suppressor gene. Mol Cancer Res **6:**735-742.

31. **Corcoran, C., A. M. Friel, M. J. Duffy, J. Crown, and L. O'Driscoll.** 2011. Intracellular and extracellular microRNAs in breast cancer. Clin Chem **57:**18-32.

32. **Cordon-Cardo, C., A. Koff, M. Drobnjak, P. Capodieci, I. Osman, S. S. Millard, P. B. Gaudin, M. Fazzari, Z. F. Zhang, J. Massague, and H. I. Scher.** 1998. Distinct altered patterns of p27KIP1 gene expression in benign prostatic hyperplasia and prostatic carcinoma. J Natl Cancer Inst **90:**1284-1291.

33. **Cortez, M. A., C. Bueso-Ramos, J. Ferdin, G. Lopez-Berestein, A. K. Sood, and G. A. Calin.** 2011. MicroRNAs in body fluids--the mix of hormones and biomarkers. Nat Rev Clin Oncol **8:**467-477.

34. **Costello, J. F., C. Plass, W. Arap, V. M. Chapman, W. A. Held, M. S. Berger, H. J. Su Huang, and W. K. Cavenee.** 1997. Cyclin-dependent kinase 6 (CDK6) amplification in human gliomas identified using two-dimensional separation of genomic DNA. Cancer Res **57:**1250-1254.

35. **Dagan, L. N., X. Jiang, S. Bhatt, E. Cubedo, K. Rajewsky, and I. S. Lossos.** 2012. miR-155 regulates HGAL expression and increases lymphoma cell motility. Blood **119:**513-520.

36. **Dar, A. A., S. Majid, D. de Semir, M. Nosrati, V. Bezrookove, and M. Kashani-Sabet.** 2011. miRNA-205 suppresses melanoma cell proliferation and induces senescence via regulation of E2F1 protein. J Biol Chem **286:**16606-16614.

37. **Darget, R.** 1955. [Ischio-rectal implantation of radium needles in certain cases of cancer of the prostate]. Bord Chir **2:**109-110.

38. **Dat le, T., T. Matsuo, T. Yoshimaru, S. Kakiuchi, H. Goto, M. Hanibuchi, T. Kuramoto, Y. Nishioka, S. Sone, and T. Katagiri.** 2012. Identification of genes potentially involved in bone metastasis by genome-wide gene expression profile analysis of non-small cell lung cancer in mice. Int J Oncol **40:**1455-1469.

39. **Denmeade, S. R., and J. T. Isaacs.** 2002. A history of prostate cancer treatment. Nat Rev Cancer **2:**389-396.

40. **Di Cristofano, A., M. De Acetis, A. Koff, C. Cordon-Cardo, and P. P. Pandolfi.** 2001. Pten and p27KIP1 cooperate in prostate cancer tumor suppression in the mouse. Nat Genet **27:**222-224.

41. **Djuranovic, S., A. Nahvi, and R. Green.** 2012. miRNA-mediated gene silencing by translational repression followed by mRNA deadenylation and decay. Science **336:**237-240.

42. **Dong, J. T., J. C. Boyd, and H. F. Frierson, Jr.** 2001. Loss of heterozygosity at 13q14 and 13q21 in high grade, high stage prostate cancer. Prostate **49:**166-171.

43. **Dueck, A., C. Ziegler, A. Eichner, E. Berezikov, and G. Meister.** 2012. microRNAs associated with the different human Argonaute proteins. Nucleic Acids Res.

44. **Duriez, P. J., and G. M. Shah.** 1997. Cleavage of poly(ADP-ribose) polymerase: a sensitive parameter to study cell death. Biochem Cell Biol **75:**337-349.

45. **Dweep, H., C. Sticht, P. Pandey, and N. Gretz.** 2011. miRWalk--database: prediction of possible miRNA binding sites by "walking" the genes of three genomes. J Biomed Inform **44:**839-847.

46. **Eis, P. S., W. Tam, L. Sun, A. Chadburn, Z. Li, M. F. Gomez, E. Lund, and J. E. Dahlberg.** 2005. Accumulation of miR-155 and BIC RNA in human B cell lymphomas. Proc Natl Acad Sci U S A **102:**3627-3632.

47. **Elkayam, E., C. D. Kuhn, A. Tocilj, A. D. Haase, E. M. Greene, G. J. Hannon, and L. Joshua-Tor.** 2012. The Structure of Human Argonaute-2 in Complex with miR-20a. Cell **150:**100-110.

48. **Ellison, L. F., and K. Wilkins.** 2012. Canadian trends in cancer prevalence. Health Rep **23:**7-16.

49. **Enciu, A. M., B. O. Popescu, and A. Gheorghisan-Galateanu.** 2012. MicroRNAs in brain development and degeneration. Mol Biol Rep **39:**2243-2252.

50. **Espinoza-Lewis, R. A., and D. Z. Wang.** 2012. MicroRNAs in heart development. Curr Top Dev Biol **100:**279-317.

51. **Fabian, M. R., and N. Sonenberg.** 2012. The mechanics of miRNA-mediated gene silencing: a look under the hood of miRISC. Nat Struct Mol Biol **19:**586-593.

52. **Feldman, B. J., and D. Feldman.** 2001. The development of androgen-independent prostate cancer. Nat Rev Cancer **1:**34-45.

53. **Fire, A., S. Xu, M. K. Montgomery, S. A. Kostas, S. E. Driver, and C. C. Mello.** 1998. Potent and specific genetic interference by double-stranded RNA in Caenorhabditis elegans. Nature **391:**806-811.

54. **Firestein, R., A. J. Bass, S. Y. Kim, I. F. Dunn, S. J. Silver, I. Guney, E. Freed, A. H. Ligon, N. Vena, S. Ogino, M. G. Chheda, P. Tamayo, S. Finn, Y. Shrestha, J. S. Boehm, S. Jain, E. Bojarski, C. Mermel, J. Barretina, J. A. Chan, J. Baselga, J. Tabernero, D. E. Root, C. S. Fuchs, M. Loda, R. A. Shivdasani, M. Meyerson, and W. C. Hahn.** 2008. CDK8 is a colorectal cancer oncogene that regulates beta-catenin activity. Nature **455:**547-551.

55. **Friedman, R. C., K. K. Farh, C. B. Burge, and D. P. Bartel.** 2009. Most mammalian mRNAs are conserved targets of microRNAs. Genome Res **19:**92-105.

56. **Fukaya, T., and Y. Tomari.** 2011. PABP is not essential for microRNA-mediated translational repression and deadenylation in vitro. EMBO J **30:**4998-5009.

57. **Gandellini, P., M. Folini, N. Longoni, M. Pennati, M. Binda, M. Colecchia, R. Salvioni, R. Supino, R. Moretti, P. Limonta, R. Valdagni, M. G. Daidone, and N. Zaffaroni.** 2009. miR-205 Exerts tumor-suppressive functions in human prostate through down-regulation of protein kinase Cepsilon. Cancer Res **69:**2287-2295.

58. **Gao, W., J. Xu, L. Liu, H. Shen, H. Zeng, and Y. Shu.** 2012. A systematic-analysis of predicted miR-21 targets identifies a signature for lung cancer. Biomed Pharmacother **66:**21-28.

59. **Garzon, R., G. Marcucci, and C. M. Croce.** 2010. Targeting microRNAs in cancer: rationale, strategies and challenges. Nat Rev Drug Discov **9:**775-789.

60. **Gibbons, R. P.** 1987. Prostate cancer. Chemotherapy. Cancer **60:**586-588.

61. **Gommans, W. M., and E. Berezikov.** 2012. Controlling miRNA regulation in disease. Methods Mol Biol **822:**1-18.

62. **Gordanpour, A., R. K. Nam, L. Sugar, and A. Seth.** 2012. MicroRNAs in prostate cancer: from biomarkers to molecularly-based therapeutics. Prostate Cancer Prostatic Dis.

63. **Gregory, R. I., T. P. Chendrimada, N. Cooch, and R. Shiekhattar.** 2005. Human RISC couples microRNA biogenesis and posttranscriptional gene silencing. Cell **123:**631-640.

64. **Gregory, R. I., T. P. Chendrimada, and R. Shiekhattar.** 2006. MicroRNA biogenesis: isolation and characterization of the microprocessor complex. Methods Mol Biol **342:**33-47.

65. **Gregory, R. I., K. P. Yan, G. Amuthan, T. Chendrimada, B. Doratotaj, N. Cooch, and R. Shiekhattar.** 2004. The Microprocessor complex mediates the genesis of microRNAs. Nature **432:**235-240.

66. **Griffiths-Jones, S., H. K. Saini, S. van Dongen, and A. J. Enright.** 2008. miRBase: tools for microRNA genomics. Nucleic Acids Res **36:**D154-158.

67. **Gu, S., L. Jin, F. Zhang, Y. Huang, D. Grimm, J. J. Rossi, and M. A. Kay.** 2011. Thermodynamic stability of small hairpin RNAs highly influences the loading process of different mammalian Argonautes. Proc Natl Acad Sci U S A **108:**9208-9213.

68. **Guo, H., N. T. Ingolia, J. S. Weissman, and D. P. Bartel.** 2010. Mammalian microRNAs predominantly act to decrease target mRNA levels. Nature **466:**835-840.

69. **Haase, A. D., L. Jaskiewicz, H. Zhang, S. Laine, R. Sack, A. Gatignol, and W. Filipowicz.** 2005. TRBP, a regulator of cellular PKR and HIV-1 virus expression, interacts with Dicer and functions in RNA silencing. EMBO Rep **6:**961-967.

70. **Hammond, S. M., S. Boettcher, A. A. Caudy, R. Kobayashi, and G. J. Hannon.** 2001. Argonaute2, a link between genetic and biochemical analyses of RNAi. Science **293:**1146-1150.

71. **Han, J., Y. Lee, K. H. Yeom, Y. K. Kim, H. Jin, and V. N. Kim.** 2004. The Drosha-DGCR8 complex in primary microRNA processing. Genes Dev **18:**3016-3027.

72. **Han, J., Y. Lee, K. H. Yeom, J. W. Nam, I. Heo, J. K. Rhee, S. Y. Sohn, Y. Cho, B. T. Zhang, and V. N. Kim.** 2006. Molecular basis for the recognition of primary microRNAs by the Drosha-DGCR8 complex. Cell **125:**887-901.

73. **Han, L., P. D. Witmer, E. Casey, D. Valle, and S. Sukumar.** 2007. DNA methylation regulates MicroRNA expression. Cancer Biol Ther **6:**1284-1288.

74. **Hassan, O., A. Ahmad, S. Sethi, and F. H. Sarkar.** 2012. Recent updates on the role of microRNAs in prostate cancer. J Hematol Oncol **5:**9.

75. **Hawkins, S. M., G. M. Buchold, and M. M. Matzuk.** 2011. Minireview: The roles of small RNA pathways in reproductive medicine. Mol Endocrinol **25:**1257-1279.

76. **He, L., and G. J. Hannon.** 2004. MicroRNAs: small RNAs with a big role in gene regulation. Nat Rev Genet **5:**522-531.

77. **Hong, L., J. Yang, Y. Han, Q. Lu, J. Cao, and L. Syed.** 2012. High expression of miR-210 predicts poor survival in patients with breast cancer: A meta-analysis. Gene **507:**135-138.

78. **Huggins, C.** 1967. Endocrine-induced regression of cancers. Science **156:**1050-1054.

79. **Huggins, C., and P. J. Clark.** 1940. Quantitative Studies of Prostatic Secretion : Ii. The Effect of Castration and of Estrogen Injection on the Normal and on the Hyperplastic Prostate Glands of Dogs. J Exp Med **72:**747-762.

80. **Humphreys, D. T., B. J. Westman, D. I. Martin, and T. Preiss.** 2005. MicroRNAs control translation initiation by inhibiting eukaryotic initiation factor 4E/cap and poly(A) tail function. Proc Natl Acad Sci U S A **102:**16961-16966.

81. **Huntzinger, E., and E. Izaurralde.** 2011. Gene silencing by microRNAs: contributions of translational repression and mRNA decay. Nat Rev Genet **12:**99-110.

82. **Huse, J. T., C. Brennan, D. Hambardzumyan, B. Wee, J. Pena, S. H. Rouhanifard, C. Sohn-Lee, C. le Sage, R. Agami, T. Tuschl, and E. C. Holland.** 2009. The PTEN-regulating microRNA miR-26a is amplified in high-grade glioma and facilitates gliomagenesis in vivo. Genes Dev **23:**1327-1337.

83. **Hutvagner, G., J. McLachlan, A. E. Pasquinelli, E. Balint, T. Tuschl, and P. D. Zamore.** 2001. A cellular function for the RNA-interference enzyme Dicer in the maturation of the let-7 small temporal RNA. Science **293:**834-838.

84. **Hutvagner, G., and P. D. Zamore.** 2002. A microRNA in a multiple-turnover RNAi enzyme complex. Science **297:**2056-2060.

85. **Jewett, H. J.** 1976. Radical perineal prostatectomy for prostatic cancer. Prog Clin Biol Res **6:**205-218.

86. **Jones, C. I., M. V. Zabolotskaya, and S. F. Newbury.** 2012. The 5' --> 3' exoribonuclease XRN1/Pacman and its functions in cellular processes and development. Wiley Interdiscip Rev RNA **3:**455-468.

87. **Jovanovic, M., and M. O. Hengartner.** 2006. miRNAs and apoptosis: RNAs to die for. Oncogene **25:**6176-6187.

88. **Jurmeister, S., M. Baumann, A. Balwierz, I. Keklikoglou, A. Ward, S. Uhlmann, J. D. Zhang, S. Wiemann, and O. Sahin.** 2012. MicroRNA-200c represses migration and invasion of breast cancer cells by targeting actin-regulatory proteins FHOD1 and PPM1F. Mol Cell Biol **32:**633-651.

89. **Kaighn, M. E., K. S. Narayan, Y. Ohnuki, J. F. Lechner, and L. W. Jones.** 1979. Establishment and characterization of a human prostatic carcinoma cell line (PC-3). Invest Urol **17:**16-23.

90. **Kalluri, R., and R. A. Weinberg.** 2009. The basics of epithelial-mesenchymal transition. J Clin Invest **119:**1420-1428.

91. **Kamitani, S., Y. Yamauchi, S. Kawasaki, K. Takami, H. Takizawa, T. Nagase, and T. Kohyama.** 2011. Simultaneous stimulation with TGF-beta1 and TNF-alpha induces epithelial mesenchymal transition in bronchial epithelial cells. Int Arch Allergy Immunol **155:**119-128.

92. **Kanwal, R., M. Pandey, N. Bhaskaran, G. T. Maclennan, P. Fu, L. E. Ponsky, and S. Gupta.** 2012. Protection against oxidative DNA damage and stress in human prostate by glutathione S-transferase P1. Mol Carcinog.

93. **Ke, N., A. Albers, G. Claassen, D. H. Yu, J. E. Chatterton, X. Hu, B. Meyhack, F. Wong-Staal, and Q. X. Li.** 2004. One-week 96-well soft agar growth assay for cancer target validation. Biotechniques **36:**826-828, 830, 832-823.

94. **Kedde, M., M. J. Strasser, B. Boldajipour, J. A. Oude Vrielink, K. Slanchev, C. le Sage, R. Nagel, P. M. Voorhoeve, J. van Duijse, U. A. Orom, A. H. Lund, A. Perrakis, E. Raz, and R. Agami.** 2007. RNA-binding protein Dnd1 inhibits microRNA access to target mRNA. Cell **131:**1273-1286.

95. **Kefas, B., L. Comeau, D. H. Floyd, O. Seleverstov, J. Godlewski, T. Schmittgen, J. Jiang, C. G. diPierro, Y. Li, E. A. Chiocca, J. Lee, H. Fine, R. Abounader, S. Lawler, and B. Purow.** 2009. The neuronal microRNA miR-326 acts in a feedback loop with notch and has therapeutic potential against brain tumors. J Neurosci **29:**15161-15168.

96. **Kelly, E. J., E. M. Hadac, S. Greiner, and S. J. Russell.** 2008. Engineering microRNA responsiveness to decrease virus pathogenicity. Nat Med **14:**1278-1283.

97. **Khvorova, A., A. Reynolds, and S. D. Jayasena.** 2003. Functional siRNAs and miRNAs exhibit strand bias. Cell **115:**209-216.

98. **Kim, V. N., and J. W. Nam.** 2006. Genomics of microRNA. Trends Genet **22:**165-173.

99. **Kjellen, L., and U. Lindahl.** 1991. Proteoglycans: structures and interactions. Annu Rev Biochem **60:**443-475.

100. **Kloosterman, W. P., and R. H. Plasterk.** 2006. The diverse functions of microRNAs in animal development and disease. Dev Cell **11:**441-450.

101. **Kolfschoten, I. G., E. Roggli, V. Nesca, and R. Regazzi.** 2009. Role and therapeutic potential of microRNAs in diabetes. Diabetes Obes Metab **11 Suppl 4:**118-129.

102. **Kong, D., Y. Li, Z. Wang, S. Banerjee, A. Ahmad, H. R. Kim, and F. H. Sarkar.** 2009. miR-200 regulates PDGF-D-mediated epithelial-mesenchymal transition, adhesion, and invasion of prostate cancer cells. Stem Cells **27:**1712-1721.

103. **Kuriyama, M., M. C. Wang, C. I. Lee, L. D. Papsidero, C. S. Killian, H. Inaji, N. H. Slack, T. Nishiura, G. P. Murphy, and T. M. Chu.** 1981. Use of human prostate-specific antigen in monitoring prostate cancer. Cancer Res **41:**3874-3876.

104. **Kwak, P. B., and Y. Tomari.** 2012. The N domain of Argonaute drives duplex unwinding during RISC assembly. Nat Struct Mol Biol **19:**145-151.

105. **Lagos-Quintana, M., R. Rauhut, W. Lendeckel, and T. Tuschl.** 2001. Identification of novel genes coding for small expressed RNAs. Science **294:**853-858.

106. **Landgraf, P., M. Rusu, R. Sheridan, A. Sewer, N. Iovino, A. Aravin, S. Pfeffer, A. Rice, A. O. Kamphorst, M. Landthaler, C. Lin, N. D. Socci, L. Hermida, V. Fulci, S. Chiaretti, R. Foa, J. Schliwka, U. Fuchs, A. Novosel, R. U. Muller, B. Schermer, U. Bissels, J. Inman, Q. Phan, M. Chien, D. B. Weir, R. Choksi, G. De Vita, D. Frezzetti, H. I. Trompeter, V. Hornung, G. Teng, G. Hartmann, M. Palkovits, R. Di Lauro, P. Wernet, G. Macino, C. E. Rogler, J. W. Nagle, J. Ju, F. N. Papavasiliou, T. Benzing, P. Lichter, W. Tam, M. J. Brownstein, A. Bosio, A. Borkhardt, J. J. Russo, C. Sander, M. Zavolan, and T. Tuschl.** 2007. A mammalian microRNA expression atlas based on small RNA library sequencing. Cell **129:**1401-1414.

107. **Lau, N. C., L. P. Lim, E. G. Weinstein, and D. P. Bartel.** 2001. An abundant class of tiny RNAs with probable regulatory roles in Caenorhabditis elegans. Science **294:**858-862.

108. **Lau, P. W., K. Z. Guiley, N. De, C. S. Potter, B. Carragher, and I. J. MacRae.** 2012. The molecular architecture of human Dicer. Nat Struct Mol Biol **19:**436-440.

109. **Lee, E. J., M. Baek, Y. Gusev, D. J. Brackett, G. J. Nuovo, and T. D. Schmittgen.** 2008. Systematic evaluation of microRNA processing patterns in tissues, cell lines, and tumors. RNA **14:**35-42.

110. **Lee, I., S. S. Ajay, J. I. Yook, H. S. Kim, S. H. Hong, N. H. Kim, S. M. Dhanasekaran, A. M. Chinnaiyan, and B. D. Athey.** 2009. New class of microRNA targets containing simultaneous 5'-UTR and 3'-UTR interaction sites. Genome Res **19:**1175-1183.

111. **Lee, K. H., C. Lotterman, C. Karikari, N. Omura, G. Feldmann, N. Habbe, M. G. Goggins, J. T. Mendell, and A. Maitra.** 2009. Epigenetic silencing of MicroRNA miR-107 regulates cyclin-dependent kinase 6 expression in pancreatic cancer. Pancreatology **9:**293-301.

112. **Lee, R. C., and V. Ambros.** 2001. An extensive class of small RNAs in Caenorhabditis elegans. Science **294:**862-864.

113. **Lee, R. C., R. L. Feinbaum, and V. Ambros.** 1993. The C. elegans heterochronic gene lin-4 encodes small RNAs with antisense complementarity to lin-14. Cell **75:**843-854.

114. **Lee, Y., C. Ahn, J. Han, H. Choi, J. Kim, J. Yim, J. Lee, P. Provost, O. Radmark, S. Kim, and V. N. Kim.** 2003. The nuclear RNase III Drosha initiates microRNA processing. Nature **425:**415-419.

115. **Lee, Y., I. Hur, S. Y. Park, Y. K. Kim, M. R. Suh, and V. N. Kim.** 2006. The role of PACT in the RNA silencing pathway. EMBO J **25:**522-532.

116. **Lee, Y., M. Kim, J. Han, K. H. Yeom, S. Lee, S. H. Baek, and V. N. Kim.** 2004. MicroRNA genes are transcribed by RNA polymerase II. EMBO J **23:**4051-4060.

117. **Lerner, M., M. Harada, J. Loven, J. Castro, Z. Davis, D. Oscier, M. Henriksson, O. Sangfelt, D. Grander, and M. M. Corcoran.** 2009. DLEU2, frequently deleted in malignancy, functions as a critical host gene of the cell cycle inhibitory microRNAs miR-15a and miR-16-1. Exp Cell Res **315:**2941-2952.

118. **Li, J., C. Yen, D. Liaw, K. Podsypanina, S. Bose, S. I. Wang, J. Puc, C. Miliaresis, L. Rodgers, R. McCombie, S. H. Bigner, B. C. Giovanella, M. Ittmann, B. Tycko, H. Hibshoosh, M. H. Wigler, and R. Parsons.** 1997. PTEN, a putative protein tyrosine phosphatase gene mutated in human brain, breast, and prostate cancer. Science **275:**1943-1947.

119. **Lim, J. T., M. Mansukhani, and I. B. Weinstein.** 2005. Cyclin-dependent kinase 6 associates with the androgen receptor and enhances its transcriptional activity in prostate cancer cells. Proc Natl Acad Sci U S A **102:**5156-5161.

120. **Liu, J., M. A. Carmell, F. V. Rivas, C. G. Marsden, J. M. Thomson, J. J. Song, S. M. Hammond, L. Joshua-Tor, and G. J. Hannon.** 2004. Argonaute2 is the catalytic engine of mammalian RNAi. Science **305:**1437-1441.

121. **Liu, J., F. V. Rivas, J. Wohlschlegel, J. R. Yates, 3rd, R. Parker, and G. J. Hannon.** 2005. A role for the P-body component GW182 in microRNA function. Nat Cell Biol **7:**1261-1266.

122. **Liu, J., M. A. Valencia-Sanchez, G. J. Hannon, and R. Parker.** 2005. MicroRNA-dependent localization of targeted mRNAs to mammalian P-bodies. Nat Cell Biol **7:**719-723.

123. **Liu, Y. N., J. J. Yin, W. Abou-Kheir, P. G. Hynes, O. M. Casey, L. Fang, M. Yi, R. M. Stephens, V. Seng, H. Sheppard-Tillman, P. Martin, and K. Kelly.** 2012. MiR-1 and miR-200 inhibit EMT via Slug-dependent and tumorigenesis via Slug-independent mechanisms. Oncogene.

124. **Llave, C., K. D. Kasschau, M. A. Rector, and J. C. Carrington.** 2002. Endogenous and silencing-associated small RNAs in plants. Plant Cell **14:**1605-1619.

125. **Llave, C., Z. Xie, K. D. Kasschau, and J. C. Carrington.** 2002. Cleavage of Scarecrow-like mRNA targets directed by a class of Arabidopsis miRNA. Science **297:**2053-2056.

126. **Lopez-Serra, P., and M. Esteller.** 2012. DNA methylation-associated silencing of tumor-suppressor microRNAs in cancer. Oncogene **31:**1609-1622.

127. **Lorenzen, J., R. Kumarswamy, S. Dangwal, and T. Thum.** 2012. MicroRNAs in diabetes and diabetes-associated complications. RNA Biol **9**.

128. **Lu, J., G. Getz, E. A. Miska, E. Alvarez-Saavedra, J. Lamb, D. Peck, A. Sweet-Cordero, B. L. Ebert, R. H. Mak, A. A. Ferrando, J. R. Downing, T. Jacks, H. R. Horvitz, and T. R. Golub.** 2005. MicroRNA expression profiles classify human cancers. Nature **435:**834-838.

129. **Lucas, J. J., J. Domenico, and E. W. Gelfand.** 2004. Cyclin-dependent kinase 6 inhibits proliferation of human mammary epithelial cells. Mol Cancer Res **2:**105-114.

130. **Lujambio, A., S. Ropero, E. Ballestar, M. F. Fraga, C. Cerrato, F. Setien, S. Casado, A. Suarez-Gauthier, M. Sanchez-Cespedes, A. Git, I. Spiteri, P. P. Das, C. Caldas, E. Miska, and M. Esteller.** 2007. Genetic unmasking of an epigenetically silenced microRNA in human cancer cells. Cancer Res **67:**1424-1429.

131. **Lund, E., S. Guttinger, A. Calado, J. E. Dahlberg, and U. Kutay.** 2004. Nuclear export of microRNA precursors. Science **303:**95-98.

132. **Ma, L., J. Teruya-Feldstein, and R. A. Weinberg.** 2007. Tumour invasion and metastasis initiated by microRNA-10b in breast cancer. Nature **449:**682-688.

133. **Maag, D., M. J. Maxwell, D. A. Hardesty, K. L. Boucher, N. Choudhari, A. G. Hanno, J. F. Ma, A. S. Snowman, J. W. Pietropaoli, R. Xu, P. B. Storm, A. Saiardi, S. H. Snyder, and A. C. Resnick.** 2011. Inositol polyphosphate multikinase is a physiologic PI3-kinase that activates Akt/PKB. Proc Natl Acad Sci U S A **108:**1391-1396.

134. **Massat, I., D. Souery, J. Del-Favero, L. Oruc, M. M. Noethen, D. Blackwood, M. Thomson, W. Muir, G. N. Papadimitriou, D. G. Dikeos, R. Kaneva, A. Serretti, R. Lilli, E. Smeraldi, M. Jakovljevic, V. Folnegovic, M. Rietschel, V. Milanova, F. Valente, C. Van Broeckhoven, and J. Mendlewicz.** 2002. Excess of allele1 for alpha3 subunit GABA receptor gene (GABRA3) in bipolar patients: a multicentric association study. Mol Psychiatry **7:**201-207.

135. **Mayr, C., and D. P. Bartel.** 2009. Widespread shortening of 3'UTRs by alternative cleavage and polyadenylation activates oncogenes in cancer cells. Cell **138:**673-684.

136. **McMenamin, M. E., P. Soung, S. Perera, I. Kaplan, M. Loda, and W. R. Sellers.** 1999. Loss of PTEN expression in paraffin-embedded primary prostate cancer correlates with high Gleason score and advanced stage. Cancer Res **59:**4291-4296.

137. **Melo, S. A., C. Moutinho, S. Ropero, G. A. Calin, S. Rossi, R. Spizzo, A. F. Fernandez, V. Davalos, A. Villanueva, G. Montoya, H. Yamamoto, S. Schwartz, Jr., and M. Esteller.** 2010. A genetic defect in exportin-5 traps precursor microRNAs in the nucleus of cancer cells. Cancer Cell **18:**303-315.

138. **Michael, M. Z., O. C. SM, N. G. van Holst Pellekaan, G. P. Young, and R. J. James.** 2003. Reduced accumulation of specific microRNAs in colorectal neoplasia. Mol Cancer Res **1:**882-891.

139. **Mickey, D. D., K. R. Stone, H. Wunderli, G. H. Mickey, and D. F. Paulson.** 1980. Characterization of a human prostate adenocarcinoma cell line (DU 145) as a monolayer culture and as a solid tumor in athymic mice. Prog Clin Biol Res **37:**67-84.

140. **Mitchell, P. S., R. K. Parkin, E. M. Kroh, B. R. Fritz, S. K. Wyman, E. L. Pogosova-Agadjanyan, A. Peterson, J. Noteboom, K. C. O'Briant, A. Allen, D. W. Lin, N. Urban, C. W. Drescher, B. S. Knudsen, D. L. Stirewalt, R. Gentleman, R. L. Vessella, P. S. Nelson, D. B. Martin, and M. Tewari.** 2008. Circulating microRNAs as stable blood-based markers for cancer detection. Proc Natl Acad Sci U S A **105:**10513-10518.

141. **Moretti, F., R. Thermann, and M. W. Hentze.** 2010. Mechanism of translational regulation by miR-2 from sites in the 5' untranslated region or the open reading frame. RNA **16:**2493-2502.

142. **Mourelatos, Z., J. Dostie, S. Paushkin, A. Sharma, B. Charroux, L. Abel, J. Rappsilber, M. Mann, and G. Dreyfuss.** 2002. miRNPs: a novel class of ribonucleoproteins containing numerous microRNAs. Genes Dev **16:**720-728.

143. **Muller, D. W., and A. K. Bosserhoff.** 2008. Integrin beta 3 expression is regulated by let-7a miRNA in malignant melanoma. Oncogene **27:**6698-6706.

144. **Nan, Y., L. Han, A. Zhang, G. Wang, Z. Jia, Y. Yang, X. Yue, P. Pu, Y. Zhong, and C. Kang.** 2010. MiRNA-451 plays a role as tumor suppressor in human glioma cells. Brain Res **1359:**14-21.

145. **Olsen, P. H., and V. Ambros.** 1999. The lin-4 regulatory RNA controls developmental timing in Caenorhabditis elegans by blocking LIN-14 protein synthesis after the initiation of translation. Dev Biol **216:**671-680.

146. **Ornstein, D. K., J. W. Gillespie, C. P. Paweletz, P. H. Duray, J. Herring, C. D. Vocke, S. L. Topalian, D. G. Bostwick, W. M. Linehan, E. F. Petricoin, 3rd, and M. R. Emmert-Buck.** 2000. Proteomic analysis of laser capture microdissected human prostate cancer and in vitro prostate cell lines. Electrophoresis **21:**2235-2242.

147. **Ortega, S., M. Malumbres, and M. Barbacid.** 2002. Cyclin D-dependent kinases, INK4 inhibitors and cancer. Biochim Biophys Acta **1602:**73-87.

148. **Pasquinelli, A. E., B. J. Reinhart, F. Slack, M. Q. Martindale, M. I. Kuroda, B. Maller, D. C. Hayward, E. E. Ball, B. Degnan, P. Muller, J. Spring, A. Srinivasan, M. Fishman, J. Finnerty, J. Corbo, M. Levine, P. Leahy, E. Davidson, and G. Ruvkun.** 2000. Conservation of the sequence and temporal expression of let-7 heterochronic regulatory RNA. Nature **408:**86-89.

149. **Peltier, H. J., and G. J. Latham.** 2008. Normalization of microRNA expression levels in quantitative RT-PCR assays: identification of suitable reference RNA targets in normal and cancerous human solid tissues. RNA **14:**844-852.

150. **Pentheroudakis, G., V. Golfinopoulos, and N. Pavlidis.** 2007. Switching benchmarks in cancer of unknown primary: from autopsy to microarray. Eur J Cancer **43:**2026-2036.

151. **Pienta, K. J., and D. C. Smith.** 2005. Advances in prostate cancer chemotherapy: a new era begins. CA Cancer J Clin **55:**300-318; quiz 323-305.

152. **Place, R. F., L. C. Li, D. Pookot, E. J. Noonan, and R. Dahiya.** 2008. MicroRNA-373 induces expression of genes with complementary promoter sequences. Proc Natl Acad Sci U S A **105:**1608-1613.

153. **Puissegur, M. P., N. M. Mazure, T. Bertero, L. Pradelli, S. Grosso, K. Robbe-Sermesant, T. Maurin, K. Lebrigand, B. Cardinaud, V. Hofman, S. Fourre, V. Magnone, J. E. Ricci, J. Pouyssegur, P. Gounon, P. Hofman, P. Barbry, and B. Mari.** 2011. miR-210 is overexpressed in late stages of lung cancer and mediates mitochondrial alterations associated with modulation of HIF-1 activity. Cell Death Differ **18:**465-478.

154. **Quero, L., L. Dubois, N. G. Lieuwes, C. Hennequin, and P. Lambin.** 2011. miR-210 as a marker of chronic hypoxia, but not a therapeutic target in prostate cancer. Radiother Oncol **101:**203-208.

155. **Ragde, H., H. C. Aldape, and C. M. Bagley, Jr.** 1988. Ultrasound-guided prostate biopsy. Biopty gun superior to aspiration. Urology **32:**503-506.

156. **Ragde, H., G. L. Grado, B. Nadir, and A. A. Elgamal.** 2000. Modern prostate brachytherapy. CA Cancer J Clin **50:**380-393.

157. **Reddy, S. D., S. B. Pakala, K. Ohshiro, S. K. Rayala, and R. Kumar.** 2009. MicroRNA-661, a c/EBPalpha target, inhibits metastatic tumor antigen 1 and regulates its functions. Cancer Res **69:**5639-5642.

158. **Rehwinkel, J., I. Behm-Ansmant, D. Gatfield, and E. Izaurralde.** 2005. A crucial role for GW182 and the DCP1:DCP2 decapping complex in miRNA-mediated gene silencing. RNA **11:**1640-1647.

159. **Reinhart, B. J., F. J. Slack, M. Basson, A. E. Pasquinelli, J. C. Bettinger, A. E. Rougvie, H. R. Horvitz, and G. Ruvkun.** 2000. The 21-nucleotide let-7 RNA regulates developmental timing in Caenorhabditis elegans. Nature **403:**901-906.

160. **Rhoades, M. W., B. J. Reinhart, L. P. Lim, C. B. Burge, B. Bartel, and D. P. Bartel.** 2002. Prediction of plant microRNA targets. Cell **110:**513-520.

161. **Ribas, J., X. Ni, M. Haffner, E. A. Wentzel, A. H. Salmasi, W. H. Chowdhury, T. A. Kudrolli, S. Yegnasubramanian, J. Luo, R. Rodriguez, J. T. Mendell, and S. E. Lupold.** 2009. miR-21: an androgen receptor-regulated microRNA that promotes hormone-dependent and hormone-independent prostate cancer growth. Cancer Res **69:**7165-7169.

162. **Ricciardelli, C., K. Mayne, P. J. Sykes, W. A. Raymond, K. McCaul, V. R. Marshall, and D. J. Horsfall.** 1998. Elevated levels of versican but not decorin predict disease progression in early-stage prostate cancer. Clin Cancer Res **4:**963-971.

163. **Ricciardelli, C., D. L. Russell, M. P. Ween, K. Mayne, S. Suwiwat, S. Byers, V. R. Marshall, W. D. Tilley, and D. J. Horsfall.** 2007. Formation of hyaluronan- and versican-rich pericellular matrix by prostate cancer cells promotes cell motility. J Biol Chem **282:**10814-10825.

164. **Ricciardelli, C., A. J. Sakko, M. P. Ween, D. L. Russell, and D. J. Horsfall.** 2009. The biological role and regulation of versican levels in cancer. Cancer Metastasis Rev **28:**233-245.

165. **Richardson, M. K., R. P. Crooijmans, and M. A. Groenen.** 2007. Sequencing and genomic annotation of the chicken (Gallus gallus) Hox clusters, and mapping of evolutionarily conserved regions. Cytogenet Genome Res **117:**110-119.

166. **Robb, G. B., and T. M. Rana.** 2007. RNA helicase A interacts with RISC in human cells and functions in RISC loading. Mol Cell **26:**523-537.

167. **Rodriguez, A., S. Griffiths-Jones, J. L. Ashurst, and A. Bradley.** 2004. Identification of mammalian microRNA host genes and transcription units. Genome Res **14:**1902-1910.

168. **Rosenwald, S., S. Gilad, S. Benjamin, D. Lebanony, N. Dromi, A. Faerman, H. Benjamin, R. Tamir, M. Ezagouri, E. Goren, I. Barshack, D. Nass, A. Tobar, M. Feinmesser, N. Rosenfeld, I. Leizerman, K. Ashkenazi, Y. Spector, A. Chajut, and R. Aharonov.** 2010. Validation of a microRNA-based qRT-PCR test for accurate identification of tumor tissue origin. Mod Pathol **23:**814-823.

169. **Ru, P., R. Steele, P. Newhall, N. J. Phillips, K. Toth, and R. B. Ray.** 2012. miRNA-29b suppresses prostate cancer metastasis by regulating epithelial-mesenchymal transition signaling. Mol Cancer Ther **11:**1166-1173.

170. **Sakr, W. A., D. J. Grignon, J. D. Crissman, L. K. Heilbrun, B. J. Cassin, J. J. Pontes, and G. P. Haas.** 1994. High grade prostatic intraepithelial neoplasia (HGPIN) and prostatic adenocarcinoma between the ages of 20-69: an autopsy study of 249 cases. In Vivo **8:**439-443.

171. **Salzman, D. W., J. Shubert-Coleman, and H. Furneaux.** 2007. P68 RNA helicase unwinds the human let-7 microRNA precursor duplex and is required for let-7-directed silencing of gene expression. J Biol Chem **282:**32773-32779.

172. **Sandberg, R., J. R. Neilson, A. Sarma, P. A. Sharp, and C. B. Burge.** 2008. Proliferating cells express mRNAs with shortened 3' untranslated regions and fewer microRNA target sites. Science **320:**1643-1647.

173. **Sarver, A. L., L. Li, and S. Subramanian.** 2010. MicroRNA miR-183 functions as an oncogene by targeting the transcription factor EGR1 and promoting tumor cell migration. Cancer Res **70:**9570-9580.

174. **Schaefer, A., M. Jung, H. J. Mollenkopf, I. Wagner, C. Stephan, F. Jentzmik, K. Miller, M. Lein, G. Kristiansen, and K. Jung.** 2010. Diagnostic and prognostic implications of microRNA profiling in prostate carcinoma. Int J Cancer **126:**1166-1176.

175. **Schmitter, D., J. Filkowski, A. Sewer, R. S. Pillai, E. J. Oakeley, M. Zavolan, P. Svoboda, and W. Filipowicz.** 2006. Effects of Dicer and Argonaute down-regulation on mRNA levels in human HEK293 cells. Nucleic Acids Res **34:**4801-4815.

176. **Sevli, S., A. Uzumcu, M. Solak, M. Ittmann, and M. Ozen.** 2010. The function of microRNAs, small but potent molecules, in human prostate cancer. Prostate Cancer Prostatic Dis **13:**208-217.

177. **Shi, X. B., L. Xue, J. Yang, A. H. Ma, J. Zhao, M. Xu, C. G. Tepper, C. P. Evans, H. J. Kung, and R. W. deVere White.** 2007. An androgen-regulated miRNA suppresses Bak1 expression and induces androgen-independent growth of prostate cancer cells. Proc Natl Acad Sci U S A **104:**19983-19988.

178. **Sikand, K., J. E. Slaibi, R. Singh, S. D. Slane, and G. C. Shukla.** 2011. miR 488* inhibits androgen receptor expression in prostate carcinoma cells. Int J Cancer **129:**810-819.

179. **Sirotkin, A. V., M. Laukova, D. Ovcharenko, P. Brenaut, and M. Mlyncek.** 2010. Identification of microRNAs controlling human ovarian cell proliferation and apoptosis. J Cell Physiol **223:**49-56.

180. **Slezak-Prochazka, I., S. Durmus, B. J. Kroesen, and A. van den Berg.** 2010. MicroRNAs, macrocontrol: regulation of miRNA processing. RNA **16:**1087-1095.

181. **Smits, M., J. Nilsson, S. E. Mir, P. M. van der Stoop, E. Hulleman, J. M. Niers, P. C. de Witt Hamer, V. E. Marquez, J. Cloos, A. M. Krichevsky, D. P. Noske, B. A. Tannous, and T. Wurdinger.** 2010. miR-101 is down-regulated in glioblastoma resulting in EZH2-induced proliferation, migration, and angiogenesis. Oncotarget **1:**710-720.

182. **Sobel, R. E., Y. Wang, and M. D. Sadar.** 2006. Molecular analysis and characterization of PrEC, commercially available prostate epithelial cells. In Vitro Cell Dev Biol Anim **42:**33-39.

183. **Statistics., C. C. S. s. S. C. o. C.** 2012. Canadian Cancer Statistics 2012. Canadian Cancer Society.

184. **Su, H., S. Meng, Y. Lu, M. I. Trombly, J. Chen, C. Lin, A. Turk, and X. Wang.** 2011. Mammalian hyperplastic discs homolog EDD regulates miRNA-mediated gene silencing. Mol Cell **43:**97-109.

185. **Sylvester, P. W.** 2011. Optimization of the tetrazolium dye (MTT) colorimetric assay for cellular growth and viability. Methods Mol Biol **716:**157-168.

186. **Szafranska, A. E., T. S. Davison, J. Shingara, M. Doleshal, J. A. Riggenbach, C. D. Morrison, S. Jewell, and E. Labourier.** 2008. Accurate molecular characterization of formalin-fixed, paraffin-embedded tissues by microRNA expression profiling. J Mol Diagn **10:**415-423.

187. **Szczyrba, J., E. Nolte, S. Wach, E. Kremmer, R. Stohr, A. Hartmann, W. Wieland, B. Wullich, and F. A. Grasser.** 2011. Downregulation of Sec23A protein by miRNA-375 in prostate carcinoma. Mol Cancer Res **9:**791-800.

188. **Takeshita, F., L. Patrawala, M. Osaki, R. U. Takahashi, Y. Yamamoto, N. Kosaka, M. Kawamata, K. Kelnar, A. G. Bader, D. Brown, and T. Ochiya.** 2010. Systemic delivery of synthetic microRNA-16 inhibits the growth of metastatic prostate tumors via downregulation of multiple cell-cycle genes. Mol Ther **18:**181-187.

189. **Thomson, D. W., C. P. Bracken, and G. J. Goodall.** 2011. Experimental strategies for microRNA target identification. Nucleic Acids Res **39:**6845-6853.

190. **van Rooij, E., and E. N. Olson.** 2007. MicroRNAs: powerful new regulators of heart disease and provocative therapeutic targets. J Clin Invest **117:**2369-2376.

191. **Visakorpi, T., E. Hyytinen, P. Koivisto, M. Tanner, R. Keinanen, C. Palmberg, A. Palotie, T. Tammela, J. Isola, and O. P. Kallioniemi.** 1995. In vivo amplification of the androgen receptor gene and progression of human prostate cancer. Nat Genet **9:**401-406.

192. **Volinia, S., G. A. Calin, C. G. Liu, S. Ambs, A. Cimmino, F. Petrocca, R. Visone, M. Iorio, C. Roldo, M. Ferracin, R. L. Prueitt, N. Yanaihara, G. Lanza, A. Scarpa, A. Vecchione, M. Negrini, C. C. Harris, and C. M. Croce.** 2006. A microRNA expression signature of human solid tumors defines cancer gene targets. Proc Natl Acad Sci U S A **103:**2257-2261.

193. **Wang, B., A. Yanez, and C. D. Novina.** 2008. MicroRNA-repressed mRNAs contain 40S but not 60S components. Proc Natl Acad Sci U S A **105:**5343-5348.

194. **Wang, S., J. Gao, Q. Lei, N. Rozengurt, C. Pritchard, J. Jiao, G. V. Thomas, G. Li, P. Roy-Burman, P. S. Nelson, X. Liu, and H. Wu.** 2003. Prostate-specific deletion of the murine Pten tumor suppressor gene leads to metastatic prostate cancer. Cancer Cell **4:**209-221.

195. **Wang, W., B. Peng, D. Wang, X. Ma, D. Jiang, J. Zhao, and L. Yu.** 2011. Human tumor microRNA signatures derived from large-scale oligonucleotide microarray datasets. International journal of cancer. Journal international du cancer **129:**1624-1634.

196. **Wang, X., and I. M. El Naqa.** 2008. Prediction of both conserved and nonconserved microRNA targets in animals. Bioinformatics **24:**325-332.

197. **Wang, X. H., R. Z. Qian, W. Zhang, S. F. Chen, H. M. Jin, and R. M. Hu.** 2009. MicroRNA-320 expression in myocardial microvascular endothelial cells and its relationship with insulin-like growth factor-1 in type 2 diabetic rats. Clin Exp Pharmacol Physiol **36:**181-188.

198. **Webber, M. M., D. Bello, and S. Quader.** 1997. Immortalized and tumorigenic adult human prostatic epithelial cell lines: characteristics and applications Part 2. Tumorigenic cell lines. Prostate **30:**58-64.

199. **Weinmann, L., J. Hock, T. Ivacevic, T. Ohrt, J. Mutze, P. Schwille, E. Kremmer, V. Benes, H. Urlaub, and G. Meister.** 2009. Importin 8 is a gene silencing factor that targets argonaute proteins to distinct mRNAs. Cell **136:**496-507.

200. **Wightman, B., I. Ha, and G. Ruvkun.** 1993. Posttranscriptional regulation of the heterochronic gene lin-14 by lin-4 mediates temporal pattern formation in C. elegans. Cell **75:**855-862.

201. **Wilting, S. M., R. A. van Boerdonk, F. E. Henken, C. J. Meijer, B. Diosdado, G. A. Meijer, C. le Sage, R. Agami, P. J. Snijders, and R. D. Steenbergen.** 2010. Methylation-mediated silencing and tumour suppressive function of hsa-miR-124 in cervical cancer. Mol Cancer **9:**167.

202. **Winter, J., S. Jung, S. Keller, R. I. Gregory, and S. Diederichs.** 2009. Many roads to maturity: microRNA biogenesis pathways and their regulation. Nat Cell Biol **11:**228-234.

203. **Wu, H., S. Zhu, and Y. Y. Mo.** 2009. Suppression of cell growth and invasion by miR-205 in breast cancer. Cell Res **19:**439-448.

204. **Wu, J., J. Qian, C. Li, L. Kwok, F. Cheng, P. Liu, C. Perdomo, D. Kotton, C. Vaziri, C. Anderlind, A. Spira, W. V. Cardoso, and J. Lu.** 2010. miR-129 regulates cell proliferation by downregulating Cdk6 expression. Cell Cycle **9:**1809-1818.

205. **Xu, B., X. Niu, X. Zhang, J. Tao, D. Wu, Z. Wang, P. Li, W. Zhang, H. Wu, N. Feng, L. Hua, and X. Wang.** 2011. miR-143 decreases prostate cancer cells proliferation and migration and enhances their sensitivity to docetaxel through suppression of KRAS. Mol Cell Biochem **350:**207-213.

206. **Xu, J., Z. Hu, Z. Xu, H. Gu, L. Yi, H. Cao, J. Chen, T. Tian, J. Liang, Y. Lin, W. Qiu, H. Ma, H. Shen, and Y. Chen.** 2009. Functional variant in microRNA-196a2 contributes to the susceptibility of congenital heart disease in a Chinese population. Hum Mutat **30:**1231-1236.

207. **Xu, J., D. Meyers, D. Freije, S. Isaacs, K. Wiley, D. Nusskern, C. Ewing, E. Wilkens, P. Bujnovszky, G. S. Bova, P. Walsh, W. Isaacs, J. Schleutker, M. Matikainen, T. Tammela, T. Visakorpi, O. P. Kallioniemi, R. Berry, D. Schaid, A. French, S. McDonnell, J. Schroeder, M. Blute, S. Thibodeau, H. Gronberg, M. Emanuelsson, J. E. Damber, A. Bergh, B. A. Jonsson, J. Smith, J. Bailey-Wilson, J. Carpten, D. Stephan, E. Gillanders, I. Amundson, T. Kainu, D. Freas-Lutz, A. Baffoe-Bonnie, A. Van Aucken, R. Sood, F. Collins, M. Brownstein, and J. Trent.** 1998. Evidence for a prostate cancer susceptibility locus on the X chromosome. Nat Genet **20:**175-179.

208. **Xu, W., and J. Y. Ji.** 2011. Dysregulation of CDK8 and Cyclin C in tumorigenesis. J Genet Genomics **38:**439-452.

209. **Xu, Y., T. Brenn, E. R. Brown, V. Doherty, and D. W. Melton.** 2012. Differential expression of microRNAs during melanoma progression: miR-200c, miR-205 and miR-211 are downregulated in melanoma and act as tumour suppressors. Br J Cancer **106:**553-561.

210. **Yamaguchi, G., M. Takanashi, M. Tanaka, K. Fujita, T. Ohira, M. Kuroda, and N. Ikeda.** 2012. Isolation of miRNAs that target EGFR mRNA in human lung cancer. Biochem Biophys Res Commun **420:**411-416.

211. **Yang, X., M. Feng, X. Jiang, Z. Wu, Z. Li, M. Aau, and Q. Yu.** 2009. miR-449a and miR-449b are direct transcriptional targets of E2F1 and negatively regulate pRb-E2F1 activity through a feedback loop by targeting CDK6 and CDC25A. Genes Dev **23:**2388-2393.

212. **Yao, B., S. Li, S. L. Lian, M. J. Fritzler, and E. K. Chan.** 2011. Mapping of Ago2-GW182 functional interactions. Methods Mol Biol **725:**45-62.

213. **Yi, R., B. P. Doehle, Y. Qin, I. G. Macara, and B. R. Cullen.** 2005. Overexpression of exportin 5 enhances RNA interference mediated by short hairpin RNAs and microRNAs. RNA **11:**220-226.

214. **Yi, R., Y. Qin, I. G. Macara, and B. R. Cullen.** 2003. Exportin-5 mediates the nuclear export of pre-microRNAs and short hairpin RNAs. Genes Dev **17:**3011-3016.

215. **Ying, S. Y., and S. L. Lin.** 2006. Current perspectives in intronic micro RNAs (miRNAs). J Biomed Sci **13:**5-15.

216. **Yu, J., D. G. Ryan, S. Getsios, M. Oliveira-Fernandes, A. Fatima, and R. M. Lavker.** 2008. MicroRNA-184 antagonizes microRNA-205 to maintain SHIP2 levels in epithelia. Proc Natl Acad Sci U S A **105:**19300-19305.

217. **Zeng, Y., and B. R. Cullen.** 2004. Structural requirements for pre-microRNA binding and nuclear export by Exportin 5. Nucleic Acids Res **32:**4776-4785.

218. **Zhang, B. G., J. F. Li, B. Q. Yu, Z. G. Zhu, B. Y. Liu, and M. Yan.** 2012. microRNA-21 promotes tumor proliferation and invasion in gastric cancer by targeting PTEN. Oncol Rep **27:**1019-1026.

CONTRIBUTIONS OF COLLABORATORS

Other scientists who contributed to this work include Huijun (Jane) Zhao, who worked with me during the *in vivo* mouse experiment. Miguel Cabrita helped me with learning and troubleshooting the microarray analysis program Flexarray. Manijeh Daneshmand helped me examine the tumour samples obtained from the mouse experiment. Grant Howe taught me how to perform scratch wound assays and allowed me to use his tools for the assay. Dr. Bruce McKay and Jeff Hamill taught me how to obtain and examine my flow cytometry data, and Dr. Jim Dimitroulakos kindly supplied certain reagents such as the Cdk6 antibody.

CURRICULUM VITAE

Education:

Master's of Biochemistry – Specialization: Human and Molecular Genetics 2010-2012
University of Ottawa, Ottawa, Ontario

- Received the Ontario Graduate Scholarship
- Average of A over two seminar courses
- Completed ESG5310: Community Outreach & Media Relations in the Sciences
- Degree to be completed Fall 2012

Bachelor of Science (Honours), SSP Life Sciences 2006-2010
Queen's University, Kingston, Ontario

- Final average of 83.6%
- Received the George and Lillian Coleman Taylor Scholarship over 4 years
- Graduated with Distinction June 2010

High School Degree
Grenville Christian College Preparatory School, Brockville, Ontario 2001-2006

- Valedictorian of my 2006 class
- Graduated with High Honours (+90%)
- Received numerous academic and extracurricular awards

Honours and Awards:

Ontario Graduate Scholarship 2011-2012
University of Ottawa

Master's Admission Scholarship 2010-2012
University of Ottawa

Dean's Honour List, all 4 years of undergraduate work 2006-2010
Queen's University

George and Lillian Coleman Taylor Scholarship 2006-2010
Queen's University

Valedictorian, Graduating Class 2006
Grenville Christian College Preparatory School

Research Experience:

Master's student in cancer research laboratory 2010-2012
University of Ottawa, Ottawa Hospital Cancer Centre

- Researched the relationship between microRNAs and prostate cancer
- Discovered novel microRNA that inhibits prostate tumour growth
- First-author publication currently in preparation
- Presented multiple posters and seminars at BMI and OHRI events

Thesis project student in cancer research laboratory September-April, 2009-2010
Queen's University

- Independent research project on the effects of the Stat3 protein on cell differentiation
- Literature review, multiple presentations, poster talk and thesis all part of the project
- Final mark of 85%

Summer student in cancer research laboratory May-August, 2009
Queen's University

- Learned many techniques such as tissue culture, Western blots, cell differentiation, staining protocols
- Helped out around the lab, performed daily and weekly chores
- Put together a paper with PI and fellow summer student based on our overall results

Publications:

Samantha Greer, Rice Honeywell, Mulu Geletu, Rozanne Arulanandam and Leda Raptis. **Housekeeping genes; expression levels may change with density of cultured cells.** Journal of Immunological Methods, 2010 Feb 19 - Published.